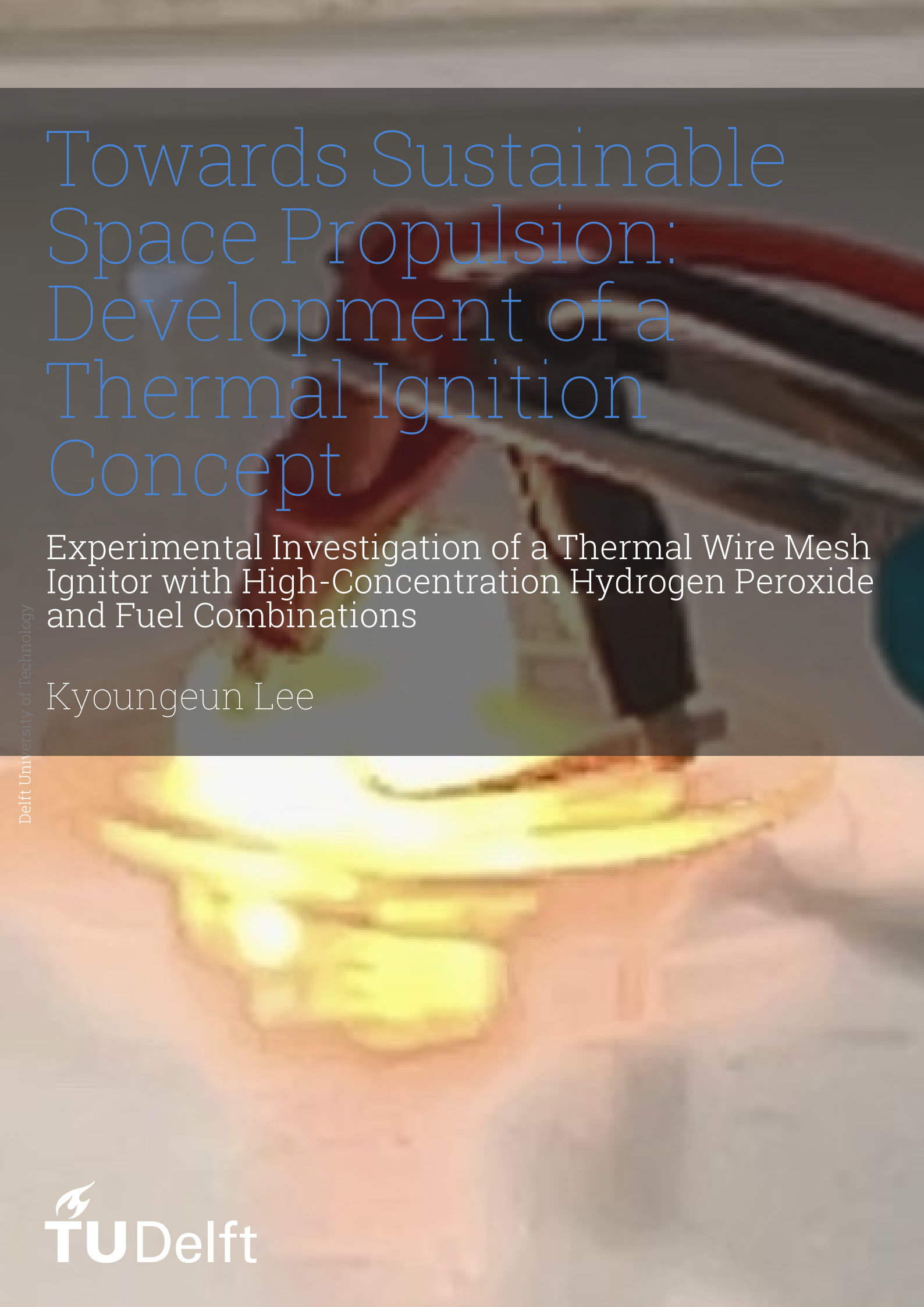

Towards Sustainable Space Propulsion: Development of a Thermal Ignition Concept

Experimental Investigation of a Thermal Wire Mesh Ignitor with High-Concentration Hydrogen Peroxide and Fuel Combinations

Kyoungeun Lee

Delft University of Technology

TU Delft

Towards Sustainable Space Propulsion: Development of a Thermal Ignition Concept

Experimental Investigation of a Thermal Wire Mesh Ignitor with High-Concentration Hydrogen Peroxide and Fuel Combinations

by

Kyoungeun Lee

to obtain the degree of Master of Science

at the Delft University of Technology,

to be defended publicly on Tuesday, July 16, 2024, at 9:00 AM.

Student number:	4843320	
Project duration:	November 20, 2023 – June 17, 2024	
Thesis committee:	Dr. B. V. S. Jyoti,	TU Delft, Supervisor, Assistant Prof. TU Delft
	Dr. Ir. J. Bouwmeester,	TU Delft, Chairman Committee
	Dr. S. Gehly,	TU Delft, External Committee Member
	Dr. S. Reichstadt,	The Exploration Company, Company Supervisor

This thesis is confidential and cannot be made public until Wednesday, July 16, 2025.

An electronic version of this thesis is available at `http://repository.tudelft.nl/`.

TU Delft

Preface

This Master Thesis was conducted in the Aerospace Faculty of Delft University of Technology, the Netherlands. It contains the outcomes of 9 months of hard work by the author, Kyoungeun Lee, and concludes the 2 years duration of a Master of Science degree as a Space Engineering, Space Flight track student. The past 5 years of my time at Delft (starting from my Bachelor's studies) left me mixed feelings since the process was successful and meaningful as the start of my journey as an aerospace engineer, but at the same time, was sometimes tough, especially during the COVID times during the 2nd and 3rd year of my BSc studies. Nonetheless, since there was lavish support from around me, including my family, friends, professors, university staff members, the Exploration Company supervisor, and many more, I was able to deal with the hard times and was able to come to this moment in time. I would like to give the honour to the supportive people and would like to show gratitude towards them. Thanks a lot, people!

One of the most important people during the MSc thesis period was my main supervisor, Dr. BVS Jyoti. Knowing her since numerous courses in the past, an external EU research project, and up to this point, she has always provided me with sincere support and encouragement. This has helped a lot during my 2 years of academic period as an MSc student and also during the MSc thesis.

Lastly, I would like to end with a famous quote that I like the most, by Sir Carl Sagan, a former university professor of astronomy at Cornell University.

> ”For myself, I like a universe that includes much that is unknown and, at the same time, much that is knowable...” - Carl Sagan

Kyoungeun Lee
Delft, June 2024

Abstract

With the urge of not only the aerospace propulsion system industry, but all industries of engineering to improve each system into a more sustainable solution, a lot of different green propellant combinations have been investigated that are less toxic, and more eco-friendly, but however efficient at the same time. This is true for liquid bi-propellant systems as well. Due to the emergence of new propellant combinations, or with the demand for more energy-efficient propulsion systems, new types of ignitor systems, which are a significant element in a bi-propellant space propulsion system, or the improvement of the conventional systems to a more efficient one are being investigated. Following the demand for research in these sectors of propulsion systems, this MSc thesis focuses on the development of a liquid bi-propellant space propulsion ignition concept, which is optimised from the perspective of power, cost, and performance.

During the literature study phase of the thesis, several ignitor systems were investigated and the thermal wire ignitor concept was chosen to be the most suitable system for the study due to its reusability function, cost-effectiveness, mass/volume, and handling features. On top of that, after understanding the features of several fuel and oxidiser combinations, ethanol and HTP were chosen as the most optimal propellant combinations. These were shown to provide performance similar to conventional propellant combinations, such as in density-specific impulse, and most importantly, were considered an eco-friendly combination.

During the experimental phase of the MSc thesis research, the first experiment aimed to measure the resulting HTP temperature when it passes through a NiCr thermal wire mesh in a glass chamber, where the chamber itself is heated up with a wire wound around the external wall. This experiment showed that a resulting temperature of almost 400 deg C was achievable with 20 W of power applied to the wire mesh down to a value of 294.37 deg C for 5 W of power applied. The most interesting point is at a power value of 12.5 W, in which the HTP reaches a temperature value right above the auto-ignition temperature of ethanol, 375.65 degrees C.

The second experiment aimed in investigating the ignition behaviour of the fuel and HTP in an open environment. The results showed that at 12 W of power applied to the NiCr thermal wire mesh, which was in contact with a premixed fuel and oxidiser pool this time, combustion and self-sustained ignition were achieved with a sufficiently short amount of IDT (around 200 ms). Also, at 10 W of power applied, combustion occurred with HTP and Jet A, which was a reference fuel used with the purpose of showing that fuel types that have an auto-ignition temperature lower than ethanol are able to ignite at lower power consumption values. The self-sustained ignition was obtained at power values slightly higher than this, 12.5 W.

The last experiment aimed in investigating the ignition behaviour of the fuel and HTP in a closed environment, which also serves as a pressurised system. The results showed that at 10 W, the ethanol and HTP combination was able to combust and self-sustain. Also, at a value of 7.5 W, the Jet A fuel and HTP combination were able to combust and provide a self-sustainable ignition. They both showed that in a pressurised system, lower levels of power values are required in order for the same fuel and oxidiser combination to achieve combustion.

Simultaneously with the experiment conducted, a simulation of the HTP decomposition temperature in a glass chamber was done using the cross-platform finite element analysis, solver and multi-physics model software, COMSOL. The simulation was able to show that at power values of 20 W, as the HTP is injected in the glass chamber, the liquid was able to achieve a temperature of 589 degrees C but decreased drastically down to the initial temperature of the volume that was inputted in the software. This simulation was done using a mesh configuration named Normal, which is an automatically available

mesh quality in the COMSOL software. Together with the same mesh quality, if 15 W of power is applied, the initial temperature that the HTP achieves is 492 degrees C and for 10 W, it is 394 degrees C. All the results presented matched the results of the experiment conducted. Lastly, 2 sensitivity analysis were performed in order to prove that the simulation was done properly.

Contents

Nomenclature

Acronyms

AWG	American Wire Gauge
DC	Direct Current
FEA	Finite Element Analysis
HS	High Speed
HTP	High Test (Hydrogen) Peroxide
IDT	Ignition Delay Time
LH2	Liquid Hydrogen
MMH	Mono-Methyl Hydrazine
NiCr	Nichrome
NTO	Nitrogen Tetroxide
PFV	Photorn FASTCAM Viewer software
PLA	Polylactic Acid
PZT	Piezoelectric Actuator
RFNA	Red Fuming Nitric Acid
RP1	Refined Petroleum 1
S/C	Spacecraft
TRL	Technology Readiness Level
UDMH	Unsymmetrical Dimethylhydrazine
WFNA	White Fuming Nitric Acid

List of Figures

List of Tables

1

Introduction

”It is difficult to say what is impossible, for the dream of yesterday is the hope of today and the reality of tomorrow.”. This is a famous quote by Robert Goddard, the pioneer of modern rocketry, which explains the significance and eagerness to pursue space travel. In pursuit of space exploration, humanity has developed launch vehicles—commonly known as rockets—and S/C, to serve as primary transportation to outer space. These sophisticated devices integrate numerous systems to support their functionality, with propulsion systems standing out as the vital force propelling vehicles forward. Comparable to a beating heart, propulsion systems infuse energy and life into the journey through outer space.

Different types of space propulsion systems exist, shown in Figure 1.1. The diagram shows three main types of systems. Chemical propulsion, also known as thermal rocket propulsion, operates by accelerating high-pressure gas to a high velocity through expansion in a nozzle, generating thrust for the vehicle [1]. Electric propulsion functions by utilizing electrical energy to accelerate a propellant through various electrical and/or magnetic methods [2]. Nuclear thermal propulsion operates similarly to a chemical propulsion system, but with a key distinction: instead of chemical reactions, nuclear reactions are used to generate the thrust [3]. In addition to the systems depicted in the diagram, there exists a diverse range of other propulsion systems that are in various stages and possess different TRLs.

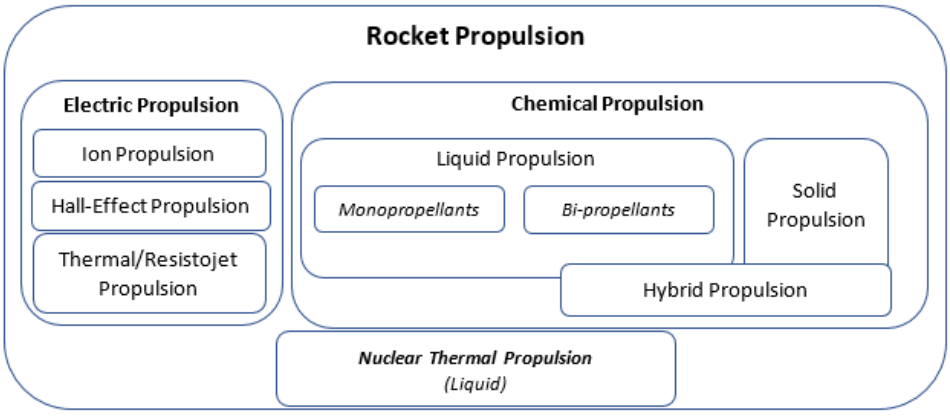

Figure 1.1: Rocket Propulsion Type Diagram [4]

A note has to be taken that this thesis concentrates on chemical propulsion systems, and in particular bi-propellant liquid propulsion systems, due to the practicality of conducting experiments within the laboratory facilities available at the Delft University of Technology, as opposed to electric or nuclear propulsion systems which may require specialised infrastructure or facilities beyond the scope of the

current study.

To briefly introduce the three main options of chemical propulsion systems, there are several differences among solid, liquid, and hybrid propulsion systems. Solid propulsion systems utilise propellants in a solid phase, typically in the form of propellant grains. Similar to a candle flame, these systems initiate a chemical reaction within the propellant grain when sufficient energy is applied, resulting in the formation of high-temperature gas. This gas is then exhausted through a nozzle, producing thrust. Solid propulsion represents one of the earliest methods of propulsion developed and was the predominant technology until the 20th century when liquid propulsion systems emerged. Despite advancements in liquid propulsion, solid systems remain in use today, particularly in military armaments and as boosters during rocket launches, due to their simple design and high reliability, which is also the main advantage of the system. A primary disadvantage of solid propulsion systems is their lack of reusability, as once the propellant grain reaction is initiated, it (mostly) cannot be halted or controlled. Additionally, these systems exhibit increased radio frequency attenuation from their reaction plumes compared to liquid propulsion systems [1]. A figure of a typical schematic of a solid propulsion system depicting its main components is shown in Figure 1.2.

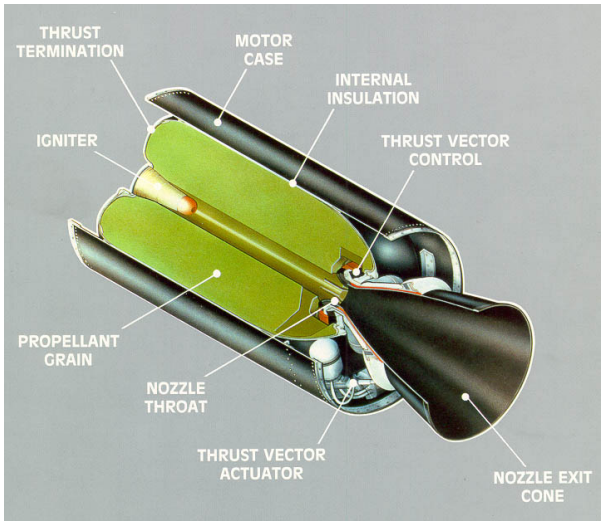

Figure 1.2: Solid Propulsion System Schematic [5]

In contrast to solid propulsion systems, liquid propulsion systems use propellants in a liquid phase, typically either mono- or bi-propellants, meaning one or two different chemicals are utilised as fuel and oxidiser. These liquids are usually sprayed into the combustion chamber using injectors to atomise them, creating a larger surface area for efficient reaction and ignition. The resulting hot gases from the combustion in the chamber are then expelled through the nozzle to produce thrust. In the case of mono-propellants, a catalyst bed is often employed where the liquid is evenly distributed over the bed, leading to chemical decomposition and the generation of thrust. Liquid propulsion systems offer several advantages, including higher specific impulse compared to solid propulsion systems and the capability of being restarted as frequently as the design permits. However, these systems also have drawbacks. They involve more subsystems for regulating and injecting the liquid, which can lead to lower reliability and increased mass compared to solid propellant options [1]. A figure of a typical schematic of a liquid propulsion system depicting its main components is shown in Figure 1.3.

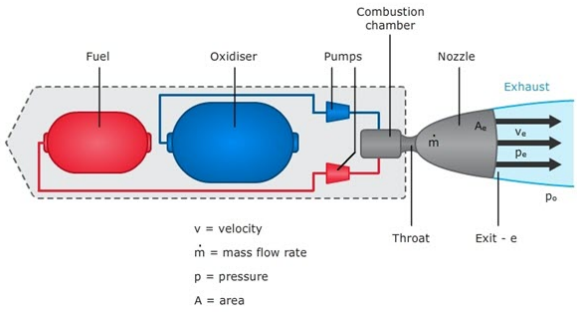

Figure 1.3: Liquid Propulsion System Schematic [6]

The hybrid propulsion system aims to combine the advantages of both solid and liquid propulsion systems while addressing their respective disadvantages. As the name suggests, these systems typically use a combination of solid and liquid propellants. The key components include a pressure vessel containing the liquid oxidiser and a combustion chamber housing the solid propellant. In hybrid systems, the oxidiser is usually in liquid form because solid oxidisers can be hazardous and exhibit lower performance compared to liquid options. When thrust is required, the valve connecting the pressure vessel and combustion chamber opens, allowing the liquid oxidiser to flow into the combustion chamber. The liquid propellant undergoes decomposition, and the resulting elevated gas reacts with the solid propellant to produce thrust. The main advantage of hybrid systems is their ability to leverage the benefits of both solid and liquid propulsion technologies. However, their performance typically falls below that of modern liquid propulsion systems, although it exceeds that of traditional solid propulsion systems. Additionally, while hybrid systems are less complex than purely liquid systems, they are still more intricate due to the regulation systems required for pressurised liquid propellants. This complexity directly impacts the reliability of the system [1]. A figure of a typical schematic of a hybrid propulsion system depicting its main components is shown in Figure 1.4.

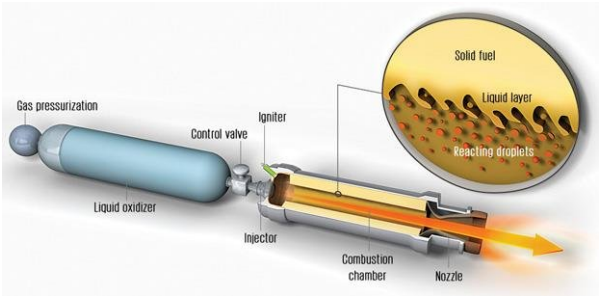

Figure 1.4: Hybrid Propulsion System Schematic [7]

In addition to liquid bi-propellant propulsion systems, which are the focus of this thesis as aforementioned, both solid and hybrid propulsion systems commonly require an important subsystem known as the ignition system. They refer to a subsystem that provides an external stimulus to induce ignition and combustion of the engine. Its primary function is to elevate the propellant temperature to a level sufficient to enable self-sustained combustion within the propulsion system. Ignition systems are crucial components of space propulsion systems, essential for igniting and operating engines successfully at the intended time and place. Failure to design these systems effectively can result in mission failure, as the spacecraft or rocket may be unable to generate the required thrust. Recognising the importance of ignition systems, numerous studies have been conducted in the past to design and develop them, aiming to ensure the reliability and performance of space missions. Early designs of ignition systems were influenced by various mechanical systems, including those used in automobiles. However, as the need for specialised and reliable ignition systems for space propulsion systems arose, dedicated designs tailored specifically for space applications were developed.

The phase of the propellant stored and utilised is a primary consideration when selecting the appropriate ignition system for a propulsion system. Pyrogen ignitors and pyrotechnic ignitors are primarily employed in solid propulsion systems, while hypergolic ignitors, catalytic ignitors, spark plugs, and torch ignitors are typically used in liquid propulsion systems. Hybrid propulsion systems, which incorporate both liquid and solid propellants, require a combination of various ignitor systems to accommodate their dual-phase propellant compositions.

Another important criterion is the type of propellant utilised. Hypergolic propulsion is commonly employed in liquid propulsion systems due to its significant advantage of high reliability. A traditional choice involves using nitrogen tetroxide (NTO) as the oxidiser paired with monomethylhydrazine (MMH) as the fuel. However, a notable drawback of this conventional ignition method is that these propellants are considered environmentally hazardous, highly toxic, and largely carcinogenic [8]. Considering these concerns, ongoing research is exploring alternative, more environmentally friendly and sustainable options for propulsion systems. One emerging combination being investigated by various institutions is hydrogen peroxide with kerosene [9]. This represents a promising direction towards developing greener propulsion solutions. Researchers are striving to explore and apply these green solutions to current systems further.

Due to the non-hypergolic nature of most green propellants, separate ignition systems are necessary to initiate ignition, combustion, and generate thrust for propelling space vehicles to their intended destinations or performing desired maneuvers. These systems require specialised components for igniting the fuel and oxidiser, such as spark plugs and thermal wire ignitors. As evident, there is a wide range of variations, categories, and types of ignition systems to consider. However, not all of these systems are at the same TRL, indicating that further development and optimisation are essential and feasible for certain types of ignition systems.

An ignition system that this thesis focuses on specifically is thermal wire ignitors. This research aims to adapt a test setup developed by a former Delft University of Technology Master student [10]. The newly adapted test setup shall be able to operate in steady-state firing, as well as short hot firing impulse modes and demonstrate the decomposition of HTP and also the auto-ignition of Ethanol and Jet A fuel which shall result in stable combustion. This research will provide a solution for an institution in Germany, the Exploration Company. This also shows the last main selection criterion for determining the suitable ignition system for a space propulsion system, the objective of the space mission.

The outline of the thesis is as follows. In chapter 2, the literature study in which the various types of ignitor systems that have been or are being investigated recently are introduced, which will support in motivating why the thermal wire ignition concept has been chosen. On top of that, the chemistry behind the ignition and combustion process of HTP and ethanol will be explained as well. This chapter will also highlight the features of liquid bi-propellant propulsion systems and the corresponding ignitor system options in more detail. In chapter 3, the research objectives and research questions, along with the propulsion system requirements both proposed by the Exploration Company as well as the adapted ones will be introduced. In chapter 4, the trial and successful test setup designed and built will be introduced. The description and objective of each experiment, as well as the step-by-step process of each experiment, will be presented. In chapter 5, the results, analysis, and observations made throughout the experiments conducted will be presented. In chapter 6, the simulation results of the pre-chamber glass chamber using a multi-physics model software named COMSOL will be presented. It will support the results presented in chapter 5. Lastly, the overall conclusion of the MSc thesis as well as the recommendations that are suggested for future work is presented in chapter 7.

2

Literature Study

In this chapter, the results of the literature study will be shown, which is initially conducted before the main objective, research questions, the system requirements, and the methodology for this thesis are presented. The main goal of this literature review is to introduce what is a liquid-bi propellant propulsion system and the working principle of ignitor systems as well as the various types, shown in section 2.1 and section 2.2, respectively. Subsequently, a trade-off among the ignition systems introduced will be done in section 2.3 with the objective of choosing the most suitable ignition system for the thesis research. Subsequently, the motivation behind the oxidiser and fuel selection will be shown in section 2.4. Afterwards, the type of thermal wire selected will be shown, along with its motivation in section 2.5. Also, the chemistry behind the ignition and combustion process of HTP and ethanol will be explained in section 2.6 and the auto-ignition temperature of several fuels commonly used in the aerospace industry is shown in section 2.7. Lastly, the operation mechanism and features of a piezoelectric disc will be explained in section 2.8.

2.1. Liquid-Bi Propellant Propulsion Systems

As mentioned in chapter 1, the main focus of this thesis is about liquid bi-propellant propulsion systems. The term 'liquid' comes from the fact that the fuel and oxidiser being used in the system are in a liquid state, which is then converted to high temperature and pressure gaseous state to be accelerated through the combustion chamber and nozzle to provide thrust. The term 'bi-propellant' comes from the fact that there are two propellants on board the system, usually the oxidiser and fuel, separately stored in a tank, which is pressurised sometimes depending on the type of propellant chemical compound. A typical schematic of a liquid-bi propellant system is shown in Figure 2.1. As can be seen from the figure, the oxidiser and fuel and stored in tanks which is connected to the actual rocket thrust chamber via feeding systems, which have valves as well to regulate the flow of the fluid.

As with any other system, it has its own advantages and limitations as well. As advantages, they offer exceptional performance and control in aerospace applications. By allowing precise adjustment of the mixture ratio and combustion processes, these systems achieve high specific impulse, leading to efficient thrust generation. Additionally, the ability to vary the engine's thrust level provides operational flexibility, allowing for precise control over acceleration and manoeuvring. Their capability to be restarted multiple times during missions enables complex manoeuvres like orbit insertion and trajectory adjustments. This flexibility in engine design not only optimises mission efficiency but also supports versatile mission profiles, making liquid bi-propellant systems a preferred choice for a wide range of space missions.

As for its limitations, the complexity of managing two different propellants simultaneously can be demanding, particularly during long-duration missions. Furthermore, certain propellant combinations may be chemically reactive or incompatible, potentially leading to issues such as corrosion or unstable combustion. Additionally, systems using cryogenic propellants require specialised handling and insulation

due to their extremely low temperatures, adding complexity and cost to the overall system. Integration challenges, including thermal management and structural considerations, further contribute to the complexity and increase in the cost of the system.

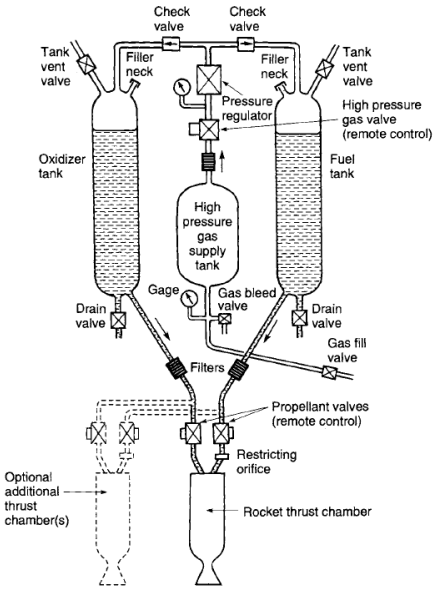

Figure 2.1: Schematic of a Typical Liquid-Bi Propellant System [6]

2.2. Ignitor Systems

The mentioned system in section 2.1, a bi-propellant propulsion system, requires an essential component in order for a successful ignition and combustion process, an ignitor system. They are an essential component in space propulsion engines where they promote the reaction, ignition, and combustion of the propellant which results in thrust. A block diagram showing the main elements of a typical ignitor system is shown in Figure 2.2. The electronics of the system ensure that the triggering of the ignitor to liberate energy is done at the right time. The safe and arm system allows for an extra safety device.

A lot of types of ignitors for rocket engines exist and have gone through investigation in the past. A typical ignitor is chosen for a rocket or space propulsion system taking into consideration several system requirements, including mass/size, cost, reusability, type of propellant usage, total energy released, temperature of the ignitor gases, ignition time, ignition delay, and many more. The reusability refers to the system being able to make several restarts, which is required for almost all types of space missions. The type of propellant used is important because, based on the phase of the chemical substance, different ignitor mechanisms are required, which will be shown in detail below. The total energy release and temperature reached by the ignitor gases are relevant because each chemical combination has a different energy level required to initiate the combustion reaction. If the chosen ignitor system is unable to provide this energy, it will lead to the propellant not reacting. Lastly, the ignition time and ignition delay time are related to how much time it takes for the chemical compounds to ignite after the required energy is released by the ignitor system. In this section, the state of the art of ignitor systems that can be found in literature will be introduced as well as their working mechanisms and advantages and disadvantages.

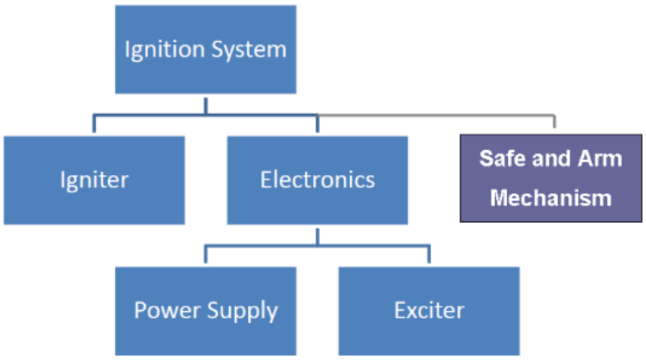

Figure 2.2: Ignitor System Main Element [1]

2.2.1. Spark Plug

Spark plugs, also known as direct spark plugs, are a well-known ignitor option when multiple starts during the flight of a liquid rocket engine are required [11]. They are used for propellant combinations that are easily vaporised, such as liquid oxygen and hydrocarbon [1]. A variation of the spark plug, the torch ignitor, will be introduced in subsection 2.2.2. They are usually built into the injector, specifically located in the flow path of the vaporised oxidiser and fuel mixture, and once the engine starts and the spark is produced, they directly ignite the gas generator or main injector propellant [11].

The spark is produced by a high voltage applied to two wires separated by a small gap. Due to this voltage, a current is produced. Once the spark plug creates an arc in the vaporised propellant mixture, ignition will occur [11]. A figure of a schematic of this system is shown in Figure 2.3. Due to its low number of components and relatively simple mechanism, it is considered an efficient and reliable system.

On the other hand, spark plugs have disadvantages as well. Unlike systems, for instance, hypergolic ignitors, introduced in subsection 2.2.5, spark plugs do not have the capability of producing infinite numbers of sparks, which limits the engine performance. This capability is highly dependent on the material usage. On top of that, as mentioned before, since the system is located in the combustion chamber directly, extra precautions must be taken to safeguard the spark plug from elevated pressures and temperatures. For this reason, normally additional spark plugs are usually installed in the engine for redundancy. Another disadvantage is that the spark generated is highly localised [11]. Consequently, in larger engines, relying on a single spark plug is insufficient to ignite the entire engine. To ensure proper ignition, multiple spark plugs must be distributed across the combustion chamber.

Figure 2.3: Schematic of a Spark Plug [1]

2.2.2. Torch Ignitor

As mentioned in subsection 2.2.1, torch ignitors, also known as augmented spark ignitors or spark torch ignitors, have a similar working mechanism as spark plugs. This variation was developed to overcome the limitations of direct spark plugs, where the spark generated is highly localised. This feature allows torch ignitors to be used in larger launch vehicles compared to direct spark plugs.

The plugs produced are used to ignite propellants in a pre-combustor or torch device, in which the

high-temperature ignitor flame is flown in the main combustion chamber via an ignitor tube or nozzle, which ensures sonic separation of the ignitor chamber with the main one [1]. Using either the same or different propellant with the main combustion chamber is possible. The propellant feeding the ignitor may be stored separately from the main propellants for the latter case. This is shown in many cases where hydrocarbons are used as propellants since they form residuals on the spark plug that can lead to ignition failure [1]. It has an even higher reliability than the direct spark plug system since the ignition occurs separately from the main combustion chamber, and thus the tips of the plugs are ensured to be better protected from the elevated temperature and pressure of the flames. A schematic of a torch ignitor is shown in Figure 2.4.

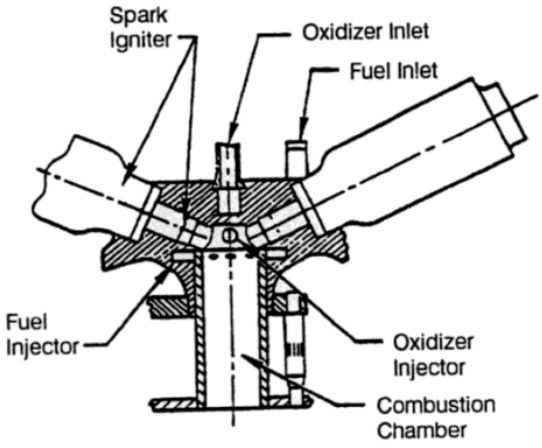

Figure 2.4: Schematic of a Torch Ignitor [12]

2.2.3. Thermal Wire Ignitor

As the name suggests, thermal wire ignitors make use of the heat generated in the wire produced by applying high electrical resistance. The heat is used to induce the decomposition of the propellant that is afterward injected into the combustion chamber. Both monopropellant as well as bipropellant rocket engines can make use of this ignitor system. In the latter case, either the oxidiser or fuel will be exposed to the thermal wire initially and decomposition of it will occur. Subsequently, that decomposed substance will come into contact with the other propellant in which ignition and thus combustion will take place. A schematic of a thermal wire ignitor that decomposes hydrogen peroxide for applications in low-thrust propulsion systems is shown in Figure 2.5.

As can be seen from the schematic, thermal wire ignitors have the advantage of having a relatively simple structure and therefore low mass and high reliability which also leads to being a cost-effective solution for space propulsion. On top of that, they are suitable for reusable usage, for instance for pulse mode firing (PMF), in which an on/off mode can be applied to the system. However, the most significant drawback is that once the size of the rocket increases to some extent, the consumption of electrical power to decompose the required amount of propellant becomes too much. This fact makes this type of ignitor system inapplicable for heavy rocket engines and limits it to only low-thrust applications or small propulsion systems. Nonetheless, note has to be taken that compared to other ignition systems, this technology has a low TRL(Technology Readiness Level) and is still under active investigation which means that vast potential remains for this ignitor system.

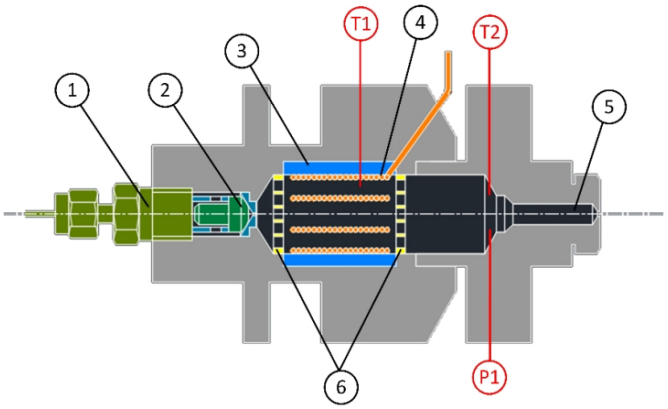

Figure 2.5: Schematic of a Thermal Wire Ignitor [13]. 1: Connector, 2: Propellant Injector, 3: Insulator, 4: Heating Wire, 5: Nozzle, 6: Holding Plates

2.2.4. Glow Plug

Glow plugs are often used in diesel engine automobiles, supporting the engine to heat the fuel easily during cold weather conditions, but have applications in rocket engines as well. Their functional purpose is similar. It is essentially a small heating element that glows red-hot when an electric current is applied, and using that heat, it decomposes the propellant to support ignition and combustion. The system can be used for both monopropellant and bipropellant rocket engines, in which the bipropellant engine, works similarly to a thermal wire ignitor shown in subsection 2.2.3. The material of the system can be made out of metal but investigations on different types also, such as ceramic glow plugs have been made [14]. It was found that the ceramic glow plugs required less voltage supply compared to the metal ones, and were also able to reach higher tip temperatures as well. A schematic of a glow plug applied to an actual rocket engine is shown in Figure 2.6.

The main advantage of the system is that it has a relatively small number of components, though being more complicated compared to spark plugs, which means the mass of the system itself is low. It is reusable to some extent as well as long as the tip material can sustain the ignition temperature. However, they have drawbacks such that the general heating time duration is 20 - 30 [sec], which may be problematic for usage in space propulsion [15]. Eventhough ceramic glow plugs have a shorter duration [14], they are still considered insufficient for applications in real space missions with today's TRL.

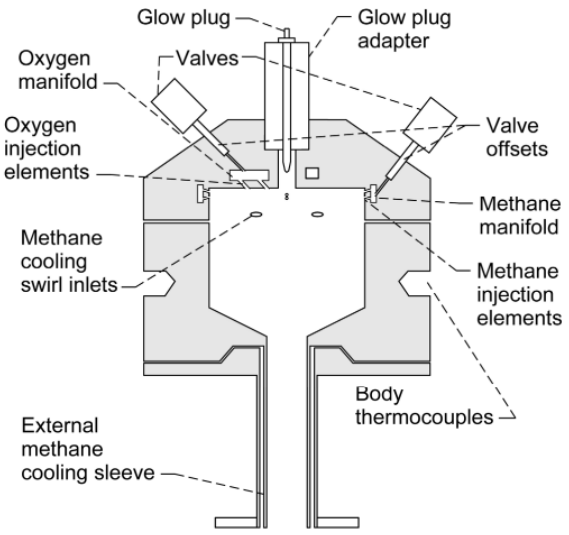

Figure 2.6: Schematic of a Glow Plug Ignitor [14]

2.2.5. Hypergolic Ignitor

The term hypergolic has the definition of spontaneously reacting upon contact of two or more components without external aid. As the term suggests, hypergolic ignitors, also known as pyrophoric ignitors, use this property of certain substances to induce combustion in a rocket engine, mostly by mixing an oxidiser and fuel combination that is hypergolic. The hot flame produced can be used to start combustion in the main engine, or the combination can be injected and come into contact directly with the main engine in which combustion will occur. The latter is preferable in a majority of cases due to it having fewer engine components and thus less mass and higher reliability.

However, a more refined method exists, which is through the use of a hypergolic slug [1]. This system injects a liquid chemical that is hypergolic with one of the main propellant components, but non-active to the other. The fluid is stored in the fluidic line of the propellant which is non-active and is injected in the main engine before the propellant. It comes into contact with the propellant that is reactive first, ignition occurs, and the flame is self-sustained since the second propellant, the one that was not active with the fluid, will be able to be continuously supplied as well. Using this method and adding a cartridge as well to the fluidic lines, the problem of conventional hypergolic ignitors not being able to stop and restart once the combustion has occurred can be possible as well [16].

Despite the advantage of being highly reliable and having a low ignition delay time, the system also has two major drawbacks, one being that the chemicals used are highly toxic. Acknowledging this fact, numerous studies have been made aiming for green hypergolic propellant combinations (Jyoti et al 2017 [17], Wojciech et al 2017 [18], S Park et al 2020 [19]). The other is that when the chemicals are in contact with air, they may ignite spontaneously making them difficult to produce, store, and handle. Extra safe measures have to be applied when considering hypergolic ignitors.

2.2.6. Catalytic Ignitor

Catalytic ignitors utilise catalysts to lower the activation energy of propellant, decompose the monopropellant and thus result in hot flames to support the combustion process in the main rocket engine. This relation follows the Arrhenius Equation, given by Equation 2.1, where k is the reaction rate, E_a is the required activation energy for a chemical reaction, and T is the temperature. The most dominantly used monopropellant used up to now is hydrogen peroxide (H_2O_2) [12], in which adiabatically decomposed 90 % HTP (High Test Peroxide) produces gases of up to 1033 K [20]. Catalysts are capable of decomposing HTP into hydrogen (H_2) and oxygen (O_2) in which the liberated oxygen molecule may react with hydrocarbons such as ethanol or kerosene, in which combustion occurs. Since most of the time, the fuel is incompatible with the catalyst, the decomposed oxidiser and fuel come into contact inside the main engine. A schematic of a catalytic ignitor is shown in Figure 2.7.

$$k = A \cdot exp(\frac{-E_a}{R \cdot T}) \tag{2.1}$$

A wide range of options are available as materials for catalysts including metals such as silver, platinum, manganese oxide, or ceramics. When selecting the right type of material, factors such as the propellant being used, the required minimum heat of the catalyst bed including the estimated decomposition temperature occurring, the pressure, and many more have to be taken into consideration. Liquid catalysts are possible too. Nonetheless, they are usually discarded since during operation, extra caution has to be made for the elaborate timing, valving, and interlocking device [1].

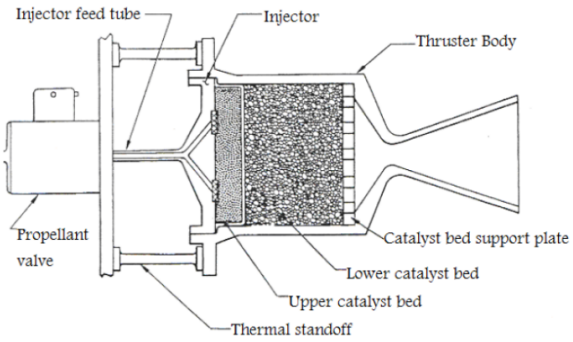

Figure 2.7: Schematic of a Catalytic Ignitor [21]

2.3. Preliminary Trade-off of Ignitor Systems

In this section, the trade-off of ignitor systems found in literature and presented in section 2.2 will be made. The trade-off scores, weighting factor as well as the criteria taken into account will be introduced as well as the Pugh matrix itself, and will show which system was chosen for further investigation.

2.3.1. Trade-off Criteria

The score of the trade-off for each system is done in -1, 0, and 1 and the weighting factor for each criterion is given a value between 1 to 3. The final score is computed by multiplying the score of each system with the weighting factor. The system with the highest score is taken to be the most suitable ignitor to be investigated and applied to the Nyx Earth propulsion system. The criteria taken into consideration and the reason behind choosing them are shown in the following.

- **Dry mass / Volume:** Dry mass and volume of, not only the propulsion system but for every system in a space propulsion system is a significant factor that has to be taken into consideration. Depending on this criterion, the cost, reliability, and many other factors are determined and therefore the weighting factor is the highest, a 3.

- **Reusability:** Reusability was considered due to it being a crucial system requirement as shown in section 3.2. If the system is inadequate for reusability, it will have to immediately be eliminated from the list of candidates. For the aforementioned reason, the weighting factor for this criterion is given a 3.

- **Cost:** The cost is also an important criterion and is usually a hard requirement for every space mission. The cost here refers mainly to the hardware and material cost, although a lot of other factors are included as well. The weighting factor of this criterion is given a 2.

- **Simplicity of the Design:** Although not as important as the other criteria, simplicity of the design must be considered as well due to it correlating with the reliability of the system, especially for space missions that have plans to be operating for a long period. The ignitor of a propulsion system is responsible for the initial stage of the ignition and combustion of the propellants. Therefore, simple propulsion system designs have less probability of malfunctioning and thus have less chance is leading to failure of the mission. The weighting factor of this criterion is given a 1.

- **Handling:** Handling of a system relates to how much it is considered safe or not. Having a system that has a low score in safeness is often considered an option that must be eliminated unless the function it possesses has a significant advantage towards conducting the space mission. The weighting factor of this criterion is given a 2.

2.3.2. Trade-off and Discussion

Considering the trade-off criteria introduced above, a Pugh matrix was made, which is shown in Figure 2.8. Out of all the ignitor systems introduced in section 2.2, the spark plug, glow plug, and thermal

wire ignitor system were the ones chosen for further trade-off since those were the only candidates that had the potential of fulfilling the propulsion system requirements, such as being reusable and considered safe. This is also the reason why, for all 3 systems, the criterion of reusability and handling scored the highest, a 1. From the trade-off table, the thermal wire ignitor resulted in the highest score, followed by the glow plug and spark plug system. Therefore, it was concluded that the thermal wire ignitor system shall be further investigated throughout this Master's thesis and is considered an adequate system for the Nyx Earth propulsion system.

Figure 2.8: Ignitor system trade-off table

Criteria	Weighting Factor	Spark Plug	Glow Plug	Thermal Wire Ignitor
Dry Mass / Volume	3	-1	1	0
Reusability	3	1	1	1
Cost	2	0	-1	1
Simplicity of Design	1	1	-1	0
Handling	2	1	1	1
Results		3	5	7

2.4. Oxidiser and Fuel Selection

Many types of oxidiser and fuel combination options exist that are advantageous in several aspects, depending on the type that is used. For instance, for oxidisers, Nitrogen Tetroxide (NTO), Nitric Acid, Red Fuming Nitric Acid (RFNA), certain fluorine compounds, and many more have been utilised as storable liquids in space propulsion [22]. In combination with these oxidiser types, certain fuels such as hydrazine are considered to have the highest performance in thrust and are also considered hypergolic as well, which the properties and advantages are explained in subsection 2.2.5 [23].

However, despite the advantages of using these propellant combinations, there are severe drawbacks as well. The main disadvantage is that these propellant combinations are mostly referred to as toxic chemicals which bring hazards to the environment and hence, to human life. Taking into account these facts, the space industry, institutions, and researchers all around the globe are striving to find solutions that are green, thus friendly to the environment, meaning emitting less hazardous chemicals. Not only are they looking for green propellant combination options, but they also looking for systems that can perform similarly to the traditional solutions. These green solutions can also lead to less cost of the space system due to them being easier to handle and thus leading to fewer safety precautions and systems required.

Out of the vast majority of green oxidiser options being investigated recently, High Test Peroxide (HTP), or in other words, Hydrogen Peroxide has been chosen to be further investigated. This is due to its emerging interest [24], [9], [25], and its low toxicity, low irritation, low corrosivity, and low volatility. They also show high performance in space propulsion systems when used in a high concentration form, 80 % or above. HTP concentration above 80 % can be made available in the chemistry lab with equipment pre-made for a research EU project conducted by me.

Other options that were candidates for usage as a green oxidiser were Hydroxylammonium Nitrate (HAN), Ammonium Dinitramide (ADN), liquid oxygen (LOX), and Nitrous Oxide. However, HAN and ADN were discarded due to them being a mixture of several types of chemicals, including methanol, which is type of fuel. Liquid oxygen was unconsidered due to it being cryogenic and thus does not match the purpose of this thesis. Lastly, Nitrous Oxide was discarded due to it requiring pressures exceeding 50 bar, which is unfeasible to operate in the chemistry lab at Delft University of Technology [26]. Due to these reasons, the only option remaining was HTP. In Table 2.1, the comparison of the performance of several oxidisers is given as a reference.

Table 2.1: Green oxidiser performance comparison [27]

Propellant	**Density [g/cm^3]**	**Theoretical Isp [s]**	**ρIsp [s · g/cm^3]**
AF-M315E	1.47	357	377
LP1846 (HAN)	1.4	262	376
SHP163 (HAN)	1.442	254	366
HNF-based	1.4	260	354
LMP-103S (ADN)	1.24	253	313
HAN/HN-based	1.4	210	294
Hydrogen peroxide (98%)	1.431	182	260
LTHG	1.3	191	254
Hydrazine	1.01	239	241

Together with the usage of HTP, several green fuel options were considered as well. As can be seen from Table 2.2, several fuel options have comparable propulsion performances with the combination of NTO and Mono-Methyl Hydrazine (MMH), which is an alternative of normal hydrazine, and in which the two combination is also a traditional option for space propulsion. Out of all the options, ethanol and methanol is readily available in the chemistry lab at Delft University of Technology. Comparing the two options, ethanol was selected for further investigation due to the fact that it has slightly higher performance in terms of propulsion compared to methanol. Apart from the chosen ethanol, Jet A fuel will be used in the experiments of this MSc thesis as well. The details will be shown in later sections.

Table 2.2: Oxidiser/Fuel combinations and their performance [28]

Oxidizer	**Fuel**	$r_{\mathbf{opt}}$ [-]	$I_{\mathbf{sp}}^{\mathbf{vac}}$ [s]	$\rho I_{\mathbf{sp}}$ [g · s/cm^3]	T_c [K]
NTO	MMH	2.1	313.6	372.2	3314
98% H2O2	Ethanol	3.79	288.9	367.7	2761
98% H2O2	Methanol	2.81	284.3	353.9	2682
98% H2O2	1-Propanol	4.29	291.2	374.9	2798
98% H2O2	2-Propanol	4.3	290.6	372.8	2790
98% H2O2	1-Butanol	4.6	292.4	378.6	2817
98% H2O2	2-Butanol	4.61	291.9	377.9	2811
98% H2O2	t-Butanol	4.62	291.4	375.8	2804

2.5. Thermal Wire Selection

For a thermal wire ignitor system to function properly, it necessitates a heating element, typically of a material having the features of high resistance, generating heat when current passes through it. There exists a range of materials suitable for this purpose. However, when selecting the heating element, compatibility with hydrogen peroxide, resilience to high temperatures, and corrosion resistance must be taken into account due to the environment of the testing of the thesis. Broadly, heating elements fall into two categories: metal-based and ceramic/silica-based materials. The latter, however, is unconventional and thus presents greater challenges in procurement. Metal-based heating elements are typically readily accessible and commonly employed in consumer goods, thus chosen for this thesis.

There are numerous possible options for metal-based heating elements available. However, the most conventional ones used, which are nickel-chromium (Nichrome), FeCrAl alloys, and CuNi alloys were selected for further trade-off [29]. As can be seen from Figure 2.9, the three criteria, that were aforementioned as well, resistance, the ability to sustain a corrosive environment, and cost were chosen. Eventhough nichrome has the worst score in the perspective of cost, due to the resistance and corrosive criteria being the highest score, and since those are more important factors compared to the cost criterion, it was chosen as the most optimal choice for the MSc thesis. Among the numerous types, particularly Type A was chosen, which is a combination of nickel and chromium in the ratio of 80/20. The compatibility of the material with HTP is confirmed from literature [30]. It is also known that it can

resist temperatures of up to 1423 K [31]. For these reasons, nichrome was selected as the material for the heating element. The specific properties of Nichrome Type A can be found in Appendix A.

Figure 2.9: Thermal Wire Type trade-off table

Criteria	Weighting Factor	Nickel - Chromium	FeCrAl alloy	CuNi alloy
Resistance	3	1	1	-1
Corrosion	2	1	-1	1
Cost	1	-1	1	0
Results		4	2	-1

On top of the type of material chosen for the thermal wire, the gauge, and thus the diameter of the wire had to be chosen as well. For this, the wire thickness that allows the highest resistance in the chart of Appendix A was chosen, which was a 30 American Wire Gauge (AWG), which corresponds to a wire diameter of 0.25 mm and a resistance of 6.5 ohms/30cm at 20 deg C.

2.6. Chemistry of High Test Peroxide and Ethanol

In this section, the chemistry behind the thermal decomposition and ignition of Ethanol will be briefly mentioned as well as the chemical reaction of HTP and Ethanol once they come in contact in the combustion chamber of the propulsion system. The temperature conditions that the environment in which the reaction is occurring will be explained as well.

2.6.1. Thermal Decomposition of HTP

For HTP to be used as a propellant in combustion processes, either as mono- or bipropellant, the energy released through thermal decomposition is necessary. The homogeneous chemical equation of the decomposition process is presented in Equation 2.2, in which the ΔH, the change in enthalpy, is -2884.5 kJ/kg, in which the minus sign means that the reaction is exothermic [32]. As can be seen from the equation, the decomposition results in hot steam and oxygen. Out of the reaction products, 46 % in the perspective of usable oxygen content mass-wise is available, thus making it an adequate oxidiser candidate when in bipropellant propulsion systems [33]. It is also known that HTP has an elevated adiabatic decomposition temperature. In fact, 90 % concentration HTP has a value of approximately 1010 K [32], in which the value varies depending on the concentration. This value is achievable by decomposing high test peroxide at temperatures equal to or higher than 150 deg C. At this temperature, hydrogen peroxide decomposes spontaneously into water vapour and oxygen molecules.

$$2\,H_2O_2[g] \longrightarrow 2\,H_2O[g] + O_2[g] + \Delta H \tag{2.2}$$

For thermal decomposition of HTP to occur, in general, 2 types of reactions are possible. One is a heterogeneous reaction, which means that the reactants in the chemical reaction consist of two or more phases [32]. An example would be the usage of a catalyst such as a wall, catalyst bed, or reactive particles in the flow, also mentioned in subsection 2.2.6. Another type is a homogeneous reaction, which means that the reactants in the chemical reaction consist of only one phase [32]. An example would be the process of decomposing the HTP by heating the concentrated aqueous solution so that the vapour produced lies within the explosive composition range, in which continuously propagating flames are available [32].

2.6.2. Auto-ignition of Ethanol

Auto-ignition temperature is the minimum temperature at which a certain chemical can spontaneously ignite in atmospheric conditions without the need for external sources to support the process. Ethanol also has an auto-ignition temperature, which varies from sources from 365 deg C [34] to 368.8 $\pm$ 7.4 deg C [35]. At those elevated temperatures, oxidisers, in this case, HTP, will be able to thermally decompose and release oxygen as mentioned in subsection 2.6.1

2.6.3. Chemical Reaction of HTP and Ethanol

Summing up all the description above in section 2.6, once a temperature is reached in which HTP can thermally decompose and release oxygen and the Ethanol can auto-ignite, the following reaction, shown in Equation 2.3, is executed. Assuming that complete combustion is available, without any residuals remaining in the combustion chamber, the equation suggests that the products are carbon dioxide (CO_2) and vapour (H_2O). Since this process is exothermic, heat is released as well as a result.

$$\mathrm{C_2H_5OH[l] + 6\,H_2O_2[g] \longrightarrow 2\,CO_2[g] + 9\,H_2O[g] + \Delta H} \tag{2.3}$$

2.7. Auto-ignition Temperature of Numerous Fuels

Apart from the auto-ignition temperature of ethanol, presented in the section above, a list of auto-ignition temperatures of numerous types of fuels will be presented. The fuels shown here are commonly used types of fuels in rocket or space engines or potential fuels that are under investigation and is expected to be used in the near future in aerospace applications.

Table 2.3: Auto-ignition temperature of numerous fuels

Type	Temperature [deg C]
Ethanol	365
Jet A fuel	210
Kerosene(RP1)	220
MMH	196
UDMH	248
Liquid Hydrogen (LH2)	571
Liquid Methane	540

2.8. Piezoelectric Disc

This section will discuss the features and functionality of a piezoelectric disc. The reason for this will be clear in chapter 4. A piezoelectric disc is a device that enables atomisation of liquids to different droplet sizes, often known as mists, depending on the Equation 2.4 [36], where κ is a proportionality constant, found to be 0.34 and F is the frequency of the piezoelectric disc. Using this formula, a disc with a vibration frequency of 113000 Hz would have a droplet size of 8.652 μm. The flow rate of the disc is 0.025mL/s. Having a droplet size this small is advantageous in combustion experiments due to the surface area to volume ratio of the interested liquid is increases, which leads to efficient chemical reactions. A note has to be taken that in practical-size rocket or space propulsion systems, the aim is to atomise the liquid injected into the combustion chamber for the same reason.

$$D_{50} = \kappa \cdot \lambda = \kappa \cdot (\frac{8 \cdot \pi \cdot \sigma}{\rho \cdot F^2})^(\frac{1}{3}) \tag{2.4}$$

In Figure 2.10 and Figure 2.11, the actual figure of a piezoelectric disc together with a microcontroller and a schematic of a piezoelectric disc is shown, respectively. As the piezoelectric actuator (PZT) vibrates, the metal plate inside will vibrate as well with the same frequency. If a liquid is injected on the opposite side of the metal plate and when it vibrates, droplets of liquids will be sprayed out through the meshes on the metal plate by breaking the surface tension of the liquid.

Figure 2.10: Piezoelectric Disc and Microcontroller Picture

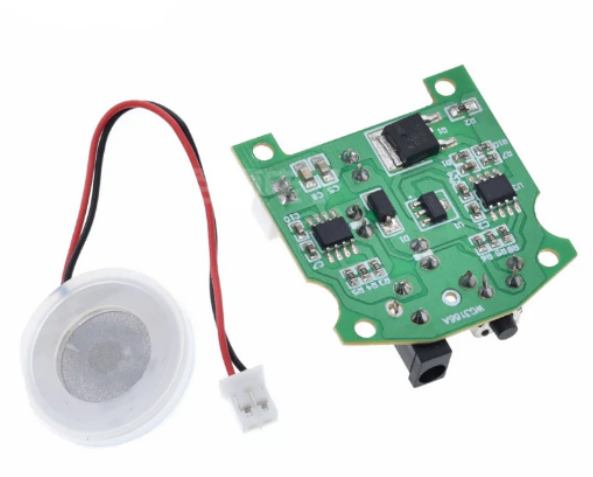

Figure 2.11: Piezoelectric Disc Schematic [37]

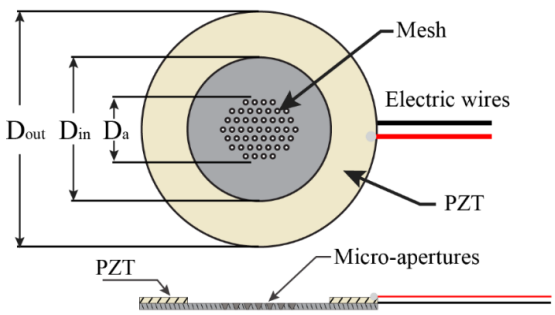

2.9. Conclusion of the Literature Study

In chapter 2, different types of ignitor systems have been investigated and published in the past along with a trade-off table to motivate why a thermal wire ignitor system must be chosen for the Nyx Earth propulsion system, the Exploration Company, Germany. It possesses the advantage of having a relatively simple structure, thus small dry mass, and therefore low cost and high reliability. However, drawbacks exist as well in which the application is mostly restricted to low-thrust applications or small propulsion systems. This would be problematic if the outcome of this Master's thesis were to be applied to those heavy propulsion systems. On top of that, the TRL is still considered low, and therefore in-depth investigation must be conducted to increase its reliability and to be used widely in actual space applications.

Alongside that, the oxidiser and fuel type, the material type of the heating element and the background chemistry of the reaction of HTP and Ethanol separately, as well as when they are in contact with each other in the combustion chamber have been introduced as well. The oxidiser was chosen to be HTP and the fuel type was chosen to be ethanol. These options, in combination with each other, are known to be a green bi-propellant option, which means that it has low toxicity, low-corrosive properties and low emissions of hazardous substances to the environment. The material of the heating element was chosen to be Nichrome Type A, which is a combination of nickel and chromium in the ratio of 80/20. This is known to be able to resist high temperatures occurring during the ignition and combustion process and also to be compatible with HTP. On top of that, a 30 AWG was selected for the thickness of the wire, which corresponds to a diameter of 0.25 mm. This was able to provide the highest resistance per meter among the conventionally available wires that were able to be procured easily.

It was shown that the fuel and oxidiser must have a temperature above the auto-ignition temperature of ethanol. At the suggested temperature, it is expected that the HTP will thermally decompose and release oxygen and heat since it is an exothermic reaction process. Using the oxygen and heat released, and combined with ethanol, ignition, reaction, and thus combustion is also expected to take place to provide thrust to the spacecraft. Lastly, the features and working principle of piezoelectric discs are shown and the approximate size of the droplets of which the piezoelectric used in the actual experiment of the thesis is calculated to be 8.652 μm. A summary of the selections based on trade-offs is provided in Table 2.4.

Table 2.4: Overall selections for the design of the test setup

Type	**Decision**
Ignitor System	Thermal Wire Ignitor
Oxidiser	HTP
Fuel	Ethanol, Jet A fuel
Thermal Wire Material	Nickel-Chromium Type A
Diameter	0.25 mm (30 AWG)

3

Research Definition

Now that the thermal wire ignitor system has been chosen throughout the literature review as the most suitable option for supporting the combustion process of Ethanol and HTP in the space propulsion system as a result of the trade-off, the research objective and research questions, as well as the propulsion system requirements can be introduced in the following chapter.

3.1. Research Objectives and Questions

During this Master's thesis study, numerous experimental and numerical types of research will be conducted to propose a thermal wire ignition concept that enables an Earth space propulsion system, named Nyx, to operate, among other functions that it must possess, especially in Steady-State Firing (SSF) mode and Pulse Mode Firing (PMF), which each correspond to a self-sustained combustion and re-ignitability of the propellant, respectively. For the case of space missions, PMF is a mode in which the valve controlling the flow of the propellant is turned on and off with a specific duty cycle to precisely control the spacecraft by applying small impulses [38]. The bi-propellant system utilises High Test Peroxide (HTP) and Ethanol as oxidiser and fuel, respectively. The objective of this thesis research can be expressed with the following statement:

Main Objective of the Thesis

This research aims to design, build, and test a lab-scale ignitor system to be used for an Earth propulsion system.

Based on the research objective presented above and in order to meet the requirements of it, the following research- and sub-questions are presented, which will be answered throughout this thesis. A note has to be taken that the solution to some sub-questions has been provided in chapter 2, in which the literature study was conducted. However, they were still included in the list because the research questions shall reflect what the total thesis aims to research and the literature study phase is considered one of the main sections of the research as well. There are 3 research questions in total to answer. Under each box, several sub-questions correspond to the main research question.

Main Research Question of the Thesis 1

What are the most significant parameters that have to be considered when designing the ignitor system to be used for an Earth propulsion system?

1. Which oxidiser and fuel combination must be chosen?

2. Which ignitor system must be chosen for further development?

3. What are the most important performance parameters in which ignition of the chosen propellant together with the ignitor system occurs?

4. What are the most important variable input parameters which influence the important performance parameters?

5. Which variable input parameters influence which performance parameters and how?

6. What are the preferred and acceptable ranges of these parameters?

Main Research Question of the Thesis 2

What lab-scale test setup can be made to prove the chosen ignitor system concept?

1. What is a viable test set-up design to measure the ignition and combustion performance as a function of the variable input parameters?

2. What is the most optimal setup for the lowest power consumption possible of the system?

3. What is the optimal ignition sequence of the chosen propellant?

4. What are the testing procedures necessary for safe and efficient calibration and use of this test set-up?

Main Research Question of the Thesis 3

What is the performance of the ignitor system in terms of self-sustained combustion (SSF mode)?

1. How does the ignitor system performance change as a function of the variable input parameters in terms of self-sustained combustion?

2. What is the total power consumption of this mode?

In the initial phase of the thesis, before the research definition has been introduced, a literature study has been conducted to get familiar with the variety of ignition system concepts existing. This phase has also supported motivating why a thermal ignitor is the most suitable system that can meet the mission requirements successfully as well as reasons for deciding on certain components or systems for the test setup. Subsequently, a test setup will be developed to investigate the ignition system further with experiments, thus resulting in practical data. The data will be used to answer the research and sub-questions presented above. Simultaneously, a multiphysics computer simulation will be performed using COMSOL, to validate the experiment results partially by comparing the experimental results with the simulated model results.

3.2. Propulsion System Requirements

One of the most important factors to take into consideration throughout the whole research process is the propulsion system requirement determination. The company, the Exploration Company, Germany, has provided a list of key requirements that the Earth propulsion system, Nyx, must fulfill, which will presented in the following.

- **COM-REQ-01:** The propulsion system shall have 20 thrusters.
- **COM-REQ-02:** Each thruster of the system shall have a thrust of 200 N.
- **COM-REQ-03:** The number of thrusters running in parallel shall not exceed 12.
- **COM-REQ-04:** The number of thrusters ignited simultaneously shall not exceed 4.

- **COM-REQ-05:** The oxidizer of the system shall be HTP.
- **COM-REQ-06:** The concentration of the oxidizer of the system shall be between 90 % to 98 %.
- **COM-REQ-07:** The fuel of the system shall be ethanol.
- **COM-REQ-08:** The system shall be able to operate in Pulse Mode Firing (PMF).
- **COM-REQ-09:** The on-time of the system PMF shall be a minimum of 50 ms.
- **COM-REQ-10:** The number of pulses of the system shall be at least 5000.
- **COM-REQ-11:** The commanding frequency of the system shall be 10 Hz.
- **COM-REQ-12:** The duty cycle of the system shall be 50 %.
- **COM-REQ-13:** The system shall be operated in Steady-State Firing (SSF).
- **COM-REQ-14:** The system shall have a maximum on-time of at least 20 min.
- **COM-REQ-15:** The system's combustion chamber temperature control shall be done by film cooling.
- **COM-REQ-16:** The system's combustion chamber temperature control shall be done using HTP.
- **COM-REQ-17:** The system's specific impulse shall be at least 300 s.
- **COM-REQ-18:** The system thrust time to 90 % shall not exceed 35 ms.
- **COM-REQ-19:** The system thrust shut-down time must not exceed 35 ms.

However, since the actual experiment is done on a lab scale, and thus a test setup would be made on a smaller scale compared to the actual propulsion engine or, for instance, a hot static fire test, i.e. a feasibility test is done in this Master's thesis, requirements will be adjusted to match the experiment environment. The adjusted requirements are shown in the following.

- **TEST-REQ-01:** The oxidiser of the system shall be HTP.
- **TEST-REQ-02:** The concentration of the oxidiser of the system shall be between 90 % to 98 %.
- **TEST-REQ-03:** The fuel of the system shall be ethanol.
- **TEST-REQ-04:** The system shall be able to operate in Pulse Mode Firing (PMF).
- **TEST-REQ-05:** The on-time of the system PMF shall be a minimum of 50 ms.
- **TEST-REQ-06:** The number of pulses of the system shall be at least 5.
- **TEST-REQ-07:** The commanding frequency of the system shall be 10 Hz.
- **TEST-REQ-08:** The duty cycle of the system shall be 50 %.
- **TEST-REQ-09:** The system shall be operated in Steady-State Firing (SSF).
- **TEST-REQ-10:** The system shall have a maximum on-time of at least 20 min.
- **TEST-REQ-11:** The system thrust time to 90 % shall not exceed 35 ms.
- **TEST-REQ-12:** The system thrust shut-down time must not exceed 35 ms.
- **TEST-REQ-13:** The cost of the setup shall not exceed 500 EUR.

- **TEST-REQ-14:** The power consumption shall not exceed 30 W.

Out of the adjusted test setup requirements presented above, most of them are the same as the requirements provided by the company. However, **TEST-REQ-06** was adjusted from 5000 to 5 number of pulses due to the test being conducted on a lab scale and not an actual propulsion system. It was considered sufficient with this requirement to prove that PMF is available with the chosen ignitor system. **TEST-REQ-13:** was a requirement added by referring to the literature study made regarding the selection of a heating element in the ignition system in section 2.5. A note has to be taken that eventhough the material type will vary the overall power consumption and lifespan of the system, only one type of material was chosen due to the purpose of the thesis being to validate the functionality of the thermal wire ignitor system itself, not on performance based on different heating element material. **TEST-REQ-14** was a requirement made due to material and facility cost constraints provided by Delft University of Technology. Lastly, **TEST-REQ-15** was added to indicate what is the range of power consumption that is expected by the ignitor system developed. The aim will be to minimise power consumption as much as possible.

3.3. Conclusion of the Research Definition

In chapter 3, the main research objective and the corresponding research questions are presented. The main research objective focused on the design, build, and testing of a lab-scale ignitor system to be used for an Earth propulsion system. The research questions and the sub-questions aim to answer what is the suitable test setup to fulfil the main objective and what results can be deduced from the results of the testing. On top of that, the propulsion system requirements provided by the Exploration Company are highlighted as well as the adjusted requirements that match the environment of the chemistry lab at Delft University of Technology. The next chapter following, chapter 4 will mention the methodologies taken to come up with a viable design for the testing as well as the details of the setup.

4

Methodology

In this chapter, the methodology of both the trial runs and the actual succeded experiments are shown. 4 trial experiments were done and after that, 3 successful experiments are introduced. In section 4.1, the 4 trial experiments methodology and there reasons of failure are presented. In section 4.2, the 3 successful experiments test setup, experiment description, and test plan are shown. Before starting the chapter, a short summary of which Trial and Experiment corresponds to which experiment type will be shown in Table 4.1 for clarification since the numbering of them could be confusing at first glance.

Table 4.1: Summary of trial and experiment numbering

Experiment	**Description**
Trial 1	3-neck beaker (pre- and main- combustion chamber)
Trial 2	3-neck beaker side neck (0-degree injector head)
Trial 3	3-neck beaker side neck (10-degree injector head)
Trial 4	Condenser (10-degree injector head)
Experiment 1	3-neck beaker side neck (HTP temperature)
Experiment 2	Round-bottom plate (contact of NiCr mesh with fuel and oxidiser)
Experiment 3	Vial (closed environment ignition)

4.1. Test Setup for Trials

When designing and building the test setup, a few points have to be taken into account. The setup shall be built accurately in order to allow the results produced to be as accurate and repeatable as possible. On top of that, modifications to the setup must be available easily, i.e. modularity must be present, to allow certain variations in the design. Most significant is the safety regarding the test setup. This must be taken into consideration both for the personnel involved as well as for the equipment and instruments that are utilised during the experiment. Lastly, the physical and chemical behaviour of the pre- and post-ignition process must be observed clearly throughout the test to meet the main objective of the thesis, which is to design, build, and test a lab-scale ignitor system.

Even after trying to take all the above considerations into account and striving to build a robust test setup, the first designed setup failed to function properly. This fact shows that making a self-build test setup is complicated and every small detail of the design has to be reflected on. In this section, the test setup which failed in deducing demanded results will be presented. A total of 4 trials were done in total.

4.1.1. Trial 1

The equipment and liquid for fuel and oxidiser used for the test setup Trial 1 are listed in the following along with their features to provide further clarification.

- **3-Neck Beaker:** This was chosen to be used as one of the necks could represent the pre-chamber being used in order to initially decompose some amount of HTP. The pre-chamber is depicted as red in Figure 4.3. After the decomposition of HTP has happened, the additional HTP and ethanol injected can meet in the main combustion chamber, depicted as blue in Figure 4.3. Also shown in the schematic is a third unused neck. This was done on purpose to avoid pressure build-up and allowing the exhaust gases resulting from the combustion process to escape during the experiment. This was done for safety reasons and to prevent incidents from occurring during the chemical process.

- **Piezoelectric Disc (0.025mL/s flow rate) and micro-controller:** This is used to inject atomised, also known as mist, liquid into the glass chamber. The liquid in this case will be either HTP or ethanol. The amount of liquid injected can not determined by the piezoelectric disc itself. It can only be done by adjusting the amount of liquid fed to the disc. All of the discs operate together with a microcontroller. Once you inject liquid into the disc and turn on the switch button, the liquid is injected into a mist form in the glass chamber. More details about piezoelectric discs and their working mechanism are presented in section 2.8.

- **Injector:** The injectors used to place the piezoelectric discs and to support the injection of the liquid were 3D printed and the material used was Polylactic Acid (PLA). The two liquid mists being injected will have an angle of 0 deg, which means that no impingement of the liquid will be present. It can fit a maximum of 2 discs. The figure of example injector heads used during the experiments is shown in Figure 4.1. The one on the very left is a 10 deg injector, and the middle and last one are both 0 deg injectors, with the middle one only able to inject one liquid and the last one capable of injecting a maximum of two liquid types.

- **Syringe:** This was used to inject the desired amount (maximum 1mL) of HTP and Ethanol into the piezoelectric disc.

- **Glass Shutter of the Fumehood:** Since the experiment was done in a fumehood, the glass shutter was used for safety purposes, in case of emergency. Also, since the shutter is transparent glass, it provided a clear view of the ignition and combustion process of the experiment both for the human eye and cameras.

- **HTP:** HTP was obtained by a self-made hydrogen peroxide concentration setup. The setup is shown in Figure 4.2. Regulated inert nitrogen gas is injected (using the green hose in the figure) on the surface of 30% concentration hydrogen peroxide, available in the chemistry laboratory at Delft University of Technology. This gas will allow water molecules to escape the hydrogen peroxide solution and will lead to the formation of highly concentrated hydrogen peroxide, also known as HTP. A magnetic stirrer and a plate, also shown in Figure 4.2 were added as well with the purpose of making the hydrogen peroxide homogeneous which thus makes the concentration process faster. In order to concentrate the hydrogen peroxide up to 90%, it took approximately 60 - 70 hours.

- **Ethanol:** Pure ethanol was available from the chemistry lab at Delft University of Technology.

- **NiCr Wire (Type A):** In order to wound a coil around the outside of the pre-chamber to support the decomposition of the HTP, Type A NiCr wire was used, which has a thickness of 0.25mm. The motivation for choosing this configuration is given in section 2.5. The 2 ends of the wires are connected to a power supply to supply power, and thus heat to the wires.

- **NiCr Mesh:** A 45 mesh configuration was used during the experiments. This means that one side of the square shaper of the mesh is 0.354mm. The mesh also is made out of Type A NiCr wire, which has a thickness of 0.25mm. The 16 mesh represents a coarse mesh, and the 45 mesh represents a fine mesh. 30mm from the entrance of the pre-chamber, there are 2 holes drilled opposite to each other. Through these holes, the mesh is placed where it can also be connected to the power supply to provide power, and thus heat to the mesh.

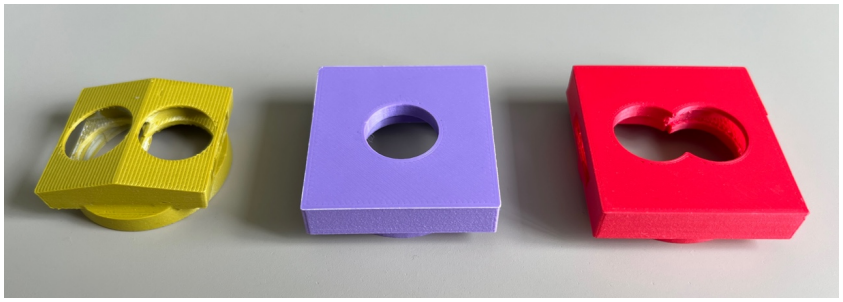

Figure 4.1: Example of injector heads used

Figure 4.2: Self-made Hydrogen Peroxide Concentration Setup

In order to record, process the data, and produce images and videos of the whole test procedures and results, especially the ignition and combustion phenomena, numerous instruments are used, which are listed in the following along with their features as well.

- **High-speed (HS) Camera:** This camera is used mostly to capture the phenomena that occur abruptly during the test, such as the flames produced during the ignition and combustion process. The one available in the aerodynamics laboratory at TU Delft is the Photron FASTCAM MINI AX100 high-speed camera with a monochrome sensor that is capable of recording up to 4000 frames per second and has a maximum resolution of 1024 by 1024 pixels. The data sheet of the high-speed camera is in Appendix B.

- **Smartphone Camera:** In order to capture the results in colour along with the high-speed camera, a smartphone camera was used.

- **High-lumen Light Source:** In order for the cameras to have a more crystal clear observance of the results, a high-lumen light source was used as well. The light was focused on the combustion chamber, where most of the physical and chemical reactions are predicted to take place. The data sheet of the high-lumen light sources is in Appendix G.

- **Computer:** To track and record all the figures and videos of the high-speed camera, a computer available in the lab is used. The high-speed camera will be connected to the computer with an

Ethernet cable.

- **Direct Current (DC) Power Supply:** During the test, several thermal wires will be applied in various locations on the test setup to provide support in the ignition of the fuel and oxidiser. In order for the thermal wires to heat up, a certain amount of voltage, and thus, power has to be applied to them by connecting the power supply to the wires using banana plug-clipper wires. This is where the power supply comes into use.

The schematic of the experiment using the 3-neck beaker and its main components are shown in Figure 4.3. In this figure, the red box represents the pre-chamber and the blue part, which is the round part of the 3-neck beaker, represents the main combustion chamber. A note has to be taken that not all connections of the wires and the instruments have been done in the schematic due to the clarity of the figure. The figure of the piezoelectric disc applied, the pre-chamber, the pre-and main-chamber, as well as the whole test setup is shown in Figure 4.4a, Figure 4.4b, Figure 4.5a, and Figure 4.5b, respectively. The red injector in Figure 4.4a has two piezoelectric discs placed and the purple one in Figure 4.4b has one disc placed. As can be seen from Figure 4.5b, the whole setup is placed inside a fumehood in order to extinguish the flames as fast as possible in case a fire occurs. There is also a glass shutter of the fumehood presented to provide extra safety of the experiment.

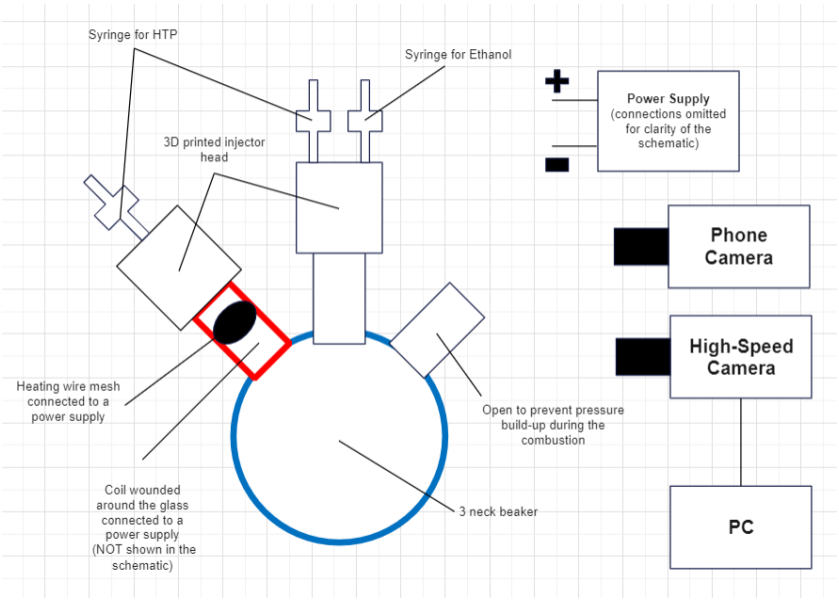

Figure 4.3: Schematic of the 3-neck beaker test setup

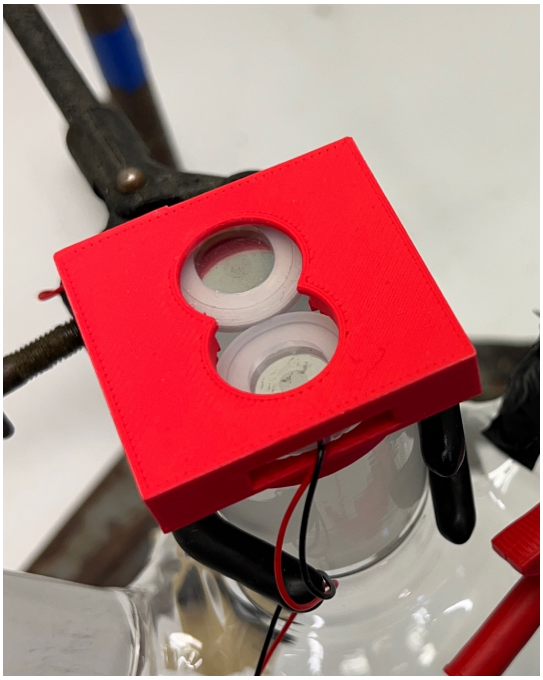

(a) Figure (a)

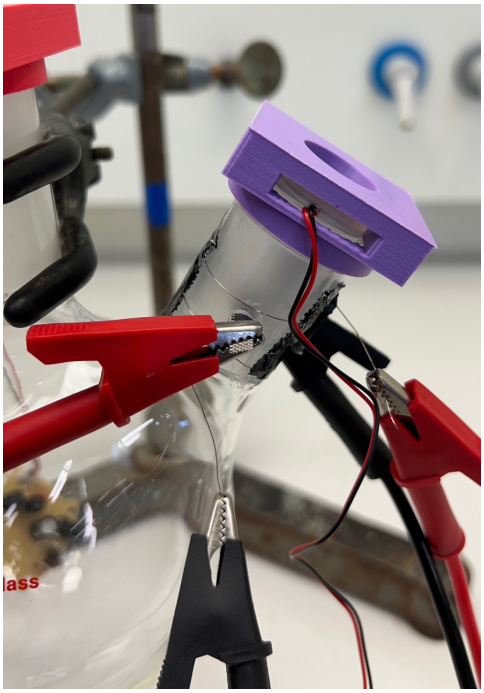

(b) Figure (b)

Figure 4.4: Figure of the piezoelectric disc mounted (a) and Figure of the pre-chamber (b)

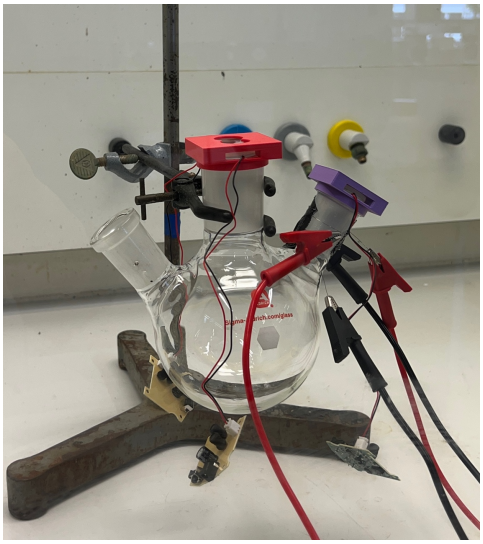

(a) Figure (a)

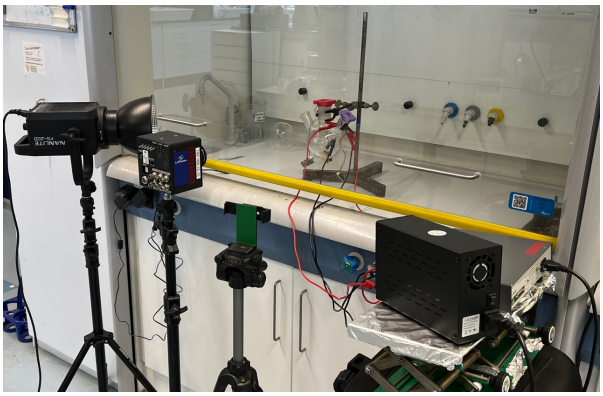

(b) Figure (b)

Figure 4.5: Figure of the pre- + main-chamber (a) and Figure of the whole test setup (b)

Eventhough the first setup was built robustly and with caution, in the end, it was not able to give valid results which match the objection of this thesis. In order words, ignition was not occurring at all in the main combustion chamber. Several causes exist, but the main one was that since the 3-neck beaker has a large volume, and compared to that, the amount of HTP and ethanol mist injected in is too less (approximately 1 ml, due to regulations in the chemistry lab), the mists were not able to completely come into contact with each other in the main combustion chamber. In addition to that, eventhough some amounts were able to come into contact with each other, due to the temperature decrease of the decomposed HTP (again, because of the too large volume of the 3-neck beaker) auto-ignition

temperature of ethanol (approximately 365 deg C) was not able to be reached and therefore, this setup resulted in a failure and modifications in the setup had to be made.

4.1.2. Trial 2 and 3

The equipment and liquid for fuel and oxidiser used for the test setup Trial 2 and 3 are listed in the following along with their features to provide further clarification. A note has to be taken that features that are the same as the equipment used in Trial 1 will only be mentioned with no further description. The same applies to the other trials introduced as well in this chapter.

- **3-Neck Beaker:** Eventhough the Trial 1 experiment test setup resulted in a failure, not all of it was scraped. One of the two side necks, which was used as the pre-chamber in Trial 1, is partially used for experiments conducted in Trial 2 and 3. The schematic of how this part is being used is shown in Figure 4.6.
- **Piezoelectric Disc (0.025mL/s flow rate) and micro-controller**
- **Injector:** In addition to the 0 deg injector, for Trial 3, a 10 deg angle injector heat would be used to inject the mist of the two liquids in the glass chamber. This will allow impingement to occur. The angle of 10 deg was found to be the most optimal number based on [10]. This was the best option that resulted in a stable combustion flame.
- **Syringe**
- **Glass Shutter of the Fumehood**
- **HTP**
- **Ethanol**
- **Jet A fuel:** Jet A fuel was available from the chemistry lab at Delft University of Technology.
- **NiCr Wire (Type A)**
- **NiCr Mesh**

In order to record, process the data, and produce images and videos of the whole test procedures and results, especially the ignition and combustion phenomena, numerous instruments are used, which are listed in the following along with their features as well. A note has to be taken that types of equipment that were used for Trial 1 as well will only be mentioned without further explanation. This is also applied to future descriptions of experiments as well.

- **High-speed (HS) camera**
- **Smartphone Camera**
- **High-lumen Light Source**
- **Computer**
- **Direct Current (DC) Power Supply**

The schematic of the experiment of Trial 2 and 3, which is partially reusing the pre-chamber part of Trial 1 and injecting the liquid in mist using a 0 deg angle injector head is shown in Figure 4.6. The figure for the 10-degree angle was omitted since the schematic is the exact same with the injector only being changed to a 10-degree angle one. In this figure, the yellow box shows where the experiment will take place, which was used as the pre-chamber in Trial 1. A note has to be taken that not all connections of the wires and the instruments have been done in the schematic due to the clarity of the figure. The figure of the 10 deg angle injector applied in Trial 3 is shown in Figure 4.7. The figure of the 0-degree angle applied is the same setup as the figure, with the only difference being that the injector head is

the 0-degree angle. The yellow injector in the figure has 2 slides on the sides in which a piezoelectric disc can be placed. The whole test setup is once again placed in a fumehood in order to extinguish the flames as fast as possible in case a fire occurs. There is also a glass shutter of the fumehood to provide extra safety for the experiment.

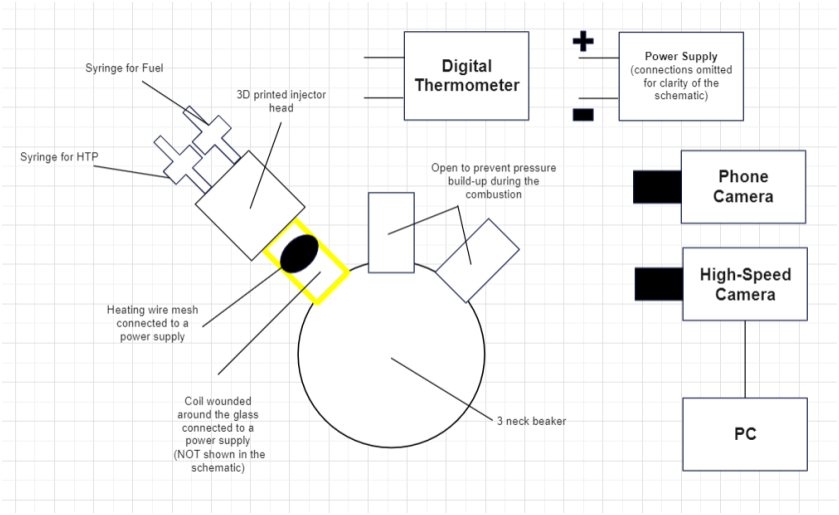

Figure 4.6: Schematic of Trial 2

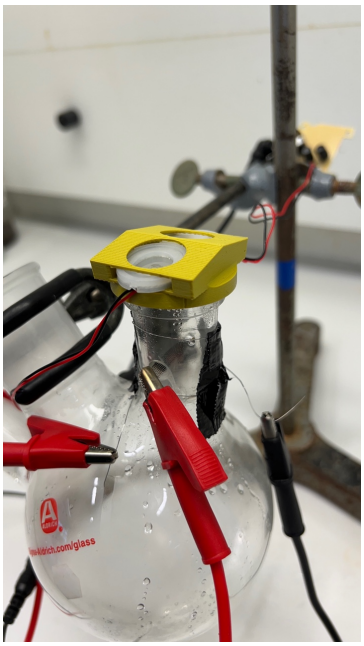

Figure 4.7: Figure of Trial 3

Eventhough the setup of Trials 2 and 3 was built again with care and was believed to work, in the end, it failed to give demanding results. There was no ignition happening on the side neck of the 3-neck beaker. It was thought to be again due to the large volume of the 3-neck beaker, a similar reason to the failure of Trial 1. The difference however with Trial 1, in addition to the fact that a 10-degree angle injector head was used to improve the impingement of the liquids, a different type of fuel was used for the experiment, Jet A fuel. This was used under the expectation that it was easier to ignite than ethanol since Jet A has a way lower auto-ignition temperature, of only 210 degrees C, compared to ethanol, which is 365 degrees C. The use of Jet A fuel alongside ethanol will be continued in future experiments

as well, whether they fail or lead to success.

4.1.3. Trial 4

The equipment and liquid for fuel and oxidiser used for the test setup Trial 4 are listed in the following.

- **Condenser:** In Trial 4, instead of a 3-neck beaker, a condenser, which is the one shown in Figure 4.8a (the left one), is used. A hole is drilled in the side of the walls using a diamond cutter drill and wires are wound around the walls of the condenser in order to provide extra heat to the setup. The bottom of the condenser is gone.
- **Piezoelectric Disc (0.025mL/s flow rate) and micro-controller**
- **Injector**
- **Syringe**
- **Glass Shutter of the Fumehood**
- **HTP**
- **Ethanol**
- **Jet A fuel**
- **NiCr Wire (Type A)**
- **NiCr Mesh**

In order to record, process the data, and produce images and videos of the whole test procedures and results, especially the ignition and combustion phenomena, numerous instruments are used, which are listed in the following along with their features as well. A note has to be taken that from this trial and on, a high-speed camera was not used due to the availability being limited. The reservation period for the equipment was limited. As future recommendation, the images of the data could be improved by using a high-speed camera to capture the behaviour and phenomena of ignition and combustion. Instead of a high-speed camera, a slow-motion camera, available in the smartphone camera software, was used, which still provided a framerate of 240, which can take videos, and thus images as accurate as 0.00417 seconds. This means that 14400 images are taken per second. The figures of the results presented in chapter 5 are also all photos from this smartphone camera slow motion video.

- **Smartphone Camera**
- **High-lumen Light Source**
- **Computer**
- **Direct Current (DC) Power Supply**

The figure of the test setup using the condenser is shown in Figure 4.8b. As can be seen from the figure, the condenser was mounted on a clamp and a 10 deg injector head was used in which two piezoelectric discs could fit. The bottom of the condenser is gone and thus can prevent pressure build-up from occurring.

(a) Figure (a)

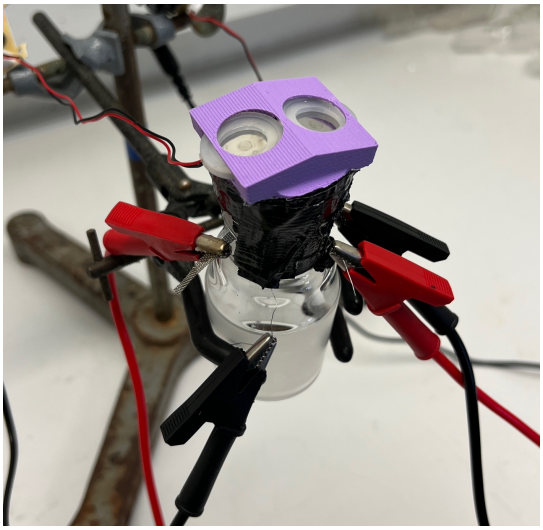

(b) Figure (b)

Figure 4.8: Figure of the condenser used (left) (a) and Figure of the whole test setup of Trial 4 (b)

Unfortunately, however, this test setup led to a failure as well. The main reason was due to lack of resources. Eventhough a lot of piezoelectric discs had been ordered numerous times, they were all damaged during trial runs, or due to the high concentration of HTP. Since future experiments had to be considered as well to capture good results, all of the discs could not be used. As future recommendations, if there would be an abundance of resources available, it would have been better and could have given good results with this setup.

4.2. Test Setup, Experiment Description, and Test Plan for Experiments Conducted

Starting from this section, the rest of the experiments lead to successful results and therefore the titles are changed to 'Experiments'. 3 experiments were done in total and the test setups, experiment description, as well as test plan will be introduced for all 3 of them.

4.2.1. Experiment 1

The equipment and liquid for fuel and oxidiser used for the test setup Experiment 1 are listed in the following.

- **3-neck beaker:** Again, the side neck of a 3-neck beaker was used in order to conduct Experiment 1. The figure of how it was used is shown in Figure 4.10.
- **Piezoelectric Disc (0.025mL/s flow rate) and micro-controller**
- **Injector**
- **Syringe**
- **Glass Shutter of the Fumehood**
- **HTP**
- **NiCr Wire (Type A)**
- **NiCr Mesh**

In order to record, process the data, and produce images and videos of the whole test procedures and

results, especially the ignition and combustion phenomena, numerous instruments are used, which are listed in the following along with their features as well, if necessary of additional explanation.

- **Smartphone Camera**
- **High-lumen Light Source**
- **Computer**
- **Direct Current (DC) Power Supply**
- **Thermocouples and Digital Thermometer:** To measure the HTP temperature resulting after contact with the heated mesh (Experiment 1), a K-type thermocouple and a corresponding digital thermometer were used. This thermocouple is in contact with the heated NiCr wire mesh. Caution has to be taken when measuring the flame temperature since the K-type thermocouple has an operation range of -200 - 1350 deg C. If the flame is bound to be over this range, the device will malfunction and be damaged. The specifications of the digital thermometer available at Delft University of Technology are in Appendix E.

During this experiment, there were some fixed parameters. A list of them is provided below.

- Using a thermal wire ignitor concept
- Using NiCr type A wires
- Thickness of the NiCr wire is 0.25mm, which corresponds to a 30 AWG wire
- HTP is used for the oxidiser
- The concentration of HTP used in the experiment is fixed to be 90 %. In real space propulsion applications, it is typical that the higher the concentration of the HTP, the better the performance. However, due to safety issues of the piezoelectric disc catching fire or due to compatibility reasons with equipment and higher HTP, 90% was chosen.
- The frequency in which the piezoelectric disc is vibrating is fixed to 113kHz, which means that the average diameter of the mist exhausted is fixed too, as shown in section 2.8.
- The length of the wire wound around the wall of the glass chamber is fixed to 30 cm
- The power applied to the wire wound around the wall is fixed to 6W.
- The distance of the mesh from the entrance of the glass chamber or vial is fixed to be 3 cm

The schematic of Experiment 1, which has the objective of measuring the resulting HTP temperature when in contact with the heated mesh is shown in Figure 4.9. In this schematic, the green box represents the pre-chamber, in which the temperature difference of HTP will be measured. A note has to be taken that not all connections of the wires and the instruments have been done in the schematic due to the clarity of the figure. The actual figure of this setup is shown in Figure 4.10, which is similar to the one presented before (Figure 4.5b) since that part of the 3-neck beaker is reused in this setup. However, an additional piece of equipment was added to the setup, which is the greenish cable in Figure 4.10. That is the K-type thermocouple which is in contact with the heated mesh and displays the resulting temperature values on a digital thermometer, connected with the thermocouple.

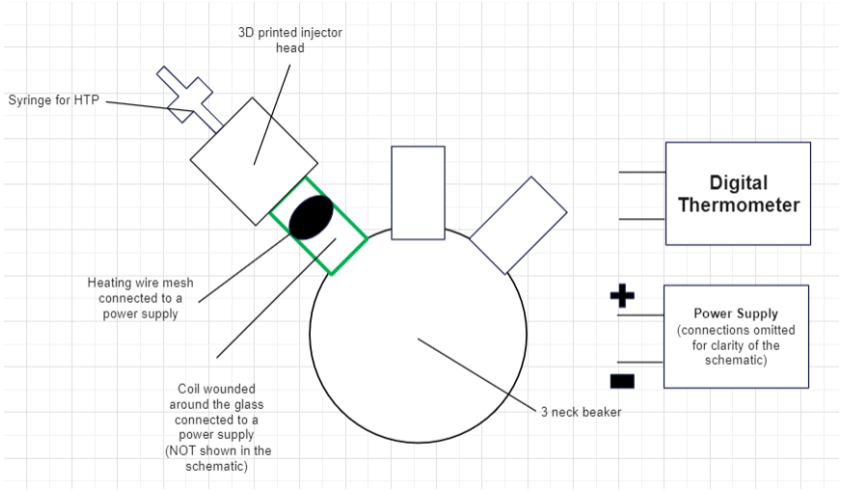

Figure 4.9: Schematic of Experiment 1

Figure 4.10: Figure of Experiment 1

The mesh and wire wounded around the glass will be heated up to the desired temperature. Using the thermocouple and a digital thermometer, the temperature of the initial heated mesh and right after the HTP liquid mist is in contact with the mesh will be measured. Since the mesh provides heat to the HTP in order for it to decompose and release heat, the mesh temperature will reduce. Subtracting the two values would provide the difference of the mesh before and after transferring heat to the hydrogen peroxide. Then using the (rearranged) heat balance equation given in Equation 4.1, where ΔT_{HTP} is the temperature difference of the hydrogen peroxide before and after being heated by the mesh, m_{mesh} is the mass of the metal mesh, c_{mesh} is the specific heat capacity of NiCr, being 420 J/kgK, ΔT_{mesh} is the temperature difference of the mesh before and after releasing heat to the hydrogen peroxide, m_{HTP} is the mass of the HTP, and c_{HTP} is the specific heat of HTP, being 2619 J/kgK, the temperature that the HTP has reached can be computed. Several power values, in the range of 5 - 20 W will be applied to the mesh and each measurement and calculation will be made.

$$\Delta T_{HTP} = \frac{m_{mesh} \cdot c_{mesh} \cdot \Delta T_{mesh}}{m_{HTP} \cdot c_{HTP}} \tag{4.1}$$

Before every batch of experiment was conducted, certain setups had to be prepared in order to allow

for a safe environment. Each will be introduced in the following.

Test Setup Assemble
The mesh shall be placed in the hole pre-drilled and a sufficient amount of it shall be sticking out in order to connect it to the power supply via the clipper wires. The coils wound around the glass chamber have to be fixed to the walls with tape robustly to prevent them from falling apart from the wall. The coils wounded shall also be connected to the power supply via a clipper wire. The injector must be tight-fit on the entrance of the glass chamber and the piezoelectric disc must be slid in with caution so that it does not fall in the glass chamber itself or the rubber wrapping the disc is damaged. The disc shall also be connected to the microcontroller. The microcontroller is connected to a wall socket via a cable and there is a switch to turn on the disc.

Smartphone Camera Operation
In the built-in camera software in a smartphone, the slow-motion video is operated. This provides a lower frame rate than the high-speed camera but is used since it can provide images in colour. Once the slow-motion video is operating, the adjustment of the focus, brightness, and exposure are all automatically done by the smartphone camera software itself. It is able to provide an additional clear slow-motion video compared to daily life videos since the high-lumen light source is operating in the background also.

Thermocouples and Digital Thermometer Operation
The tip of the K-type thermocouple is placed at a location where the measurement is required to be made. Connected to the thermocouple is the digital thermometer. The measured temperature result is shown on a digital screen.

Safety Measures
After the setup is built, the glass chamber is clamped with a metal clamp to a rod available in the chemistry lab. A rubber or cork clamp shall not be used since if HTP leaks on there on accident, there are chances of a fire occurring. Whenever a test is ongoing, the glass shutter of the fumehood must be shut in order for extra safety in case a glass breaks or fire occurs. Even when making the setup, the fumehood glass shutter is required to not go up a certain limit for caution. Despite these precautionary measures, a fire might unintendedly occur. In this case, it must be extinguished by either spraying a sufficient amount of water on the flame or by shutting down the fumehood glass shutter completely. On top of that, the power supply switch shall be turned off immediately.

Step-by-step process of Experiment 1
The number step list shown below will show the step-by-step process of the first experiment, in which the objection was to measure the temperature of the HTP once in contact with the heated-up mesh in the pre-chamber.

1. Mount the test setup on a stand and fix it tight so that it is stable.

2. From the big batch of HTP (90%) collected, extract a small amount of HTP into a smaller vial in order to prevent degradation and contamination of the HTP.

3. Plug in the power supply of the microcontroller of the piezoelectric disc and turn it on.

4. Turn on the power supply while making sure that the clipper wires are connected in pairs, with the wounded coil around the glass chamber and the Nichrome mesh.

5. Set the coil wounded around the pre-chamber to a power value of 6W.

6. Start with a power value of 20 W down to 5 W in an interval of 2.5W by adjusting the current value on the power supply with the nob on the device for the NiCr mesh.

7. Wait for a few seconds (not more than 30 seconds) until the coil wounded is able to sufficiently heat up the glass chamber.

8. Measure the temperature of the NiCr mesh using a thermocouple and digital thermometer.
9. Fill a syringe with 1mL of HTP.
10. Inject the HTP into the piezoelectric disc gently so that the HTP does not leak or overflow.
11. Measure the minimum temperature the heated NiCr mesh reaches when the HTP mist is injected.
12. When confirmed that all the liquid has been injected into the glass chamber, turn off the power supply.
13. Write the minimum temperature that the heated mesh has reached in an Excel sheet pre-made for computation later on.

4.2.2. Experiment 2

The equipment and liquid for fuel and oxidiser used for the test setup Experiment 2 are listed in the following.

- **Round-shape plate:** A round-bottom shape glass plate that can be found in the chemistry lab at Delft University of Technology, shown in Figure 4.11, was used in order to conduct Experiment 2.
- **Syringe**
- **Glass Shutter of the Fumehood**
- **HTP**
- **Ethanol**
- **Jet A fuel**
- **NiCr Mesh**

In order to record, process the data, and produce images and videos of the whole test procedures and results, especially the ignition and combustion phenomena, numerous instruments are used, which are listed in the following along with their features as well, if necessary of additional explanation.

- **Smartphone Camera**
- **High-lumen Light Source**
- **Computer**
- **Direct Current (DC) Power Supply**

During this experiment, there were some fixed parameters. A list of them is provided below.

- Using a thermal wire ignitor concept
- Using NiCr type A wires
- Thickness of the NiCr wire is 0.25mm, which corresponds to a 30 AWG wire
- HTP is used for the oxidiser
- The concentration of HTP used in the experiment is fixed to be 90 %.

The figure of the experiment conducted is shown in Figure 4.11.

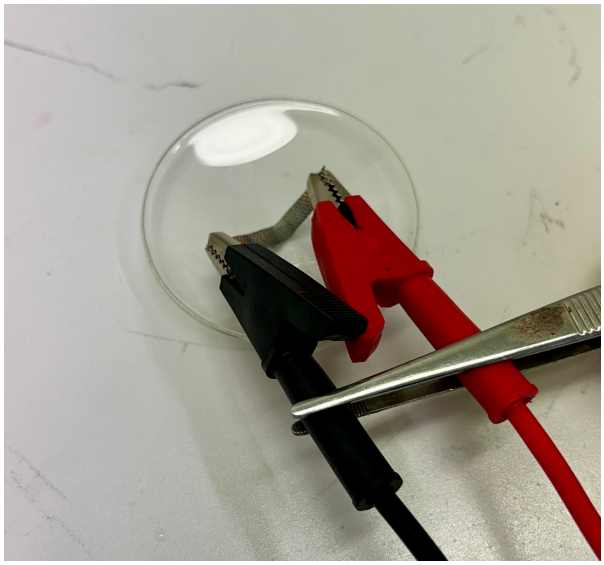

Figure 4.11: Figure of Experiment 2

In the round-bottom glass plate, 1mL each of fuel, either ethanol or Jet A fuel, and HTP will be placed prior of the experiment. Then, a heated NiCr wire mesh, in which the two ends are clipped to a cable that is connected to a DC power supply, will come in contact with the fuel and oxidiser. By adjusting the power values and contacting the heated mesh, the minimum value of power that is available to make the combination ignite and which can result in a self-sustained combustion will be determined. Similar to the Experiment 1 description, certain setups had to be prepared which will be introduced below. If the information is the same as Experiment 1, it was not added again.

Test Setup Assemble
Since it is impossible to clamp the round-bottom glass plate due to its geometry, it shall at least be fixed to the ground of the fumehood in order to remain stable. The mesh shall be connected to the power supply via clip cables in a sufficient amount of distance in order for the heat wire mesh to have sufficient contact area with the liquid.

Smartphone Camera Operation

Safety Measures
As mentioned above, the glass plate must be fixed to the ground of the fumehood not only for accurate results but also due to safety reasons. Similarly, the fumehood glass shutter shall be closed a sufficient amount. Also, in case of an incident occurring, such as a fire, it must be extinguished immediately by either shutting the fumehood glass shutter if the fire is small or by spraying a sufficient amount of water on the plate and the DC power supply must be switched off.

Step-by-step process in Experiment 2
The number step list shown below will show the step-by-step process of Experiment 2.

1. Place the glass plate fixed to the ground of the fumehood.
2. From the big batch of HTP (90%) or either fuel (ethanol or Jet A fuel) extract a small amount of liquid into a smaller vial in order to prevent degradation and contamination of it.
3. Plug in the power supply and connect the clip wires to the two ends of the mesh to be used.
4. Turn on the power supply while making sure that the clipper wires are connected in pairs with the Nichrome mesh.
5. Start with a power value of 5 W up to 20 W in an interval of 2.5W by adjusting the current value

on the power supply with the nob on the device for the NiCr mesh.

6. Capture any ignition and combustion behaviour of the experiment.
7. When the experiment is done, turn off the DC power supply.
8. Write the observations in an Excel sheet pre-made for analysis later on.

4.2.3. Experiment 3

The equipment and liquid for fuel and oxidiser used for the test setup Experiment 3 are listed in the following.

- **Vial:** A 50mL vial will be used, which are available for use in the chemistry lab at Delft University of Technology, for Experiment 3. This vial represents the combustion chamber when compared to a real rocket or space vehicle engine. 2 holes were drilled using diamond drills at the side of the walls to place the mesh and connect it to a power supply. A note has to be taken that normally the bottom of the vial should have been cut off or at least numerous holes must have been made in order to prevent pressure build-up in the vial. However, this was not done on purpose to resemble somewhat a pressurised environment and to see the combustion behaviour of the chemicals. This has led to damage to the setup and the equipment for obvious reasons but was able to give demanding results.
- **Piezoelectric Disc (0.025mL/s flow rate) and micro-controller**
- **Injector**
- **Syringe**
- **Glass Shutter of the Fumehood**
- **HTP**
- **Ethanol**
- **Jet A fuel**
- **NiCr Wire (Type A)**
- **NiCr Mesh**

In order to record, process the data, and produce images and videos of the whole test procedures and results, especially the ignition and combustion phenomena, numerous instruments are used, which are listed in the following along with their features as well, if necessary of additional explanation.

- **Smartphone Camera**
- **High-lumen Light Source**
- **Computer**
- **Direct Current (DC) Power Supply**

During this experiment, there were some fixed parameters. A list of them is provided below.

- Using a thermal wire ignitor concept
- Using NiCr type A wires
- Thickness of the NiCr wire is 0.25mm, which corresponds to a 30 AWG wire

- HTP is used for the oxidiser
- The concentration of HTP used in the experiment is fixed to be 90 %.
- The distance of the mesh from the entrance of the glass chamber or vial is fixed to be 3 cm

The figure of the experiment conducted is shown in Figure 4.12. The vial that was used is also shown in Figure 4.8a (right).

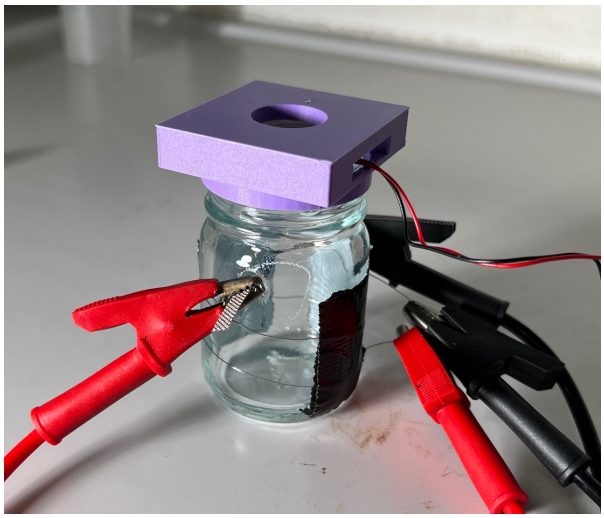

Figure 4.12: Figure of Experiment 3

In the 50mL vial, 1mL of either ethanol or Jet A will be injected. Then, through the pre-drilled holes, the NiCr mesh will be placed which will be clipped to the cables that are connected to the DC power supply. Also, 30cm of NiCr wires will be wound around the vial and fixed firmly to avoid it from falling off. Through the injector on the vial, HTP will be injected through a piezoelectric disc. By adjusting the power values of the wire mesh, the minimum value of power that is available to make the chemicals ignite will be determined. Similar to the Experiment 1 description, certain setups had to be prepared which will be introduced below. If the information is the same as Experiment 1, it was not added again.

Test Setup Assemble
Similar to Experiment 2, since it is impossible to clamp the vial due to it needing wires wound around the wall, it shall again be fixed to the ground of the fumehood in order to remain stable.

Smartphone Camera Operation

Safety Measures
As mentioned above, the vial must be fixed to the ground of the fumehood not only for accurate results but also for safety reasons. Similarly, the fumehood glass shutter shall be closed a sufficient amount. Also, in case of an incident occurring, such as a fire, it must be extinguished immediately by either shutting the fumehood glass shutter if the fire is small or by spraying a sufficient amount of water on the plate and the DC power supply must be switched off.

Step-by-step process in Experiment 3
The number step list shown below will show the step-by-step process of Experiment 3.

1. Place the vial fixed to the ground of the fumehood.
2. From the big batch of HTP (90%) or either fuel (ethanol or Jet A fuel) extract a small amount of liquid into a smaller vial in order to prevent degradation and contamination of it.

3. Plug in the power supply of the microcontroller of the piezoelectric disc and turn it on.
4. Turn on the power supply while making sure that the clipper wires are connected in pairs, with the wounded coil around the vial and the Nichrome mesh.
5. Set the coil wounded around the pre-chamber to a power value of 6W.
6. Start with a power value of 5 W up to 20 W in an interval of 2.5W by adjusting the current value on the power supply with the nob on the device for the NiCr mesh.
7. Wait for a few seconds (not more than 30 seconds) until the coil wounded is able to sufficiently heat up the glass chamber.
8. Capture any ignition and combustion behaviour of the experiment.
9. When the experiment is done, turn off the DC power supply.
10. Write the observations in an Excel sheet pre-made for analysis later on.

4.3. Conclusion of the Methodology

In chapter 4, 4 test setups of the trial experiment runs of the test as well as 3 successful experiments test setups, test plan, and experiment description are presented. Out of the 3 successful ones, Experiment 1 (the summary of the numbering of these can be found in Table 4.1) has the objective of measuring the mist HTP temperature once it is in contact with the heating mesh and is in an elevated temperature environment, due to the wound coil around the glass chamber. Experiment 2 has the objective of investigating the ignition and combustion behaviour and phenomena of selected fuel and HTP in an open environment once in contact with the heated NiCr mesh. Lastly, Experiment 3 has the objection of observing the combustion behaviour of the chosen chemicals in a closed environment by injecting HTP into the pool of fuel placed in a vial. The results of these methods introduced will be shown in the next chapter, chapter 5.

5

Results, Analysis and Observations

In this chapter, the results, analysis, and observations of the three successful Experiments conducted during this MSc thesis are presented. In section 5.1, the results of Experiment 1, which aimed to measure the temperature of the HTP after contact with the NiCr heated wire mesh are presented. In section 5.2, the results of Experiment 2, which has the objective of determining the ignition behaviour of fuel and HTP in an open environment are shown. Lastly, in section 5.3, the results of Experiment 3, which aims to determine the ignition phenomena of fuel and HTP in a closed environment are introduced.

5.1. Results of Experiment 1: Measurement of HTP temperature after contact with heated NiCr wire mesh

This section will present the results of Experiment 1, in which the objection was to measure the HTP temperature after contact with the heated NiCr wire mesh.

In order to do so, the initial mesh temperature and the final mesh temperature after the HTP had been injected through the piezoelectric disc were measured using a thermocouple and digital thermometer. A note has to be taken that, for the initial mesh temperature, the temperature shall be measured after waiting for a few seconds in order for the glass chamber to be sufficiently heated up by the coils wound around the external wall. The heated coils were able to provide an extra amount of heat to the chamber of about 80 - 100 deg C.

The result of Experiment 1 is shown in Table 5.1. In the table, before HTP injected is the temperature value reached by the wire mesh before the HTP is injected and after HTP injected is the temperature value reached by the mesh after the HTP is injected. The minimum temperature reached by the mesh wire was documented. Lastly, the Resulting HTP is the temperature the HTP reaches, which is the result of calculation using Equation 4.1. The temperature for power values between 12.5 W to 20 W are shown to have values higher than the auto-ignition temperature of ethanol, which is 365 deg C. This implies that once these power values are applied to the heated mesh, the decomposition of HTP is achieved to the right amount so that a sufficient amount of oxygen is released and thus the combination of ethanol will result in ignition.

Table 5.1: Result of Experiment 1

Power[W]	Before HTP inject [deg C]	After HTP inject [deg C]	Resulting HTP [deg C]
20	530	130	403.3
17.5	500	120	392.24
15	472	100	387.82
12.5	420	70	375.65
10	380	95	339.71
7.5	320	70	320.36
5	270	67	294.37

On top of that, the trend of the resulting HTP temperature depending on the power value applied to the heated wire mesh is shown in Figure 5.1. A note has to be taken that the power applied to the wire wound around the glass chamber was always fixed to 6 W for consistency. As can be seen from the graph, there is an annual increase in temperature value, as expected, since increasing the power value of the wire mesh definitely increases the initial temperature of the mesh as well. Eventhough only power ranges of 5 - 20 W in 2.5 W intervals were measured, an interpolation is available for the measurements in between.

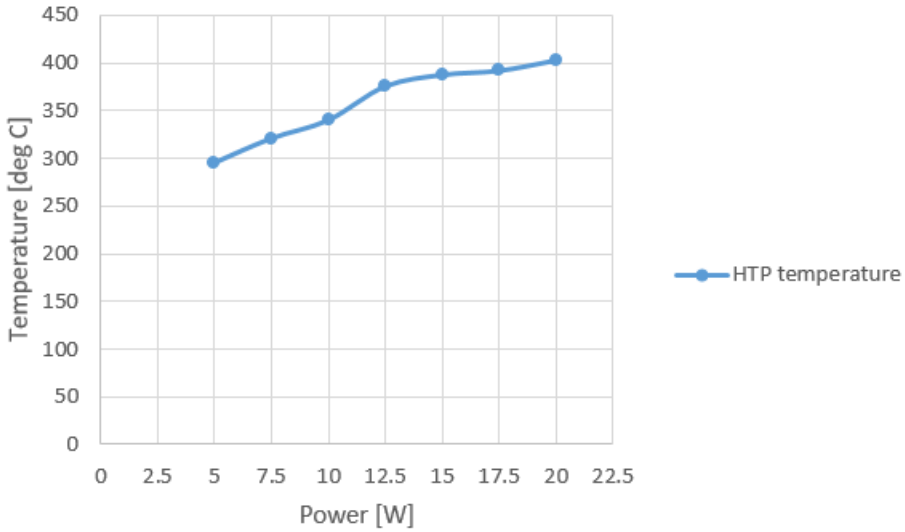

Figure 5.1: Graph showing the trend of HTP temperature depending on power value

5.2. Results of Experiment 2: Ignition behaviour of fuel and HTP in open environment

This section will present the results of Experiment 2, in which the objection was to examine the ignition behaviour of 2 different types of fuel (ethanol and Jet A fuel) and HTP as an oxidiser in an open environment. It was done by contacting a heated wire mesh in a pool of fuel and oxidiser combination placed in a round-bottom glass plate.

The results of the experiment using ethanol are presented in Table 5.2. From the table, it can seen that at power value applied to the heated wire mesh of 12.5 W was the minimum power value that was able to obtain combustion and self-sustained ignition with a nominal IDT value. The exact value of the IDT under the precise ms level was not able to be captured since a high-speed camera was not available at the time this experiment was being held. However, the IDT was about 200 ms, according to the slow-motion video taken on the smartphone. This is still a large value but this is just a estimate from a 240 fps video. If a high-speed camera were to be used, a more accurate result would have

been deduced. The figure of the ethanol ignition at the moment the combustion was achieved is shown in Figure 5.2a. Also, the figure of intensive ignition occurring when a power value of 15 W has been applied to the wire mesh with ethanol is shown in Figure 5.3. The intensive reaction implies that the amount of decomposed HTP was large and that there were a lot of oxygen molecules available to react with the molecules consisting of ethanol. This shows that eventhough 12.5 W is the minimum value in which combustion is achieved, the propellant combination contains more energy, which is related to higher power available and thrust in a real space propulsion engine when higher power is applied to the heated wire mesh. A trade-off for practical systems must be made here whether a lower power consumption of the engine or a higher thrust value is preferable.

The yellow-, orange-ish colour in the figure is the soot emissions that has been formed during the combustion process, which implies that the mixture was a fuel-rich mixture. An excess of carbon molecules is the cause of soot emissions. However, no NOx emissions can be captured since there is no nitrogen molecules contained in either ethanol nor hydrogen peroxide. This shows that the fuel and oxidiser combination investigated during this experiment is indeed a green propellant combination, as the whole objective of this MSc thesis is aiming for, apart from investigating a thermal wire mesh option for space propulsion.

Self-sustained ignition was also reached at the same power value of 12.5 W. By self-sustained here, it means that once combustion has happened, the power supply of the heated wire mesh will be turned off immediately. If the flame is still able to sustain for a sufficient amount of time, it is called a self-sustained ignition flame. A note has to be taken that a power value of 12 W was taken as well for the experiment, eventhough initially 2.5 W interval values was told to be taken because the goal of the experiment is to determine the minimum power value available for combustion and self-sustained combustion. Since 12.5 W was able to reach this, a power value that was 0.5 W below this was taken. However, this power value did not lead to combustion, but rather only a very intensive reaction. The figure of the self-sustained flame after combustion occurred for ethanol is shown in Figure 5.4a.

Table 5.2: Result of Experiment 2 for Ethanol

Power [W]	**Combustion**	**Self-sustained Ignition**	**Comments**
5	NO	NO	Small reaction
7.5	NO	NO	Reaction
10	NO	NO	Reaction
12	NO	NO	Intensive Reaction
12.5	YES	YES	Nominal IDT
15	YES	YES	Nominal IDT
17.5	YES	YES	Short IDT
20	YES	YES	Very Short IDT

The results of the experiment using Jet A fuel are presented in Table 5.3. From the table, it is examined that at a power value of 10 W, the minimum power value that was able to result in combustion was reached, with a nominal IDT value. The IDT value was approximately 200 ms also, according to the slow-motion recorded by the smartphone.

Compared to ethanol, the power value in which combustion was achieved is lower, 2.5 W difference. This is mainly due to the low auto-ignition temperature of Jet A fuel, 210 deg C, compared to ethanol, 365 deg C. The lower the auto-ignition temperature, the lower the amount of energy that needs to be provided to the chemicals in order for the reaction to occur. This also shows as a reference that different fuel types, such as the ones introduced in section 2.7, that have a lower auto-ignition temperature compared to ethanol are also able to ignite with a power value applied lower than 12.5 W. The examples shown in the table are RP1, MMH, and UDMH. However, eventhough auto-ignition temperature is the main consideration in combustion, there are a lot of side effects as well, which are different depending on the chemical type of the fuel. This has to be taken into account when experiments are conducted for different fuel and HTP combinations. The figure of the Jet A ignition the moment the combustion process occurred is shown in Figure 5.2b. Again, it can be seen that soot has been formed, and thus

it is a fuel-rich mixture with similar reasons as mentioned above for the ethanol combustion. Similarly, no NOx emissions resulted from this fuel and oxidiser combination.

Self-sustained ignition was reached, however, at a higher power value of 12.5 W. A note has to be taken again that a power value of 12 W was taken as well for the experiment for similar reasons as for the ethanol combustion explained above. For the 12 W results also, combustion was occurring, which was expected since combustion has occurred for 10 W as well. However, again, a self-sustained flame was not achievable with this power value. The figure of the self-sustained flame after combustion happened for Jet A fuel is shown in Figure 5.4b.

Table 5.3: Result of Experiment 2 for Jet A fuel

Power [W]	**Combustion**	**Self-sustained Ignition**	**Comments**
5	NO	NO	Small reaction
7.5	NO	NO	Reaction
10	YES	NO	Nominal IDT
12	YES	NO	Nominal IDT
12.5	YES	YES	Nominal IDT
15	YES	YES	Short IDT
17.5	YES	YES	Short IDT
20	YES	YES	Very Short IDT

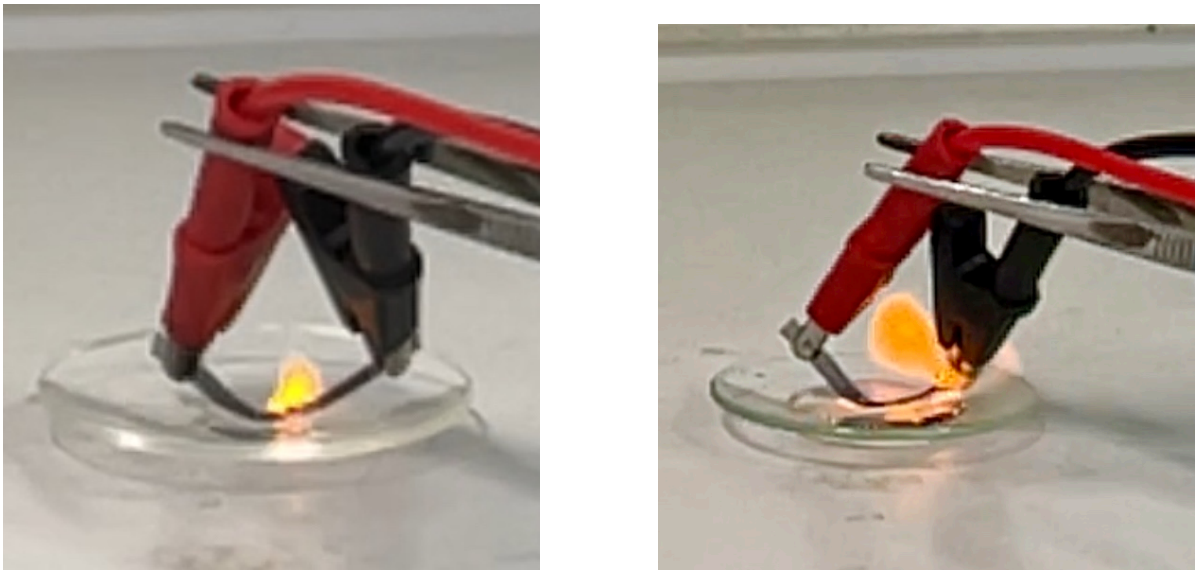

(a) Figure (a) (b) Figure (b)

Figure 5.2: Figure of ignition of ethanol at 12.5 W (a) and Figure of ignition of Jet A fuel at 10 W (b)

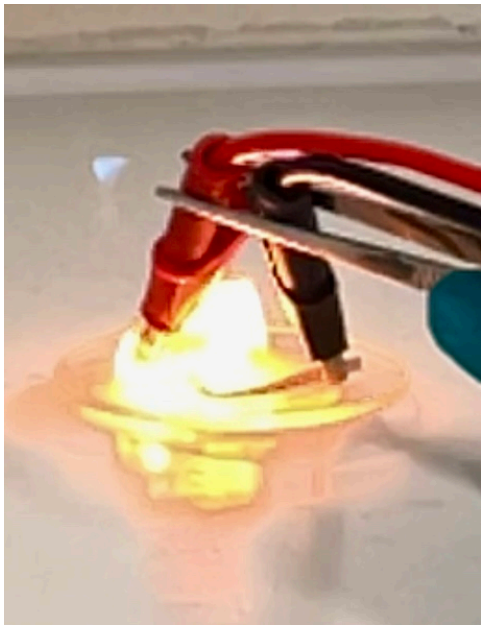

Figure 5.3: Figure of intensive ignition of ethanol at 15 W

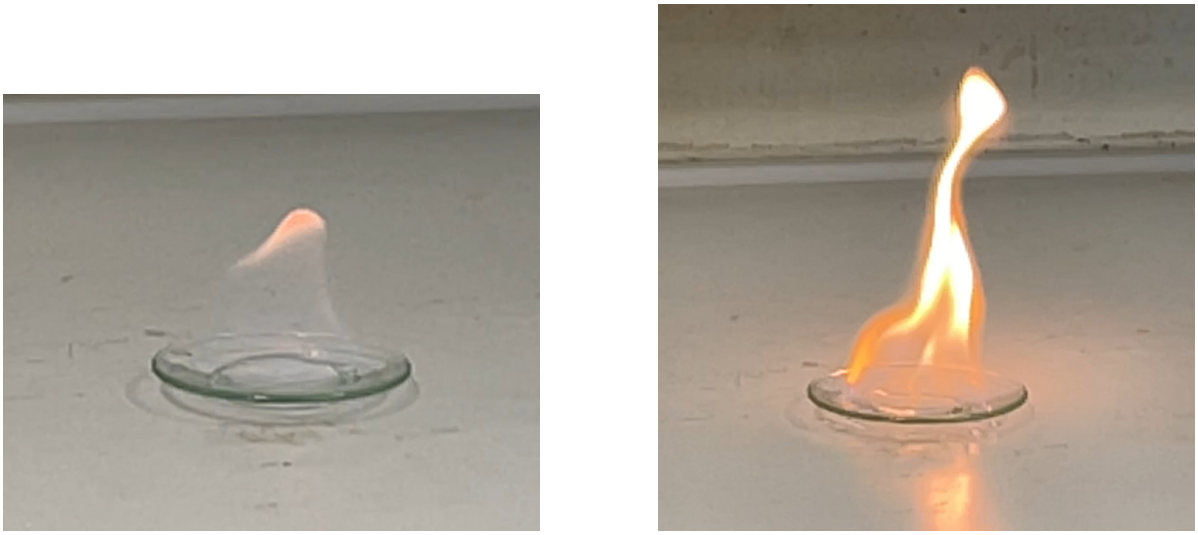

(a) Figure (a)

(b) Figure (b)

Figure 5.4: Figure of self-sustained ignition of ethanol at 12.5 W (a) and Figure of self-sustained ignition of Jet A fuel at 12.5 W (b)

The results of the experiment in this section could have been improved, i.e. combustion and self-sustained combustion could have been achieved, if the experiment was done in a glass chamber where coils could be wound around the external wall to provide extra heat, and thus energy, just like the experiment setup used in section 5.1 or the many setups that resulted in failure introduced in chapter 4.

5.3. Results of Experiment 3: Ignition behaviour of fuel and HTP in closed environment

This section will present the results of Experiment 3, in which the objective was to determine the ignition behaviour of the 2 different types of fuel (ethanol and Jet A fuel) and HTP as the oxidiser in a closed, pressurised environment. This was done by placing the fuel in a 50 mL vial and injecting a mist of HTP

to it while bypassing a heated wire mesh. The heat was added to the vial with the coils wound around it as well.

A note has been taken that for both experiments using ethanol and Jet A fuel, described below, it was expected that the whole setup, including the piezoelectric disc and injector head used, would be damaged due to it being a closed environment setup and additional heat source of the coil wound around the vial to be present as well. The additional pressure build up occurring was expected to result in an explosion, in which the pressure waves would be directed to the entrance of the beaker to escape the vial. Unfortunately, at this period of time of the experiment, even after several attempts of purchasing piezoelectric discs, there were only 2 left due to several attempts in the past as well. Therefore, once the reaction happens, and the equipments has been damaged for the ethanol batch, the next fuel type, the Jet A fuel experiment had to be carried on without any further experiments in the ethanol batch due to needing at least 1 each of piezoelectric discs for each experiment.

The results of the experiment using ethanol for Experiment 3 are presented in Table 5.4. As can be seen from the table, at a power value of 10 W, combustion was achieved with a short IDT and as expected, the piezoelectric disc was destroyed. It was interesting to see that since a closed environment experiment was conducted, as well as adding heat to the glass chamber, unlike Experiment 2, the power value of the heated mesh at which ignition happened decreased by 2.5 W. This implies that in real engine combustors, where an excessive amount of pressure is built up in the combustion chamber, where the temperature of the injected liquid is much higher, and where, except for the exit of the thruster, the chamber is tightly sealed, the amount of power and thrust produced by the engine would be massive. Also, similar to Experiment 2, the flame is yellow-, orange-ish which shows that soot was formed during the ignition process and the mixture was fuel-rich. No NOx formation can be seen here as well. The figure of the ethanol ignition at the moment the combustion occurred is shown in Figure 5.5a.

Self-sustained ignition was also reached at the same power value of 10 W. Eventhough experiments at power values slightly lower than this value was intended to be performed, due to several constraints, this could not be done. It would be better in the future to resolve this issue and to conduct experiments using different power values as well. The figure of the self-sustained flame after combustion occurred for ethanol is shown in Figure 5.6a.

Table 5.4: Result of Experiment 3 for Ethanol

Power [W]	**Combustion**	**Self-sustained Ignition**	**Comments**
5	NO	NO	Small reaction
7.5	NO	NO	Reaction
10	YES	YES	Short IDT, Piezoelectric disc damaged
12	NO	NO	-
12.5	YES	YES	-
15	YES	YES	-
17.5	YES	YES	-
20	YES	YES	-

The results of the experiment using Jet A fuel are presented in Table 5.5. From the table, it can be seen that at a power value of 7.5 W, combustion was available with short IDT. Again in this experiment, similar to ethanol, combustion occurred at a power value lower than in Experiment 2. This is due to similar reasons presented for the ethanol. The figure of the Jet A fuel ignition is shown in Figure 5.5b.

Self-sustained ignition was also reached at the same power value of 7.5 W. Similar to the ethanol case, further experiments considering the reduction of ethanol could not be made due to similar reasons. The figure of the self-sustained flame after combustion occurred for ethanol is shown in Figure 5.6b.

Table 5.5: Result of Experiment 3 for Jet A fuel

Power [W]	Combustion	Self-sustained Ignition	Comments
5	NO	NO	Small reaction
7.5	YES	YES	Short IDT, Piezoelectric disc damaged
10	N/A	N/A	-
12	N/A	N/A	-
12.5	N/A	N/A	-
15	N/A	N/A	-
17.5	N/A	N/A	-
20	N/A	N/A	-

(a) Figure (a)

(b) Figure (b)

Figure 5.5: Figure of ignition of ethanol at 10 W (a) and Figure of ignition of Jet A fuel at 7.5 W (b)

(a) Figure (a)

(b) Figure (b)

Figure 5.6: Figure of self-sustained ignition of ethanol at 10 W (a) and Figure of self-sustained ignition of Jet A fuel at 7.5 W (b)

Figure 5.7a shows the detachment of the injector head as combustion had occurred in the vial. This is due to the energy release of the flame. Figure 5.7b shows the damaged 50 mL vial slightly after the detachment of the injector head was done. The piezoelectric disc and the attached microcontroller, as can be seen in the figure, are damaged as well. This shows how dangerous a closed environment can be in a lab-scale experiment and that extra precautions have to be made and considered compared to open-environment, low-pressure test setup executions.

(a) Figure (a)

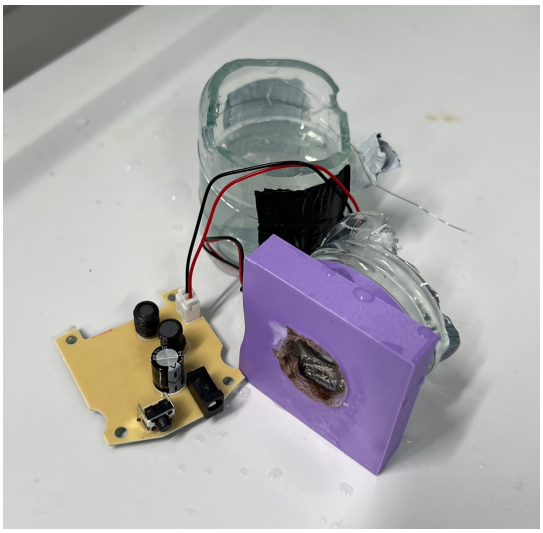

(b) Figure (b)

Figure 5.7: Figure of the detachment of the injector head due to the energy released (a) and Figure of damaged 50 mL vial after combustion (b)

5.4. Conclusion of the Results and Observations

In chapter 5, the results of 3 experiments conducted were shown. Experiment 1 showed the resulting HTP temperature once in contact with the heated NiCr wire mesh, which was calculated using Equation 4.1. The temperature of the power values of 12.5 W up to 20 W was higher than the auto-ignition temperature of ethanol, which is 365 deg C. This shows at these power values, reaction, ignition, and combustion is bound to happen with the combination of ethanol and HTP, which means that a sufficient amount of oxygen molecules can be released at these power values in order for combustion to occur.

Experiment 2 shows the ignition behaviour of 2 fuel types (ethanol and Jet A fuel) with HTP in an open environment. It was done by placing the fuel and oxidiser premixed in a glass plate and contacting them with the heated mesh while modifying the power values. Results showed that for ethanol, the minimum power in which combustion and self-sustained ignition were achieved was 12.5 W. On the other hand, for Jet A fuel, combustion was achieved at a minimum power value of 10 W and self-sustained ignition was reached at 12.5 W minimum. Also, from the colour of the flames, the types of emission particles released can be seen, which are soot due to the carbon and all the mixtures were fuel-rich for both fuels.

Experiment 3 shows the ignition behaviour of 2 fuel types (ethanol and Jet A fuel) with HTP in a closed environment. It was done by placing the fuel in a 50 mL vial and injecting a mist of HTP onto it using a piezoelectric disc to atomise the liquid. The vial was also pre-heated with the coils wound around it and a heated mesh was placed as well in the passage of the HTP through pre-drilled holes. Results showed that for ethanol, at 10 W power value, combustion and self-sustained ignition was achieved. On the other hand, for Jet A fuel, combustion and self-sustained combustion were achieved at power values of 7.5 W. These values are lower compared to Experiment 2 due to the environment difference between the two experiments, one being open and the other being closed. Lastly, similar to Experiment 2, the soot formation was captured and the mixture was seen to be fuel-rich. This experiment reflected how dangerous closed-environment experiments could be and that extra precautions have to be present when these types of experiments were to be conducted.

6

Simulation of the HTP Decomposition Chamber

In this chapter, the simulation results of the decomposition chamber of the glass chamber will be presented, which was done by using the cross-platform finite element analysis, solver and multi-physics model software, COMSOL. It is one part of the total test setup that was built in the chemistry lab at the Delft University of Technology. The data obtained from the simulation will be used to support and validate the results obtained during the actual practical experiment.

For the model, certain simplifications and assumptions will be introduced in section 6.1 in order to reduce the complexity of the model to match the timeframe of the MSc thesis. The geometry and mesh built and used will be shown in section 6.2 and the interface settings of the COMSOL software will be shown in section 6.3. Then, the simulation results and the analysis of them will be shown in section 6.4 following by the verification and sensitivity analysis of the model in section 6.5. This chapter only shows the key elements in the COMSOL model, which are the most significant settings. A more detailed document about the information of the settings is available in Appendix F, which is a report exported from the COMSOL software itself, showing the settings in detail.

6.1. Simplifications and Assumptions

The simulation done and presented in this chapter has several points for improvement in the future. Due to the timeframe of the MSc thesis, a really sophisticated model could not be built. Therefore, several simplifications and assumptions had to be made during the simulation process. In the following list, the simplifications and assumptions made during the simulation as well as a description and motivations of them will be presented.

- **Ignition Occurrence:** During the experiment, and the process of ignition and combustion of a rocket or space engine propulsion system, numerous chemical reactions that place. When taking, for instance, into consideration the fact that the chemical process is not one-step chemistry, but a multiple-step process and dissociations occur during the process, it becomes hard to simulate the results and would require more sophisticated software only taking into consideration combustion chemistry. Due to these reasons, and many more, the simulation presented in this MSc thesis focused on only whether the HTP, when being in contact with the heated mesh, was able to reach, or at least have a similar value with the auto-ignition temperature of the fuel that was used during the experiments. It is assumed that once the auto-ignition temperature is reached, ignition will occur automatically between the fuel and oxidiser.

- **No atomisation process of the liquid injected:** In the real experiment, a piezoelectric is utilised in order to atomise the liquid into small droplets in order to increase the efficiency of the com-

bustion process. However, in the simulation, the liquid will be injected into the glass chamber with a low-speed laminar flow. However, the mass flow rates will be the same as the values the piezoelectric disc injects liquid.

- **HTP decomposition chamber simulation:** In the real experiment, there is a pre-and main-combustion chamber existing. However, due to the timeframe of the thesis, only the pre-chamber of the setup will be simulated and therefore, only HTP will be injected in the glass chamber in the simulation.

- **Omit of the coil wound around the glass chamber:** In the experiment, there are two heat sources existing. One is the NiCr mesh and the other is the coil wound around the external wall of the glass chamber. However, in the simulation, the effect of heat transfer due to the heating mesh is presented for simplicity.

- **Use of 3 coils instead of a mesh configuration:** In the experiments conducted, a heated NiCr wire mesh was used to act as a thermal ignition source. After attempting to build the mesh configuration in COMSOL, however, it was impossible to do so. Therefore, 3 coils were placed at the location where the mesh was located in the experiment. This was considered a valid assumption since the 3 coils cover most of the surface area of the cylinder and thus are similar to a mesh configuration, where nearly all the surface area is covered.

6.2. Geometry and Mesh

Following the last point in the previous section, the glass chamber in the simulation will be simulated only and it will have a cylindrical shape, which is the same in the experiment as well. The length of the cylinder is 50 mm and the diameter is 26 mm. The dimensions are also determined by measuring the one used in the actual test setup. The heating coil is located 30mm from the entrance of the glass chamber and the diameter of the coil is 0.25mm which corresponds to a wire thickness of 30 AWG. The reason that coils are used instead of a mesh will be given later on. The geometry of the simulation is shown in Figure 6.1.

A note has to be taken that instead of the Nichrome Types A mesh configuration used in the experiment, 3 heating coils are used in the simulation of the COMSOL model. This was done due to the fact that applying a mesh configuration in COMSOL while applying heat to it takes too much time in order to simulate the model. Making a mesh shape itself is possible using the array function in the geometry section of the software. However, since they are all separate lines, on each line, a material will have to be specified, explained in detail in section 6.3, and also an initial temperature value would have to be applied as well, explained in detail in section 6.3. This will result in a computation running time of over 6 hours per simulation, especially for the Normal mesh, explained below.

Therefore, taking this fact into account, but still with the purpose of trying to simulate somewhat a mesh configuration, 3 heating coils were placed instead. 1 heating coil was considered insufficient since there is an abundance of area in which the liquid injected does not have contact too, which does not match with the MSc thesis objection of having a mesh configuration to heat up. All three of the coils included in the model have the same thickness of 0.25mm. However, they have different lengths due to the middle of the cylinder having the maximum diameter value and decreasing as it goes to the edge.

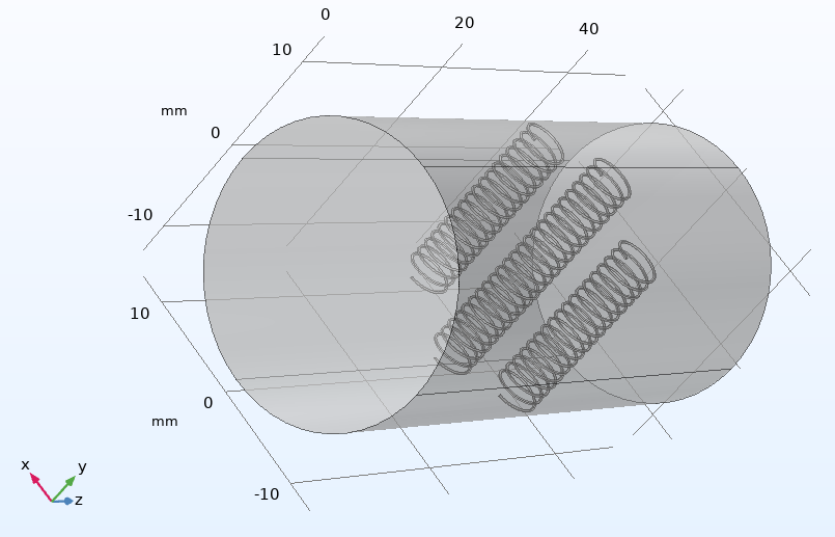

Figure 6.1: Geometry of the Simulation

In order to compute the simulation results, the geometry presented above needs a mesh configuration. The mesh that is automatically available in the COMSOL simulation is being used. The setting is named physics-controlled mesh and will adjust the mesh to the best fit with the simulation type the user is using. The mesh element used in this setting uses a hybrid mesh, consisting of a combination of tetrahedrons and hexehedrons. The user of the software gets a variety of choices of mesh quality as well, which is distinguished into 9 levels in total. They have names ranging from Extremely coarse to Extremely fine, with Normal being the quality in the middle. Due to the computer specification limitations and the running time of the computation taking too long, the Normal setting was the best quality that could be simulated, which was also selected as the final simulation mesh quality. With the Normal mesh quality setting, the number of mesh domain elements is 805383.

Two other simulations, with a different coarser mesh quality, were done in order to evaluate the sensitivity of the simulation. This will be presented in section 6.5. The mesh quality that was chosen were the Coarse and Coarser mesh quality, which are 1 and 2 levels under the Normal quality, respectively, and corresponds to a mesh domain element number of 238936, and 116605, respectively. The figure of the mesh of the Normal and Coarser mesh quality is shown in Figure 6.2a and Figure 6.2b , respectively. The image of the Coarse mesh quality is shown in Figure 6.3.

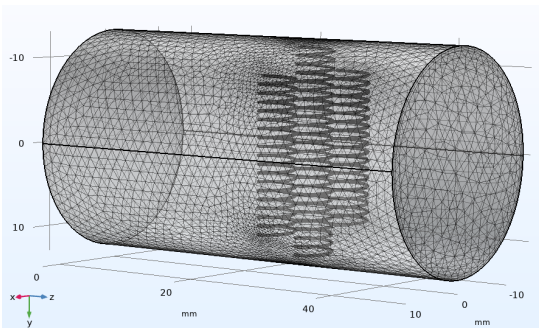

(a) Figure (a)

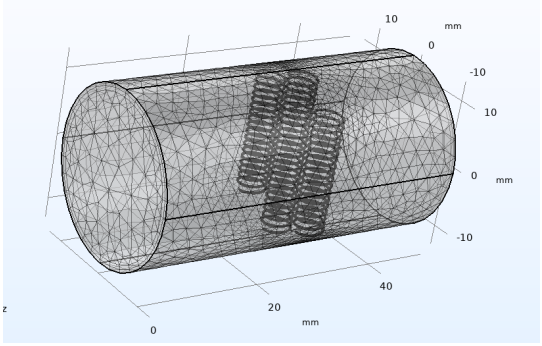

(b) Figure (b)

Figure 6.2: Mesh quality Normal (a) and Mesh quality Coarser (b)

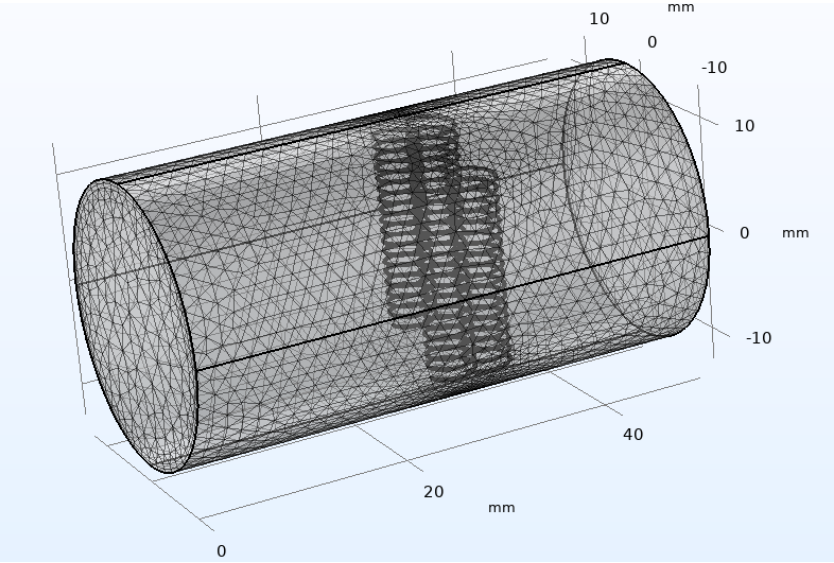

Figure 6.3: Mesh quality Coarse

6.3. COMSOL interfaces and Settings

COMSOL, since it is a multi-physics computation software, allows one to divide and select the numerous physics that the user would like to apply to the simulation. One, or multiple interfaces could be selected based on what problem the user would like to simulate. For this MSc thesis simulation, the following interfaces were chosen as shown in the following list.

- **Heat transfer in Solids and Fluids (ht):** Allows to simulate the heat transfer between the fluid (HTP) and solid (the heating coils) and the walls to the surroundings.
- **Laminar Flow (spf):** Allows to inject of a low-speed laminar flow (HTP) in the glass chamber.
- **Surface-to-Surface Radiation (rad):** Allows radiation heat transfer to be simulated at the wall.

6.3.1. Initial and Boundary Conditions

Inside the interface, the selection of initial and boundary conditions, just like any other computer simulation software, has to be determined as well. This subsection will introduce, out of the numerous types of settings being done, the main contributing initial and boundary conditions.

For the Normal mesh quality, 3 different simulations have been computed, which are when the heated coil has an input power of 20W, 15W, and 10W. All 3 of the simulations were time-dependent since the main interest of the MSc thesis experiment was about the IDT of the ignition and combustion process of the fuel and oxidiser, which shall ideally be in a split of a ms unit. A lot of numerous types of initial and boundary conditions were given to the simulation, in which the most important values will be shown in a list below.

- **Initial volume temperature of the glass chamber:** The initial volume temperature of the glass chamber before the liquid is injected must to specified before the computation can be made. In order to measure its value in the experiment, a thermocouple as well as a digital thermometer explained in section 4.1 was used. By sticking in the K-type thermocouple, the value of the temperature of the initial volume was measured to be around 230 degrees C, independent of the power input value on the heating coil. Therefore, this value was used for the simulation.
- **Initial temperature of the heating coil:** Similar to the initial volume temperature of the glass chamber, the temperature of the heating coil once the power required was input had to measured as well in order to add to the settings of the interface in COMSOL. Here, also a thermocouple

and digital thermometer explained in detail in section 4.1, were used to measure the value of the temperature. The results were 400 degrees C, 500 degrees C, and 600 degrees C, for 10W, 15W, and 20W, respectively. These temperature values were used in the simulation as the initial temperature of the heating coils right before the liquid was injected.

- **Injected laminar flow liquid temperature:** The initial temperature of the liquid injected, HTP, had to be measrured as well. This was done with a normal thermometer and the value was approximately 20 degrees C, which was used for the simulation.

- **Surrounding temperature:** The surrounding temperature of the chemistry lab had to measured as well for the interface settings. Eventhough the weather and thus the temperature of the surroundings in the chemistry lab at Delft University of Technology is always different, an average temperature of 20 degrees C was selected and used in the simulation.

- **Flow rate of the laminar flow:** The flow rate of the liquid injected in the glass chamber had to be given as well in the interface settings. As explained in section 6.1, instead of the mist flow of HTP from the piezoelectric disc, a low-speed laminar flow was assumed, but with the same flow rate as the disc produces. This had a value of 0.05mL/s, which was added to the settings of the interface.

6.3.2. Materials

After the geometry is been built, the corresponding material has to be chosen from a built-in library in COMSOL. A user can always use a self-defined material, if necessary, but the MSc thesis only focused on the existing materials in the list because those were sufficient to compute the physics. For the heating coils of this simulation, Nichrome wires were selected, which is the same as in the experiment. For the fluid, hydrogen peroxide was selected which is selected to be simulated in the pre-chamber. If the hydrogen peroxide simulated is able to reach a temperature value similar to or higher than the auto-ignition temperature of the fuel chosen, it means that ignition will occur.

Eventhough in the actual experiment, glass was used as the pre-chamber, in the COMSOL model it was assumed that a model that simulated heat dissipation was sufficient to investigate the physics behind the setup which had the advantage of being able to simplify the model even further, which matched with the scope of the MSc thesis timeframe and reduces the simulation time of the model significantly as well. A note has to be taken that, with the the computer available to be used for the simulation, for the Normal quality mesh already, without adding these sophisticated interfaces and models, took 3 hours to simulate each power value.

6.4. Simulation Results and Analysis

As explained in section 6.3, a time-dependent simulation was conducted in order to study the phenomena happening to the HTP injected in the pre-chamber. In order to do so, and the thesis is interested in a short period of time of less than 1 second, due to the IDT, a simulation in the range of 0 to 1 seconds, in an interval of 0.01 seconds was conducted. Further decreasing the interval allowed to have more results between the instant the liquid was injected and came into contact with the heating coil and reacted. However, since the computation time is already 3 hours, the interval was decided to be 0.01 seconds, which was also sufficient to investigate the physics properly. This section will present the results the COMSOL model has computed with descriptions and analysis of the results.

The results of the simulation model, after computation, show that initially, instantaneously as the liquid is injected in the chamber, it is able to reach a really high value of 589 deg C for the 20W simulation done with the Normal mesh, which is the finest mesh used for the simulation. The figure of the surface that is cut at approximately 30mm from the inlet in the x-y plane is shown in Figure 6.4.

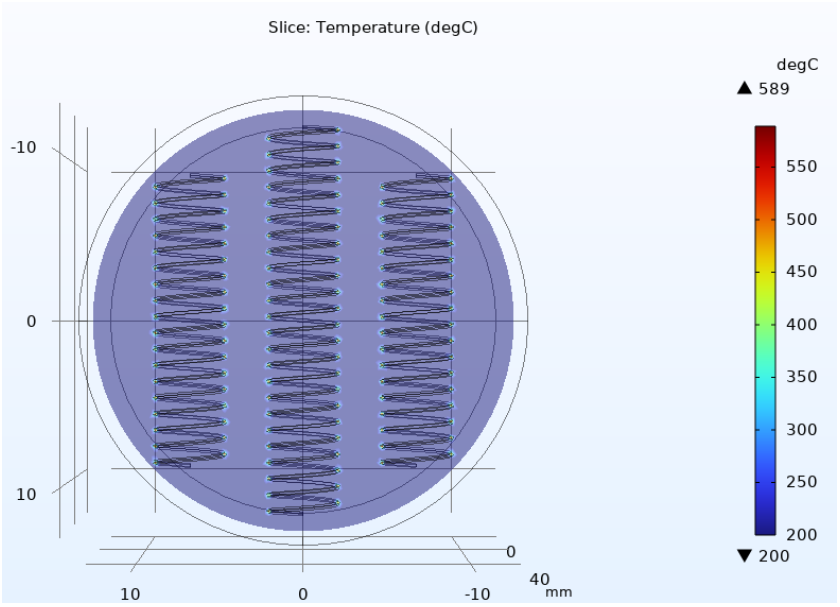

Figure 6.4: Temperature instantaneously as the liquid is injected for 20W heated coil value

However, the slope of the temperature graph is shown to decrease drastically in not only the 20W simulation but the 15W and 10W also. The graph for 20W is given in Figure 6.5. The graph for the 15W and 10W will be given later on, together with the 20W graph in order to compare. The graph shows that the initial temperature of the glass chamber, which is 230 deg C is reached again when a sufficient amount of time has passed for all three simulations. This is mainly due to the heating coil cooling down in temperature as it is in contact with the liquid. As this process proceeds, the heated coil shows expansion in area due to thermal expansion. Also, from Figure 6.6, it can be seen that even after 0.05 seconds after the liquid is injected, the maximum temperature has dropped significantly to 292 deg C. This figure again is a figure of the cylinder cut in the x-y plane at a location approximately 30 mm from the inlet. This simulation result also aligns with the experiment results shown in section 5.1. At a power value of 20 W heated wire mesh, the resulting mist HTP injected has a computed temperature value of 403.3 deg C, which is similar with the simulation results. This is also shown to have similar values for other power values (15 W and 10 W) as well, as can be seen by comparing the results from section 5.1 and the Figure 6.9.

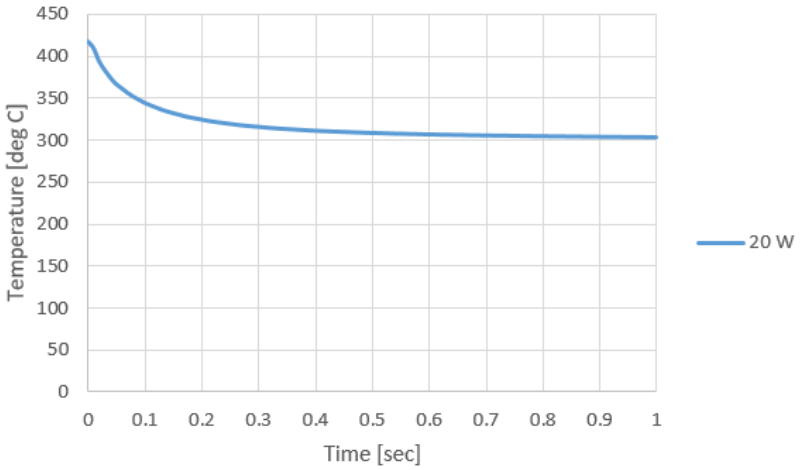

Figure 6.5: Graph of 20 W heat coil value

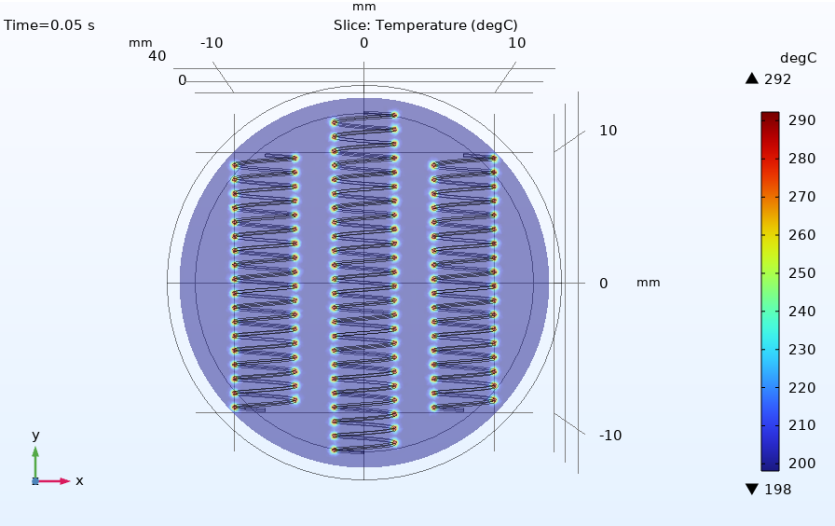

Figure 6.6: Temperature 0.05 seconds after the liquid is injected for 20 W heated coil value

6.4.1. Comparing the Three Simulation Results Depending on Power Applied to the Heating Coil

This section will discuss about the three simulation results that were conducted based on different power values applied to the heating coil placed at 30mm from the inlet. All three simulations used the Normal mesh quality configuration, which is the finest out of the three simulations conducted. As can be seen in Figure 6.7a and Figure 6.7b, which is the figure of the simulation result right after the liquid is injected in the cylindrical chamber for 15W and 10W heated coil, respectively, it can be seen that the initial temperature of both of them are high, 492 and 394 deg C, respectively. However, Figure 6.8a and Figure 6.8b shows that as a time of 0.5 seconds has passed, the temperature of the liquid near the heated coil has decreased tremendously, to a value of 271 and 248 deg C, respectively. This is shown to again be due to the heated coils being cooled as the initial room temperature liquid of HTP is in contact with the coil for some time.

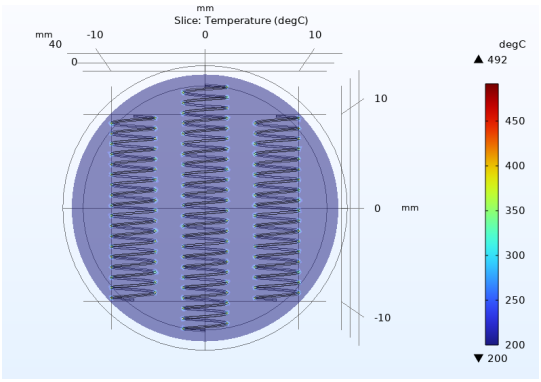

(a) Figure (a)

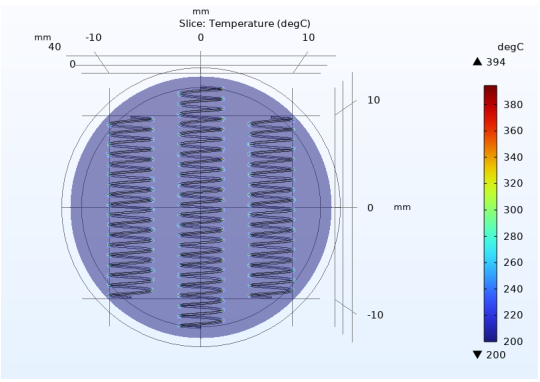

(b) Figure (b)

Figure 6.7: Temperature instantaneously as the liquid is injected for 15 W heated coil value (a) and 10 W (b)

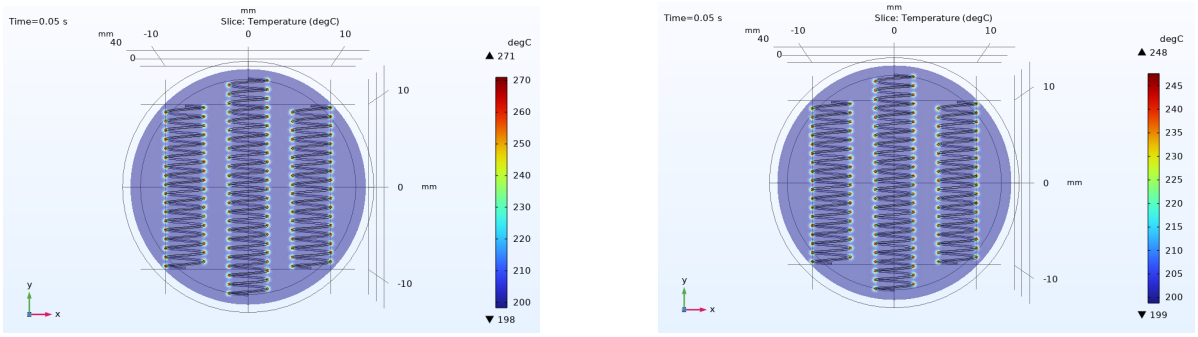

(a) Figure (a)

(b) Figure (b)

Figure 6.8: Temperature 0.05 seconds after the liquid is injected for 15 W heated coil value (a) and 10 W (b)

On top of the results above, a graph was produced by extracting the data of the temperature value change in a point that was chosen, after several attempts, to maintain the highest temperature value on the boundary of the heating coil. This value was chosen to be (x, y, z) = (0.58, 0.55, 29.76). The same coordinates were taken for all three simulations, the 20W, 15W, and 10W in order to keep consistency in the results. The graph of the temperature decrease time-dependently from the whole time range the simulation was conducted, 0 to 1 seconds in 0.01-second intervals for the three heated coil power values is shown in Figure 6.9. Together with the three graphs, the auto-ignition temperature of ethanol and Jet A fuel, which were used in the experiments as well, shown in chapter 5, is depicted as well to provide a reference value.

This simulation result also matches the result of the practical experiment using ethanol. From section 5.2 and section 5.3, it can be seen that combustion of ethanol and HTP is reached with a minimum power value applied to the heated mesh of 12.5 W and 10 W, respectively, for the open and closed environment experiment. The 12.5 W is a similar value as shown in Figure 6.9 and the 10 W resulted in ignition due to the environment of the experiment being pressurised which adds an extra amount of heat, and thus is available to heat up the HTP more compared to an open environment experiment.

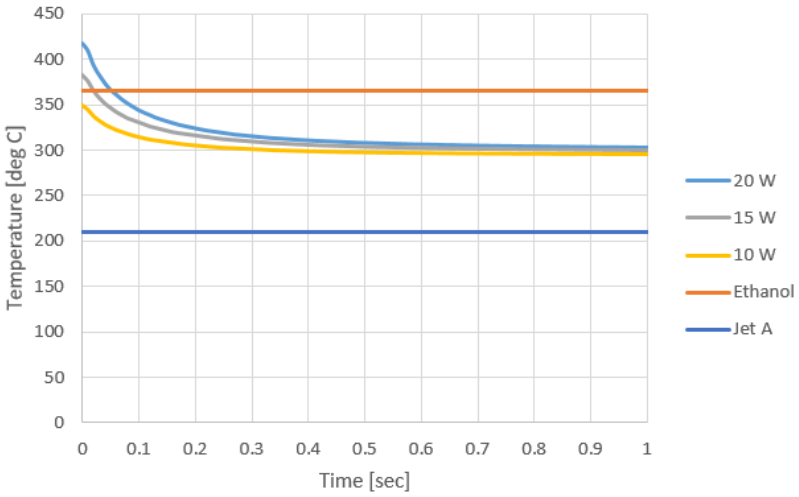

Figure 6.9: Graph comparing the 3 simulation results depending on power applied to the heating coil

6.5. Validation and Sensitivity Analysis

In order to validate the simulation results and perform a sensitivity analysis, some parameters were altered to compare with the actual model. The parameters modified were the mesh quality and the distance of the heated coils from the inlet of the cylinder. These will show proof of whether the model

built is accurate or not.

6.5.1. Mesh Sensitivity on the Results

Apart from the Normal mesh quality configuration, which was the finest option and used to present the results in the above sections, two other meshes were generated with the purpose of conducting a sensitivity analysis of the model. They are the coarse and coarser meshes, which are 1 and 2 levels coarser than the Normal mesh, and each has a domain element number of 238936 and 116605, respectively. The figure of the meshes is presented in section 6.2. The same point that was determined in subsection 6.4.1, (x, y, z) = (0.58, 0.55, 29.76), was used in order to compare the three simulation results and the same time range of 0 to 1 seconds and a stepsize of 0.01 seconds was used.

As can be seen from Figure 6.10, the Normal mesh is able to show the steep decrease in temperature the most and the Coarser mesh, which is the coarsest mesh that was simulated, was not able to capture this phenomenon. There are several reasons that can be thought of. One is due to the finer mesh being able to accurately capture the spatial temperature and the heat dissipation of the liquid and heating coil better than the coarser mesh options. Another one is due to the temporal accuracy of the simulation. A finer mesh allows the simulation process in more smaller time steps which leads to more accurate results where the steep of the heat dissipation is large. Therefore, the finer mesh is able to predict better what is the decrease in heat of the liquid as time advances. Lastly, the heat source is better represented if the mesh is finer. It can predict the heat locally more accurately and the distribution of heat around it. This is also a reason why the finer mesh can better predict the decrease in temperature of the liquid compared to the coarser mesh configurations. From this section and from Figure 6.10, we can see that the simulation is validated to have been done well.

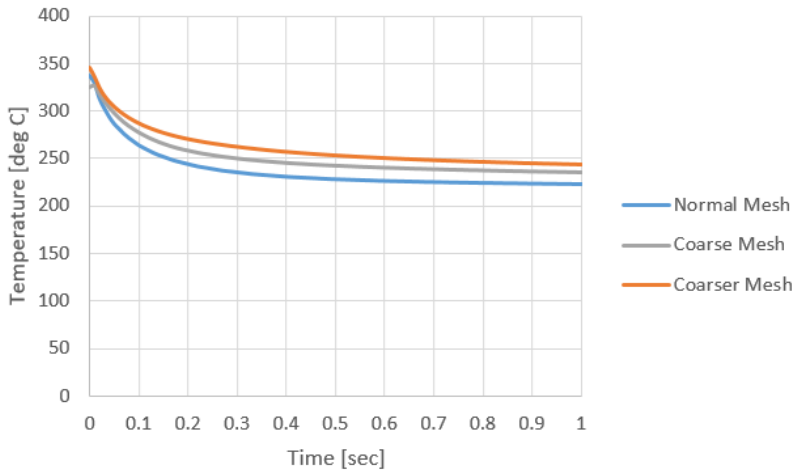

Figure 6.10: Graph comparing the 3 simulation results depending on different mesh quality

6.5.2. Dependency of the Distance of the Heated Coils on the Results

Another sensitivity analysis of the simulation was done by placing the heating source, i.e. the heating coil, at a different distance than 30mm. It will also be able to show that the distance of the heating source from the inlet of the glass chamber does not influence the ignition behaviour. In order to validate this, the same simulation of 20 W and using a Normal mesh quality was done with the only difference being the distance from the inlet to the heating source being 20mm. The same point of (x, y, z) = (0.58, 0.55, 29.76), which was determined in subsection 6.4.1, was used to show the results depending on time. As can be seen in Figure 6.11, the results of the two simulations in almost the same. They start at the same temperature at 0 seconds and end up at the initial temperature of the volume. This shows that only the residence time of the fluid injected near the heating source matters, not from what distance the fluid was injected. This is also able to validate that the simulation model was done correctly in COMSOL.

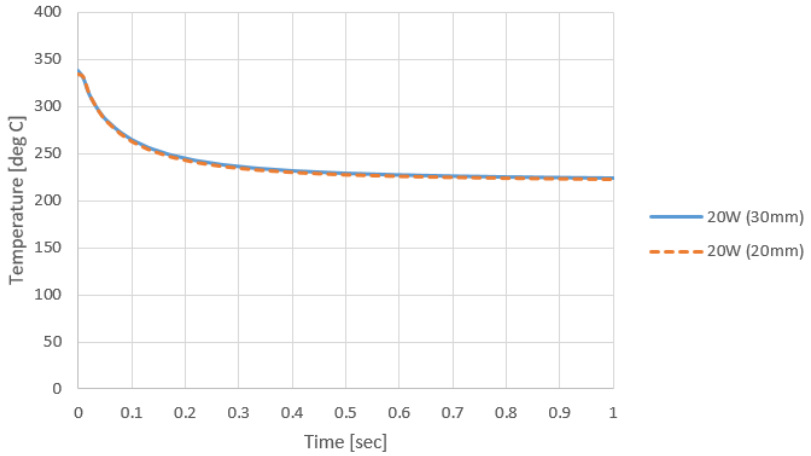

Figure 6.11: Graph comparing the 2 simulation results depending on different heating source distances from the inlet

6.6. Conclusion of the Simulation

In chapter 6, the process and results of the model for the decomposition chamber of HTP were shown using the cross-platform finite element analysis, solver and multi-physics model software COMSOL. The 5 simplifications and assumptions made while building the model were presented. Firstly, an assumption was made that ignition is bound to occur if the simulation results are equal to or higher than the auto-ignition temperature of the fuel investigated. The second simplification made was that the HTP injected in the chamber of the model will not be atomised, but would be a rather low-speed laminar flow. Also, the simplification of the model to only simulate the HTP decomposition chamber was done and the coil wound around the glass chamber's external wall was omitted as well. Lastly, the assumption of using 3 heating coils instead of a mesh configuration, which was used in the experiment, was made.

The geometry and the mesh were presented as well. There were three mesh types used during the simulation for sensitivity analysis purposes. A Mesh quality of Normal, Coarser, and Coarse was used. The Normal option is the middle quality mesh that can be chosen by the automatically generated COMSOL mesh settings, and the Coarser and Coarse correspond to 1 and 2 level coarse mesh, respectively. A mesh option higher than Normal could not be selected due to the limitation of the computer specifications used for the simulation.

After that, the COMSOL interfaces and settings chosen were presented. For the interfaces, which is the physics that the user would like to include in the model, the heat transfer in solids and fluids, laminar flow, and surface-to-surface radiation were chosen. There were several initial and boundary conditions that were selected as well. The initial volume temperature of the glass chamber, as well as the initial temperature of the heating coil depending on the power applied, the injected laminar flow liquid temperature, the surrounding temperature, and the flow rate of the laminar flow were determined and added to the COMSOL model. Lastly, the materials were shown as well.

After all the settings have been specified, the results and analysis of the simulation was made. Using the Normal mesh quality, and a heating value of 20 W, the HTP injected was shown to reach an initial temperature of 589 degrees C followed by a steep decrease in the slope of the temperature value due to the heat dissipation and cooling of the heated coils as time passed. Also, the comparison of two different power values, 15W and 10W, using the same Normal mesh quality was made. The comparison temperature values obtained from the simulation were also compared with the auto-ignition temperature of ethanol and Jet A fuel, which were the 2 fuel types used during the experiment.

Lastly, a validation and sensitivity analysis was conducted by altering the mesh quality and adjusting the distance of the heated coil from the inlet. For the former, the Coarse and Coarser Mesh were used to simulate, and the same point was taken as a reference to compare the temperature behaviour of the

HTP as time passed. Also, the distance of the heating coil was adjusted to 20 mm, in which the initial distance was 30mm. Both sensitivity analyses were able to validate the simulation results and thus it was concluded that the simulation was successful.

7

Conclusion and Recommendations

In this chapter, the conclusion and recommendations of the work conducted in this MSc thesis will be made. This thesis started off with the main objective as the following:

Main Objective of the Thesis

This research aims to design, build, and test a lab-scale ignitor system to be used for an Earth propulsion system.

At the very first, a literature study was conducted in chapter 2 in which the keywords in the statement were touched upon. Since the Earth propulsion system, mentioned in the main objective statement, is a liquid bi-propellant space propulsion system, the details of the system were described following with several ignitor systems concepts available or under development in the aerospace industry. Taking into consideration the main advantages and disadvantages of these ignitor system types, a trade-off was made, in which a thermal wire ignitor system was chosen as the most optimal type of ignition system suitable to answer the main objective.

Later on, the selection of hydrogen peroxide as oxidiser and ethanol (and Jet A fuel for reference) was motivated following with the chemistry behind the chosen chemicals. When HTP is able to reach a temperature of 150 deg C, or higher, it is able to decompose spontaneously into water vapour and oxygen molecules and releases an adiabatic decomposition temperature of around 1010 K for 90 % concentration HTP. On the other hand, ethanol has an auto-ignition temperature of 365 degrees C, meaning that at this temperature, the fuel is available to spontaneously ignite without any other ignition source. Later on in the test setup, this had to be taken into account. The thermal wire ignitor concept selected had to be able to provide this heat to the chemical combinations in order for ignition to occur.

The type of thermal wire selection, such as the material and the thickness of the wire were shown and the literature review was concluded by explaining the equipment used during the experiments conducted, a piezoelectric disc. The main feature of this equipment is the availability of atomising the liquid into micro-level droplet sizes (8.652 μm).

Now that the background knowledge necessary in order to dive deep into the thesis were presented, the research definition was introduced in chapter 3. The main objective mentioned above was introduced along with the 3 main research questions and sub-questions that were aimed to be answered together with the main objective of the MSc thesis. The main research questions were as follows:

Main Research Question of the Thesis 1

What are the most significant parameters that have to be considered when designing the ignitor system to be used for an Earth propulsion system?

Main Research Question of the Thesis 2

What lab-scale test setup can be made to prove the chosen ignitor system concept?

Main Research Question of the Thesis 3

What is the performance of the ignitor system in terms of self-sustained combustion (SSF mode)?

On top of these main research questions, the system requirement that was provided by the company, the Exploration Company, as well as the adjusted system requirements chosen to match the lab-scale test setup conducted in the chemistry lab of Delft University of Technology were presented.

With the aim of answering the main objective and the 3 research questions, several trial concepts were designed, shown in chapter 4, and at the end, 3 test setups were designed and experiment was conducted to answer the main objective and the research questions, in which the results are presented in chapter 5.

The first experiment aimed in measuring the resulting HTP temperature when it passes through a NiCr thermal wire mesh in a glass chamber where the chamber itself is heated up with a wire wound around the external wall. This experiment showed that a resulting temperature of almost 400 deg C was achievable with 20 W of power applied to the wire mesh down to a value of 294.37 deg C for 5 W of power applied. The most interesting point is at a power value of 12.5 W, in which the HTP reaches a temperature value right above the auto-ignition temperature of ethanol, 375.65 degrees C.

The second experiment aimed in investigating the ignition behaviour of the fuel and HTP in an open environment. The results showed that at 12 W of power applied to the NiCr thermal wire mesh, which was in contact with a premixed fuel and oxidiser pool this time, combustion and self-sustained ignition were achieved with a sufficiently short amount of IDT (around 200 ms). Also, at 10 W of power applied, combustion occurred with HTP and Jet A, which was a reference fuel used with the purpose of showing that fuel types that have an auto-ignition temperature lower than ethanol are able to ignite at lower power consumption values. The self-sustained ignition was obtained at power values slightly higher than this, 12.5 W.

The last experiment aimed in investigating the ignition behaviour of the fuel and HTP in a closed environment, which also serves as a pressurised system. The results showed that at 10 W, the ethanol and HTP combination was able to combust and self-sustain. Also, at a value of 7.5 W, the Jet A fuel and HTP combination were able to combust and provide a self-sustainable ignition. They both showed that in a pressurised system, lower levels of power values are required in order for the same fuel and oxidiser combination to achieve combustion. The second and third experiments were also able to show that different fuel types, such as RP1, MMH, and UDMH, which have auto-ignition temperatures lower than ethanol, are able to combust and have a self-sustained ignition with the combination of HTP.

Simultaneously with the experiment conducted, a simulation of the HTP decomposition temperature in a glass chamber was done using the cross-platform finite element analysis, solver and multi-physics model software, COMSOL was shown in chapter 6. Several simplifications and assumptions were made during the simulation which are shown in the following:

- Ignition is bound to occur once the HTP temperature is able to reach the auto-ignition temperature of the fuel. For the case of ethanol, 365 degrees C and for Jet A fuel, 220 degrees C.
- No atomisation of the HTP injected is applied.

- Only the HTP decomposition chamber is simulated.
- The coil that was wound around the glass chamber is omitted.
- In the simulation, instead of the mesh configuration used in the experiment, 3 coils were used.

The simulation was able to show that at power values of 20 W, as the HTP is injected in the glass chamber, the liquid was able to achieve a temperature of 589 degrees C but decreased drastically down to the initial temperature of the volume that was inputted in the software. This simulation was done using a mesh configuration named Normal, which is an automatically available mesh quality in the COMSOL software. Together with the same mesh quality, if 15 W of power is applied, the initial temperature that the HTP achieves is 492 deg C and for 10 W, it is 394 deg C. All the results presented matched the results of the experiment conducted. Lastly, two sensitivity analysis were conducted in order to prove the simulation model. The mesh quality used was modified as well as the distance where the heated coils were placed from the inlet and both tests proved that the simulation conducted was validated.

7.1. Overall Recommendations

In this section, the overall recommendations that were thought for sources of future improvement will be presented. There are aspects of both the practical experiment itself and the simulation conducted as well.

- **Experiment - Increase the amount of fuel and oxidiser:** Since the experiments conducted were lab-scale ones, the amount of fuel and oxidiser that could be used for the experiment was limited to 1 mL each. If the allowed quantity of chemicals during the experiment were to be more, the duration of the experiment would have been longer and thus the capture of a self-sustained ignition and the behaviour of the flame when combustion occurred could have been better. In future experiments, the test setup and the material used during the experiment shall be improved if were to be a experiment at a larger scale and the safety precautions would have to be improved more at the same time.
- **Experiment - More variations in parameters:** There were a limited amount of parameters used during the test due to limitations in timeframe and the amount of available resources of the MSc thesis study. In the future, better and more accurate results could be achieved if more parameters were to be applied to the experiment, such as finer or coarse mesh options, higher concentrated HTP as oxidiser, more types of fuels to be used as reference, different frequency values of the piezoelectric disc in order to take into consider the variations of the test results depending on the atom size of the HTP mist, different wire thickness NiCr wires, and many more. These would be able to further optimise the power consumption value of the thermal wire ignitor system.
- **Experiment - More precautions applied when conducting a closed environment system:** The third experiment conducted was a closed environment, somewhat pressurised test setup. As can be seen in chapter 5, during the experiment, the test setup was damaged as well as the equipment used during the experiment. In future studies, a more robust and safe system must be built in order to ensure more data obtained and last but not least, the safety of the test setup.
- **Experiment - Usage of a High-Speed camera:** The usage of a high-speed camera was limited and therefore the results obtained were taken using a smartphone camera which has a slow-motion video function available with 240 fps. Eventhough, this is better than a normal video, if a high-speed camera had been used, which has fps values of over 4000, the results of the test would have been better captured.
- **Simulation: Improving the COMSOL model:** Several assumptions and simplifications were made during the COMSOL model, such as not including the atomisation process of the liquid injected, or using 3 heated wire coils instead of a wire mesh. If these simulation settings were to be included in the future, a more robust simulation would be available and more accurate results that resemble the experiment even better would have been shown.

- **Simulation - Considering chemical kinetics:** The recent simulation only focuses on one-step chemistry and assumes that ignition were to occur once the liquid injected reached the auto-ignition temperature of the fuel. However, in reality, several chemical phenomena such as dissociation, heat dissipation, diffusion, and many more are present. Also, since there are different molecules existing in the chemical reaction, the Lewis number or certain models have to be applied to them to take into account differential diffusion. If these settings, and many more, would have been included in the simulation in the future, it would have produced more accurate results.

Bibliography

[1] Ir. B.T.C. Zandbergen. *Thermal Rocket Propulsion*. Online PDF: https://brightspace.tudelft.nl/d2l/le/content/498944/viewContent/2915988/View. Accessed: 10-09-2023. Delft, the Netherlands, Sept. 2022.

[2] European Space Agency (ESA). *What is Electric propulsion?* Accessed: May 4, 2024. Accessed 2024.

[3] Australian Nuclear Science and Technology Organisation (ANSTO). *Nuclear Propulsion Systems*. Accessed: May 4, 2024. Accessed 2024.

[4] NASA Glenn Research Center. *Chemical Propulsion Systems*. https://www1.grc.nasa.gov/research-and-engineering/chemical-propulsion-systems/. Accessed: May 4, 2024. Accessed 2024.

[5] Purdue Propulsion Engineering. *Solid Rockets - Purdue Propulsion Engineering*. Year Accessed. URL: https://engineering.purdue.edu/~propulsi/propulsion/rockets/solids.html.

[6] AerospaceNotes. *Salient Features of Liquid Propellant Rockets*. Year Accessed. URL: https://aerospacenotes.com/salient-features-of-liquid-propellant-rockets/.

[7] Hammad Shah et al. "Design and Prototyping of a Solid Fuel/Gaseous Oxidizer Hybrid Rocket Engine". PhD thesis. Dec. 2016. DOI: 10.13140/RG.2.2.12066.22728.

[8] Stephen M Davis and Nadir Yilmaz. "Advances in hypergolic propellants: Ignition, hydrazine, and hydrogen peroxide research". In: *Advances in Aerospace Engineering* 2014 (2014).

[9] Hongjae Kang et al. "Development of 500 N Scale Green Hypergolic Bipropellant Thruster using Hydrogen Peroxide as an Oxidizer". In: July 2015. DOI: 10.2514/6.2015-4062.

[10] Emre Tambag. "Thermal ignition system for green rocket propulsion: Experimental study on thermal ignition of high concentration hydrogen peroxide and ethanol propellant". MA thesis. Delft University of Technology, 2022. URL: http://resolver.tudelft.nl/uuid:951c9f37-4128-4d87-b834-7872a9b57670.

[11] Alessandro Veris. *Fundamental Concepts of Liquid-Propellant Rocket Engines*. Jan. 2021. ISBN: 978-3-030-54703-5. DOI: 10.1007/978-3-030-54704-2.

[12] D.K. Huzel, D.H. Huang, and H. Arbit. *Modern Engineering for Design of Liquid-propellant Rocket Engines*. Modern engineering for design of liquid-propellant rocket engines v. 147. American Institute of Aeronautics and Astronautics, 1992. ISBN: 9781563470134. URL: https://books.google.nl/books?id=fclbnQEACAAJ.

[13] Lukasz Mezyk et al. "Possibility of Using Thermal Decomposition of Hydrogen Peroxide For Low Thrust Propulsion System Application". In: (July 2017). DOI: 10.13009/EUCASS2017-626.

[14] Kevin Breisacher and Kumud Ajmani. "LOX / Methane Main Engine Igniter Tests and Modeling". In: (July 2008). DOI: 10.2514/6.2008-4757.

[15] Marek WOZNIAK, Gustavo OZUNA, and Krzysztof SICZEK. "Problems with glow plug – a review". In: *Combustion Engines* 186.3 (2021), pp. 11–30. ISSN: 2300-9896. DOI: 10.19206/CE-140114. URL: https://doi.org/10.19206/CE-140114.

[16] Eric S Taylor, W Neill Myers, and Michael A Martin. "Hypergolic ignitor". In: (2005).

[17] Botchu Vara Siva Jyoti et al. "Hypergolicity and ignition delay study of gelled ethanolamine fuel". In: *Combustion and Flame* 183 (2017), pp. 102–112. ISSN: 0010-2180. DOI: https://doi.org/10.1016/j.combustflame.2017.05.007. URL: https://www.sciencedirect.com/science/article/pii/S0010218017301748.

[18] Wojciech Florczuk and Grzegorz P Rarata. “Performance evaluation of the hypergolic green propellants based on the HTP for a future next generation spacecrafts”. In: *53rd AIAA/SAE/ASEE Joint Propulsion Conference*. 2017, p. 4849.

[19] Seonghyeon Park et al. “A review of the technical development on green hypergolic propellant”. In: *Journal of the Korean Society of Propulsion Engineers* 24.4 (2020), pp. 79–88.

[20] Wouter A Jonker, Alfons EHJ Mayer, and Barry TC Zandbergen. “Development of a rocket engine igniter using the catalytic decomposition of hydrogen peroxide”. In: *green propellant for space propulsion* (2006).

[21] Hatem Belal. “Modeling of Hydrazine Decomposition for Monopropellant Thrusters”. In: (May 2009).

[22] D Altman. *Rocket Motor, Hybrid*. Encyclopedia of Physical Science and Technology, 2003.

[23] Wim De Groot. “Propulsion Options for Primary Thrust and Attitude Control of Microspacecraft”. In: *Microsatellites as Research Tools*. Ed. by Fei-Bin Hsiao. Vol. 10. COSPAR Colloquia Series. Pergamon, 1999, pp. 200–209. DOI: https://doi.org/10.1016/S0964-2749(99)80027-4. URL: https://www.sciencedirect.com/science/article/pii/S0964274999800274.

[24] Marco Santi et al. “Design and Testing of a Hydrogen Peroxide Bipropellant Thruster”. In: Aug. 2020. DOI: 10.2514/6.2020-3827.

[25] J. Sisco et al. “Autoignition of Kerosene by Decomposed Hydrogen Peroxide in a Dump-Combustor Configuration”. In: *Journal of Propulsion and Power - J PROPUL POWER* 21 (May 2005), pp. 450–459. DOI: 10.2514/1.5287.

[26] Vadim Zakirov et al. “Nitrous oxide as a rocket propellant”. In: *Acta Astronautica* 48.5 (2001), pp. 353–362. ISSN: 0094-5765. DOI: https://doi.org/10.1016/S0094-5765(01)00047-9. URL: https://www.sciencedirect.com/science/article/pii/S0094576501000479.

[27] Dylan DeSantis. “Satellite Thruster Propulsion- H2O2 Bipropellant Comparison with Existing Alternatives”. In: (Apr. 2014).

[28] S. Frolik et al. “Development of hypergolic liquid fuels for use with hydrogen peroxide”. In: *36th AIAA/ASME/SAE/ASEE Joint Propulsion Conference and Exhibit*. DOI: 10.2514/6.2000-3684. eprint: https://arc.aiaa.org/doi/pdf/10.2514/6.2000-3684. URL: https://arc.aiaa.org/doi/abs/10.2514/6.2000-3684.

[29] Alloy Network. *Types of Heating Elements*. Accessed: 04/03/2024. n.d. URL: https://www.heating-element-alloy.com/article/heating-elements-properties-and-types.html.

[30] Mei-feng HE et al. “Effect of hydrogen peroxide concentration on surface properties of Ni–Cr alloys”. In: *Transactions of Nonferrous Metals Society of China* 26.5 (2016), pp. 1353–1358. ISSN: 1003-6326. DOI: https://doi.org/10.1016/S1003-6326(16)64238-3. URL: https://www.sciencedirect.com/science/article/pii/S1003632616642383.

[31] Omega Engineering. *Omega Engineering: NI80 Thermocouple Alloy*. Accessed: 14/03/2024. n.d. URL: https://www.omega.nl/pptst/NI80.html.

[32] Jong Mok et al. “Thermal Decomposition of Hydrogen Peroxide, Part I: Experimental Results”. In: *Journal of Propulsion and Power - J PROPUL POWER* 21 (Sept. 2005), pp. 942–953. DOI: 10.2514/1.13284.

[33] Wioleta Kopacz et al. “Hydrogen peroxide – A promising oxidizer for rocket propulsion and its application in solid rocket propellants”. In: *FirePhysChem* 2.1 (2022). Progress in Solid Rocket Propulsion - Part A, pp. 56–66. ISSN: 2667-1344. DOI: https://doi.org/10.1016/j.fpc.2022.03.009. URL: https://www.sciencedirect.com/science/article/pii/S2667134422000141.

[34] Magnus Sjoberg and John Dec. “Ethanol Autoignition Characteristics and HCCI Performance for Wide Ranges of Engine Speed, Load and Boost”. In: *SAE International Journal of Engines* 3 (Aug. 2010), pp. 84–106. DOI: 10.4271/2010-01-0338.

[35] Chan-Cheng Chen et al. “Autoignition Temperature Data for Methanol, Ethanol, Propanol, 2-Butanol, 1-Butanol, and 2-Methyl-2,4-pentanediol”. In: *Journal of Chemical and Engineering Data - J CHEM ENG DATA* 55 (Aug. 2010). DOI: 10.1021/je100619p.

[36] Stefan Kooij et al. “Size distributions of droplets produced by ultrasonic nebulizers”. In: *Scientific Reports* 9.1 (2019), p. 6128. DOI: 10.1038/s41598-019-42599-8. URL: https://doi.org/10.1038/s41598-019-42599-8.

[37] Jorge Esteban Guerra Bravo et al. “Vibration Analysis of a Piezoelectric Ultrasonic Atomizer to Control Atomization Rate”. In: *Applied Sciences* 11 (Sept. 2021), p. 8350. DOI: 10.3390/app11188350.

[38] Go Fujii et al. “Visualization of Pulse Firing Mode in Hypergolic Bipropellant Thruster”. In: *Journal of Propulsion and Power* 36 (Apr. 2020), pp. 1–8. DOI: 10.2514/1.B37637.

A

Thermal Wire Data Sheet

Resistance Heating Wire Nickel-Chromium Alloy

80% Nickel / 20% Chromium

- **Withstands High Temperatures up to 1150°C (2100°F)**
- **Quick Heating, Long Life**
- **Corrosion Resistant**
- **Used to Make Straight or Helical Coil Resistance Heaters**
- **Convenient 15 m and 60 m Spools Available**

See Page G-39 for Coiled Resistance Wire

OMEGA® NIC80 wire is a resistance heating wire comprised of 80% Nickel and 20% Chromium. NIC80 wire is commonly used as a resistor at elevated temperatures. NI/CR-80/20 is essential for resistor elements in high temperature applications such as electric furnaces, electric ranges and radiant heaters operating at temperatures up to 1150°C (2100°F).

In addition to these qualities and standard uses, it has found wide application in technical applications due to its combination of high electrical resistance and its temperature coefficient of resistance much less than that of Nickel-Chrome 60.

Specifications

Composition: 80% Ni, 20% Cr
Specific Resistance: 650 Ohms per circular mil-foot at 20°C (68°F). See table below for multiplication factors to obtain resistance at other temperatures.
Specific Gravity: 8.41
Density: 8.4g/cm^3
Melting Point: approx. 1400°C (2550°F)
Nominal Coefficient of Linear Expansion: 0.000017 (10-1000°C)
Tensile Strength (Kg/cm^2) 20°C: Hard Drawn: 14,060 Soft Annealed: 7,030
Nominal Temperature Coefficient of Resistance: 0.00011 Ohms/Ohm/°C (20-500°C)

Factor by Which Resistance at Room Temperature Is to Be Multiplied to Obtain Resistance at Indicated Temperatures
(These figures are given as a basis for engineering calculations and represent average material as supplied.)

Temp. °F	68	200	400	600	800	1000	1200	1400	1600	1800	2000°F
Temp. °C	20	93	204	315	427	538	649	760	871	982	1093°C
Factor	1.000	1.016	1.037	1.054	1.066	1.070	1.064	1.062	1.066	1.072	1.078

To Order ***(Specify Model Number)*** ***IN STOCK FOR FAST DELIVERY!***

AWG	Dia. mm	Ohms per 30cm @ 20°C (68°F)	Current Temperature Characteristics* °C (°F) 425 (800)	550 (1000)	650 (1200)	750 (1400)	875 (1600)	1100 (2000)	Model No.	Price 15 m	Price 60 m
18	1 (.040)	.4062	8.32	10.17	12.48	15.11	18.06	24.03	**NI80-040-(†)**	**£17.25**	**£52.00**
20	.8 (.032)	.6348	6.17	7.56	9.24	11.13	13.23	17.57	**NI80-032-(†)**	**13.00**	**39.50**
22	.64(.0253)	1.015	4.62	5.62	6.85	8.20	9.69	12.85	**NI80-025-(†)**	**13.00**	**39.50**
24	.5 (.0201)	1.609	3.46	4.18	5.06	6.04	7.10	9.40	**NI80-020-(†)**	**13.00**	**39.50**
26	.4 (.0159)	2.571	2.62	3.12	3.76	4.49	5.27	6.90	**NI80-015-(†)**	**8.20**	**24.50**
28	.3 (.0126)	4.094	1.98	2.38	2.84	3.37	3.93	5.09	**NI80-012-(†)**	**8.20**	**24.50**
30	.25 (.010)	6.50	1.50	1.81	2.14	2.53	2.93	3.75	**NI80-010-(†)**	**8.20**	**24.50**

****** Showing approximate amperes necessary to produce a given temperature, applying only to a straight wire stretched horizontally in free air.*
***Note:** This wire is **not** intended for use in making thermocouple elements. † Specify desired length in metres: 15m or 60m*
Ordering Example: NI80-040-15m** is a 15 m spool of 1.0mm bare wire, **£17.25.

B

High-Speed Camera Data Sheet

PRODUCT DATASHEET

Mini AX

FASTCAM series by Photron

FASTCAM Mini AX50 / AX100 / AX200

1-Megapixel CMOS Image Sensor:
1024 x 1024 pixels at 2,000fps (Mini AX50)
1024 x 1024 pixels at 4,000fps (Mini AX100)
1024 x 1024 pixels at 6,400fps (Mini AX200)

Maximum Frame Rate:
170,000fps (Mini AX50 type 170K-S)
212,500fps (Mini AX100 type 200K-S)
540,000fps (Mini AX100 type 540K-S)
216,000fps (Mini AX200 type 200K-S)
540,000fps (Mini AX200 type 540K-S)
900,000fps (Mini AX200 type 900K-S)

Class Leading Light Sensitivity:
ISO 50,000 monochrome
ISO 25,000 color

Global Electronic Shutter:
1ms to 1µs independent of frame rate
(Mini AX200 model 900K-S only: 260ns shutter available subject to export control)

Dynamic Range (ADC):
12-bit monochrome, 36-bit color

Compact and Lightweight:
120mm (H) x 120mm (W) x 94mm (D)
4.72″ (H) x 4.72″ (W) x 3.70″ (D)
Weight: 1.5Kg (3.30 lbs.)

Internal Recording Memory:
8GB, 16GB, or 32GB

Fast Gigabit Ethernet Interface:
Provides high-speed image download to standard notebook/PC

Flexible Frame Synchronization:
Frame rate may be synchronized to external unstable frequencies

High-G Rated:
Suitable for application in high-G environments; operation tested to 100G, 10ms, 6-axes

Fan Stop Function:
Remotely switch off cooling fans to eliminate vibration

COMPACT HIGH-SPEED CAMERAS WITH HIGH LIGHT SENSITIVITY

The FASTCAM Mini AX is Photron's highest performance model within the FASTCAM Mini series of high-speed cameras. The Mini AX delivers exceptional light sensitivity, excellent image quality and flexible region of interest (ROI) features for customers who do not require the ultimate frame rate performance of the FASTCAM SA-Z, but would benefit from the same high-end camera image sensor features.

Three performance level models - Mini AX50, AX100 and AX200 - deliver 1-megapixel image resolution (1024 x 1024 pixels) at frame rates up to 2,000fps, 4,000fps and 6,400fps respectively. All three Mini AX models offer a minimum exposure duration of 1µs as standard with recording memory options up to 32GB providing extended recording times and triggering flexibility.

Subject to export approval the Mini AX100 can be offered with maximum frame rates up to 540,000fps and the Mini AX200 with maximum frame rates up to 900,000fps with a minimum exposure time of 260 nanoseconds.

Standard operational features of the FASTCAM Mini AX include a mechanical shutter to allow remote system calibration, Gigabit Ethernet Interface for reliable system control with high-speed data transfer to PC, and the ability to remotely switch off cooling fans to eliminate vibration when recording at high magnifications.

With the combination of high frame rates, high image quality and exceptional light sensitivity contained within a 120mm x 120mm x 94mm rugged camera body weighing just 1.5kg, the FASTCAM Mini AX is ideally suited for use in a wide range of demanding scientific and industrial applications.

Image Sensor Technical Data

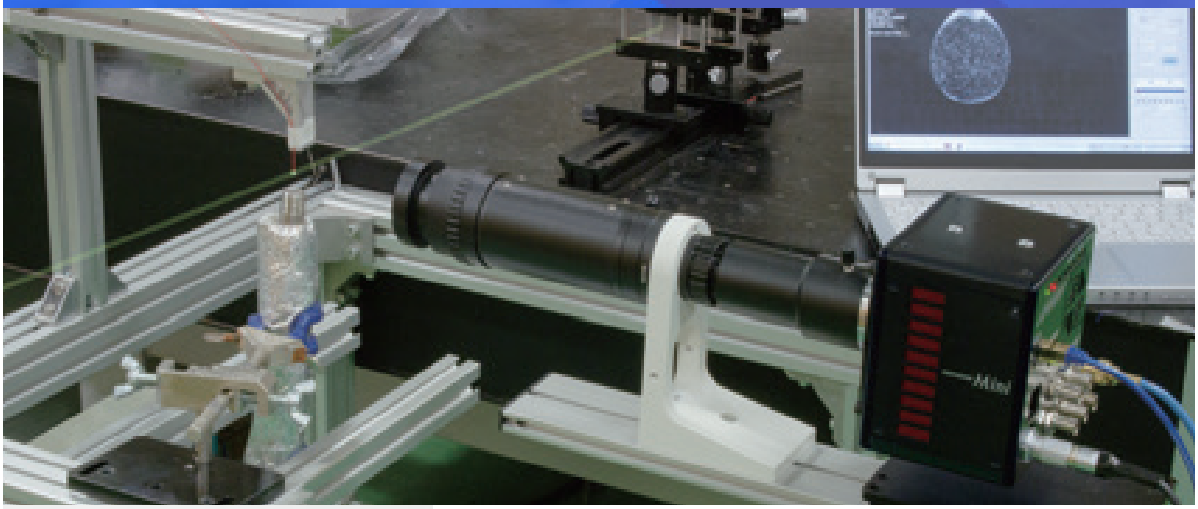

Light Sensitivity:

FASTCAM MINI AX	
Monochrome models	ISO 50,000
Color models	ISO 25,000

Monochrome sensors used in the FASTCAM Mini AX cameras are supplied without an IR absorbing filter, extending the camera spectral response beyod 900nm. When the sensitivity of the FASTCAM Mini AX camera is measured to tungsten light including near IR response an equivalent value of ISO 125,000 is obtained.

Image Sensor:
The FASTCAM Mini AX system uses an advanced CMOS image sensor optimized for light sensitivity and high image quality that is unique to Photron.

A 20-micron pixel pitch gives a sensor size at full image resolution of 20.48 x 20.48mm (diagonal 28.96mm).

Lenses designed for both FX (35mm full frame) and also DX (APS-C digital SLR) formats are fully compatible with the FASTCAM Mini AX at full image resolution.

Sensor Type	Proprietary Design Advanced CMOS
Maximum Resolution (pixels)	1024 x 1024 pixels
Sensor Size / Diagonal	20.48 x 20.48mm / 28.96mm
Pixel Size (microns)	20µm x 20µm
Quantum Efficiency	46% at 630nm
Fill Factor	58%
Color Matrix	Bayer CFA (single sensor)
Light Sensitivity	ISO 50,000 monochrome ISO 25,000 color (monochrome sensor equivalent ISO 125,000 including near IR response)
Shutter	Global Electronic Shutter 1ms to 1µs independent of frame rate (Mini AX200 model 900K-S only: 260ns shutter available subject to export control)

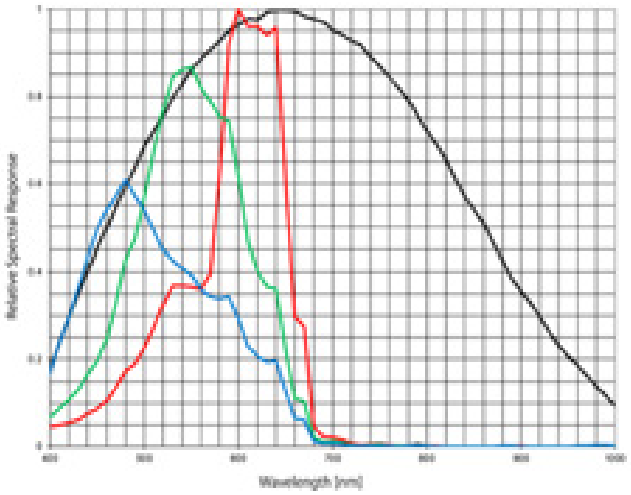

Camera Performance Specifications

Camera Performance Specifications

Model	Mini AX50	Mini AX100	Mini AX200
Full Frame Performance	2,000fps 1024 x 1024 pixels	4,000fps 1024 x 1024 pixels	6,400fps 1024 x 1024 pixels
Maximum Frame Rate	Type 170K-S: 170,000fps (128 x 16 pixels)	Type 200K-S: 212,500fps (128 x 16 pixels) Type 540K-S: 540,000fps* (128 x 16 pixels)	Type 200K-S: 216,000fps (128 x 16 pixels) Type 540K-S: 540,000fps* (128 x 16 pixels) Type 900K-S: 900,000fps* (128 x 16 pixels)
Minimum Exposure Time	Global electronic shutter to 1.05µs selectable independent or frame rate (260ns option available with Mini AX200 type 900K only) *		
Inter Frame Time (for PIV)	1.71µs		
Ruggedized Mechanical Calibration Shutter	Standard feature		
Dynamic Range (ADC)	12-bit monochrome 36-bit color		
Memory Capacity Options	8GB: 5,457 frames at full resolution 16GB: 10,918 frames at full resolution 32GB: 21,841 frames at full resolution		
Memory Partitions	Up to 64 memory segments		
Region of Interest	Selectable in steps of 128 pixels (horizontal) x 16 pixels (vertical)		
Trigger Inputs	Selectable +/- TTL 5V and switch closure		
Trigger Delay	Programmable on selected input / output triggers: 100ns resolution		
Input / Output	Input: Trigger (TTL/Switch), sync, ready, event, IRIG Output: trigger, sync, ready, rec, exposure		
Trigger Modes	Start, end, center, manual, random, random reset, image trigger, time lapse, record on command		
Time Code Input	IRIG-B		
External Sync	+/- TTL 5Vp-p Variable frequency sync		
Camera Control Interface	High-speed Gigabit Ethernet		
Image Data Display	Frame rate, shutter speed, trigger mode, date/time, status, real time / IRIG time, frame count, resolution		
Saved Image Formats	BMP, TIFF, JPEG, PNG, RAW, RAWW, MRAW, AVI, WMV, FTIF, MOV - Images can be saved with or without image data and in 8-bit, 16-bit or 36-bit depth of sensor where supported		
Supported OS	Microsoft Windows operating system including: 7, 8, 8.1, 10, 11 (32/64-bit)		

* Frame rates above 225,000fps and exposure times below 1µs may be subject to export control regulations in some areas

High-Speed Gigabit Ethernet Interface:
The FASTCAM Mini AX camera system is equipped with a high-speed Gigabit Ethernet Interface to provide reliable network communication and fast download of image data.

Dedicated I/O:
A dedicated BNC connection for a contact closure hardware trigger input is provided. In addition, two programmable inputs and two programmable output channels provide direct connection for common tasks such as synchronization of multiple cameras and operation in conjunction with Data Acquisition (DAQ) hardware.

High-G Mechanical Calibration Shutter:
The ruggedized mechanical shutter fitted as standard to the FASTCAM Mini AX camera allows sensor black balance calibration to be carried out remotely from the system control software.

Nikon G-Type Compatible Lens Fitting:
The FASTCAM Mini AX camera is equipped with an objective lens mount compatible with readily available Nikon G-type lenses. Controls provided within the lens mount allow the control of lens aperture on lenses without external iris control.

Operational Features

Camera Operation Features

Frame Synchronization	Accurate frame synchronization with other cameras and with external and unstable frequencies.
Dual Slope Shutter (Extended Dynamic Range)	Selectable in 20 steps (0 to 95% in 5% increments) to prevent pixel overexposure without post processing.
Memory Partitions	Up to 64 memory segments allow multiple events to be stored in camera memory before downloading, with automatic progression to the next available partition.
Low Light Mode	Operation at minimum frame rate with separately adjustable shutter time to allow easy camera set-up and focus in ambient lighting.
IRIG Phase Lock	Enables multiple cameras to be synchronized together with other instrumentation equipment or to a master external time source.
Internal Time Delay Generator	Allows programmable delays to be set on input and output triggers; 100ns resolution.
Event Markers	Up to ten user-entered event markers to define specific events within the recorded image sequence .
Download While Recording	FASTCAM Mini AX supports Partition Recording Mode, allowing image data captured in one memory partition to be downloaded while at the same time recording into another partition.
Automatic Download	The system can be set to automatically download image data to the control PC and, when download is complete to re-arm in readiness for the next trigger with automatically incremented file names.
Software Binning	Virtual pixel binning (2x2, 4x4 etc.) allows increased light sensitivity with reduced image resolution without changing camera field of view.

Operation Software Features

Image Calibration	2D image calibration allows the measurement of distance and angle from the image. A calibration grid overlay can be superimposed on the image.
Image Overlay	A stored reference image may be overlaid on the live image to allow accurate camera positioning to achieve the same view as a previous test.
Import of Multiple Image Sequences	Multiple image sequences can be loaded and simultaneously replayed. Timing of image sequences can be adjusted to create a common time reference. Time based synchronization allows images captured at different frame rates to be synchronized.
High Dynamic Range Mode	Making use of the full sensor dynamic range, HDR mode allows enhanced detail in both light and dark areas of an image to be displayed simultaneously.
Motion Detector	In order to highlight subtle changes in an image, Motion Detector allows a reference image to be subtracted from a recorded sequence. Details including propagation of shock waves and surface changes during impact can be visualized using the feature.
Line Profile	A line profile representing grey levels along a line drawn across any region of the image is displayed. In live mode the Line Profile can be used to ensure optimum image focus is achieved.
Histogram	A histogram displaying grey levels within a user-defined image area is displayed. In live mode the Histogram can be used to ensure that optimum exposure levels are set for the scene being recorded.

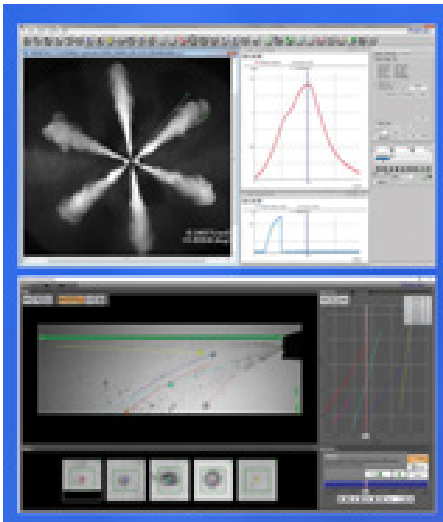

Photron FASTCAM Viewer:
Photron FASTCAM Viewer software (PFV) has been designed to provide an intuitive and feature rich user interface for the control of Photron high-speed cameras, data saving, image replay and simple motion analysis. Advanced operation menus provide access to features for advanced camera operation and image enhancement. Tools are provided to allow image calibration and easy measurement of angles and distances from image data. Also included are a C++ SDK and wrappers for LabView and MATLAB ®.

An optional software plug-in module provides synchronisation between Photron high- speed cameras and data acquired through National Instruments data acquisition systems. Synchronised data captured by the DAQ system provides waveform information which can be viewed alongside high-speed camera images.

Photron FASTCAM Analysis:
PFV software allows image sequences to be exported directly to optional Photron FASTCAM Analysis (PFA) Motion Analysis software. This entry level Motion Analysis software with an on screen 'step by step guide' function launches automatically from Photron FASTCAM Viewer software, and provides automated tracking of up to 5 points using feature or correlation tracking algorithms for the automated analysis of motion within an image sequence.

Frame Rate / Image Resolution

Variable Region of Interest:
Region of Interest (ROI) or sub-windowing allows a user-specified portion of the sensor to be defined to capture images. By using a reduced portion of the image area, the frame rate at which images are recorded can be increased. FASTCAM Mini AX allows the ROI to be set in increments of 128 pixels horizontal and 16 pixels vertical.

Square Image Sensor Format:
Unlike broadcast and media applications where image formats such as 16:9 have now become standard, in scientific and industrial imaging applications an image sensor with a 1:1 image format is generally accepted to be advantageous. To capture the maximum useful image data in applications including microscopy, detonics, combustion imaging and many others, a 1:1 sensor format provides greater flexibility than 'letterbox' image formats. The FASTCAM Mini AX image sensor allows the user to choose either square or rectangular image formats in order to obtain the maximum subject information.

External Frame Synchronization:
The FASTCAM Mini AX camera can be fully synchronized with an external event to allow the timing of when each individual image is captured to be precisely referenced. The camera can be accurately synchronized to unstable frequencies allowing complex events such as combustion in rapidly accelerating or decelerating engines to be recorded and studied.

Record During Download Operation:
FASTCAM Mini AX recording memory can be divided into multiple active sections. The user can record an on-going event in one memory partition while at the same time downloading a previously recorded image sequence in order to improve workflow and optimize camera operation.

Mini AX200

Resolution	Frame Rate	8GB		16GB		32GB	
(h x v pixels)	Max fps	Frames	Time (sec)**	Frames	Time (sec)**	Frames	Time (sec)**
1024 x 1024	6,400	5,457	0.85	10,918	1.71	21,841	3.41
1024 x 896	7,200	6,236	0.87	12,478	1.73	24,961	3.47
896 x 896	8,100	7,127	0.88	14,261	1.76	28,527	3.52
768 x 768	10,800	9,701	0.90	19,410	1.80	38,829	3.60
512 x 512	22,500	21,829	0.97	43,674	1.94	87,365	3.88
512 x 256	43,200	43,658	1.01	87,349	2.02	174,730	4.04
256 x 256	67,500	87,317	1.29	174,698	2.59	349,461	5.18
256 x 128	120,000	174,634	1.46	349,397	2.91	698,922	5.82
128 x 128	162,000	349,269	2.16	698,794	4.31	1,397,845	8.63
128 x 64	259,200	698,538	2.69	1,397,589	5.39	2,795,690	10.79
128 x 32	360,000	1,397,077	3.88	2,795,178	7.76	5,591,381	15.53
128 x 16	540,000	2,794,154	5.17	5,590,357	10.35	11,182,762	20.71
128 x 16	900,000						

Mini AX100

Resolution	Frame Rate	8GB		16GB		32GB	
(h x v pixels)	Max fps	Frames	Time (sec)**	Frames	Time (sec)**	Frames	Time (sec)**
1024 x 1024	4,000	5,457	1.36	10,918	2.73	21,841	5.46
1024 x 896	4,500	6,236	1.39	12,478	2.77	24,961	5.55
896 x 896	5,400	7,127	1.32	14,261	2.64	28,527	5.28
768 x 768	6,800	9,701	1.43	19,410	2.85	38,829	5.71
512 x 512	13,600	21,829	1.61	43,674	3.21	87,365	6.42
512 x 256	25,500	43,658	1.71	87,349	3.43	174,730	6.85
256 x 256	37,500	87,317	2.33	174,698	4.66	349,461	9.32
256 x 128	61,200	174,634	2.85	349,397	5.71	698,922	11.42
128 x 128	76,500	349,269	4.57	698,794	9.13	1,397,845	18.27
128 x 64	127,500	698,538	5.48	1,397,589	10.96	2,795,690	21.93
128 x 32	170,000	1,397,077	8.22	2,795,178	16.44	5,591,381	32.89
128 x 16	540,000	2,794,154	5.17	5,590,357	10.35	11,182,762	20.71

Mini AX50

Resolution	Frame Rate	8GB		16GB		32GB	
(h x v pixels)	Max fps	Frames	Time (sec)**	Frames	Time (sec)**	Frames	Time (sec)**
1024 x 1024	2,000	5,457	2.73	10,918	5.46	21,841	10.92
1024 x 896	2,500	6,236	2.49	12,478	4.99	24,961	9.98
896 x 896	2,500	7,127	2.85	14,261	5.70	28,527	11.41
768 x 768	3,600	9,701	2.69	19,410	5.39	38,829	10.79
512 x 512	7,200	21,829	3.03	43,674	6.07	87,365	12.13
512 x 256	13,600	43,658	3.21	87,349	6.42	174,730	12.85
256 x 256	20,400	87,317	4.28	174,698	8.56	349,461	17.13
256 x 128	37,500	174,634	4.66	349,397	9.32	698,922	18.64
128 x 128	45,900	349,269	7.61	698,794	15.22	1,397,845	30.45
128 x 64	76,500	698,538	9.13	1,397,589	18.27	2,795,690	36.54
128 x 32	127,500	1,397,077	10.96	2,795,178	21.92	5,591,381	43.85
128 x 16	170,000	2,794,154	16.44	5,590,357	32.88	11,182,762	65.78

* Specifications subject to change without notice.
** Recording time is an estimate and may be different depending on recording conditions and settings.

Photo
Schlieren imaging of fuel injection and engine combustion
20,000fps

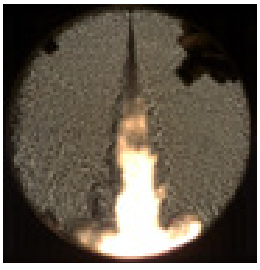

Mechanical & Environmental Specifications

Compatibility with Specialist Lens Systems:
A combination of small physical size, low weight and high light sensitivity allows the FASTCAM Mini AX to be coupled to a range of optical systems such as scientific and long distance microscopes, rigid endoscopes or borescopes, and image intensifiers for applications ranging from imaging flows in microfluidic devices to combustion diagnostics.

PIV and DIC Requirements:
FASTCAM Mini AX specifications match with the requirements for optical measurement techniques such as Particle Image Velocimetry (PIV) and Digital Image Correlation (DIC). The FASTCAM Mini AX has many key performance specifications desired for these measurement systems.

In PIV the detection of low light levels from small particles is fundamental. A high sensitivity image sensor allows the use of smaller tracer particles and/or lower laser power.

For DIC applications a highly sensitive camera allows the use of smaller objective lens apertures yielding greater depth of field and enhanced measurement of out of plane displacements.

Small Physical Size:
The small physical size and weight of the Mini camera range allows the use of conventional opto-mechanical hardware for rigid and stable mounting of multiple cameras, and for the location of cameras in space limited locations.

Specifications subject to change without notice.

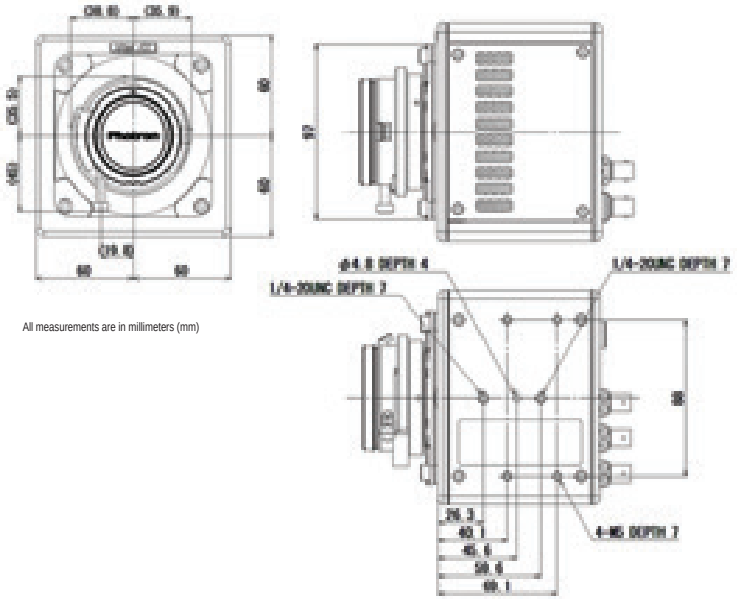

All measurements are in millimeters (mm)

Mechanical and Environmental Specifications

Mechanical	
Lens Mount	F-mount (G-type lens compatible) and C-mount provided - Optional lens mounts available include M42 adapter
Camera Mountings	4 x 1/4 - 20 UNC (base and top), 4 x M5 (base)
External Dimensions	
Camera Body (excluding protrusions)	120mm (H) x 120mm (W) x 94mm (D) 4.72" (H) x 4.72" (W) x 3.70" (D)
Weight	
Camera Body	1.5kg (3.30lbs)
Environmental	
Operating Temperature	0 to 40C, 32˚ to 104˚F
Storage Temperature	-20 to 60C, -4˚ to 140˚F
Humidity	85% or less (non-condensing)
Cooling	Internal fan cooling (fan-off mode supported)
Operational Shock	100G, 10ms, 6-axes
Power	
AC Power (with supplied adapter)	100 to 240V, 50 to 60Hz
DC Power	22 to 32V, 55VA

PHOTRON USA, INC.
9520 Padgett Street, Suite 110
San Diego, CA 92126
USA

Tel: 858.684.3555 or 800.585.2129
Fax: 858.684.3558
Email: image@photron.com
www.photron.com

PHOTRON EUROPE LIMITED
The Barn, Bottom Road
West Wycombe
Bucks. HP14 4BS
United Kingdom

Tel: +44 (0) 1494 481011
Fax: +44 (0) 1494 487011
Email: image@photron.com
www.photron.com

PHOTRON (Shanghai)
Room 20C, Zhao-Feng
World Trade Building
No. 369, JiangSu Road
Chang Ning District
Shanghai, 200050 China
Tel: +86 (21) 5268-3700
Fax: +86 (21) 5268-3702
Email: info@photron.cn.com
www.photron.cn.com

PHOTRON LIMITED
21F, Jinbocho Mitsui Bldg.
1-105 Kanda Jimbocho
Chiyoda-ku, Tokyo 101-0051
Japan

Tel: +81 (3) 3518-6271
Fax: +81 (3) 3 3518-6279
Email: image@photron.co.jp
www.photron.co.jp

REV# 24.4.25

C

Hydrogen Peroxide Safety Data Sheet

ThermoFisher SCIENTIFIC

SAFETY DATA SHEET

Creation Date 22-Sep-2009 **Revision Date** 24-Dec-2021 **Revision Number** 12

1. Identification

Product Name **Hydrogen Peroxide (30% in water)**

Cat No. : **BP2633-500; NC1592410**

Synonyms Hydrogen Dioxide; Peroxide; Carbamide Peroxide

Recommended Use Laboratory chemicals.
Uses advised against Food, drug, pesticide or biocidal product use.

Details of the supplier of the safety data sheet

Company
Fisher Scientific Company
One Reagent Lane
Fair Lawn, NJ 07410
Tel: (201) 796-7100

Emergency Telephone Number
For information **US** call: 001-800-ACROS-01 / **Europe** call: +32 14 57 52 11
Emergency Number **US:**001-201-796-7100 / **Europe:** +32 14 57 52 99
CHEMTREC Tel. No.**US:**001-800-424-9300 / **Europe:**001-703-527-3887

2. Hazard(s) identification

Classification
This chemical is considered hazardous by the 2012 OSHA Hazard Communication Standard (29 CFR 1910.1200)

Oxidizing liquids	Category 2
Acute oral toxicity	Category 4
Acute Inhalation Toxicity - Dusts and Mists	Category 4
Skin Corrosion/Irritation	Category 1 A
Serious Eye Damage/Eye Irritation	Category 1

Label Elements

Signal Word
Danger

Hazard Statements
May intensify fire; oxidizer
Harmful if swallowed or if inhaled
Causes severe skin burns and eye damage

Precautionary Statements
Prevention
Wash face, hands and any exposed skin thoroughly after handling
Do not eat, drink or smoke when using this product
Use only outdoors or in a well-ventilated area
Do not breathe dust/fume/gas/mist/vapors/spray
Wear protective gloves/protective clothing/eye protection/face protection
Keep away from heat/sparks/open flames/hot surfaces. - No smoking
Keep/Store away from clothing/ other combustible materials
Take any precaution to avoid mixing with combustibles
Response
Immediately call a POISON CENTER or doctor/physician
Inhalation
IF INHALED: Remove victim to fresh air and keep at rest in a position comfortable for breathing
Skin
IF ON SKIN (or hair): Take off immediately all contaminated clothing. Rinse skin with water/shower
Wash contaminated clothing before reuse
Eyes
IF IN EYES: Rinse cautiously with water for several minutes. Remove contact lenses, if present and easy to do. Continue rinsing
Ingestion
Rinse mouth
Do NOT induce vomiting
Fire
In case of fire: Use water spray/fog or regular foam to extinguish
Storage
Store locked up
Store in a well-ventilated place. Keep container tightly closed
Disposal
Dispose of contents/container to an approved waste disposal plant
Hazards not otherwise classified (HNOC)
None identified

3. Composition/Information on Ingredients

Component	CAS No	Weight %
Water	7732-18-5	65 - 80
Hydrogen peroxide	7722-84-1	20 - 35

4. First-aid measures

General Advice Show this safety data sheet to the doctor in attendance. Immediate medical attention is required.

Eye Contact Rinse immediately with plenty of water, also under the eyelids, for at least 15 minutes. Immediate medical attention is required.

Skin Contact Wash off immediately with plenty of water for at least 15 minutes. Remove and wash contaminated clothing and gloves, including the inside, before re-use. Call a physician

immediately.

Inhalation If not breathing, give artificial respiration. Remove from exposure, lie down. Do not use mouth-to-mouth method if victim ingested or inhaled the substance; give artificial respiration with the aid of a pocket mask equipped with a one-way valve or other proper respiratory medical device. Call a physician immediately.

Ingestion Do NOT induce vomiting. Clean mouth with water. Never give anything by mouth to an unconscious person. Call a physician immediately.

Most important symptoms and effects Causes severe eye damage. Ingestion causes severe swelling, severe damage to the delicate tissue and danger of perforation

Notes to Physician Treat symptomatically

5. Fire-fighting measures

Suitable Extinguishing Media Water spray. Foam. Carbon dioxide (CO_2).

Unsuitable Extinguishing Media Dry chemical

Flash Point Not applicable
Method - No information available

Autoignition Temperature No information available

Explosion Limits
Upper No data available
Lower No data available

Oxidizing Properties Oxidizer

Sensitivity to Mechanical Impact No information available
Sensitivity to Static Discharge No information available

Specific Hazards Arising from the Chemical
Oxidizer: Contact with combustible/organic material may cause fire. In the event of fire and/or explosion do not breathe fumes. Containers may explode when heated. May ignite combustibles (wood paper, oil, clothing, etc.).

Hazardous Combustion Products
Hydrogen. Oxygen.

Protective Equipment and Precautions for Firefighters
As in any fire, wear self-contained breathing apparatus pressure-demand, MSHA/NIOSH (approved or equivalent) and full protective gear. Thermal decomposition can lead to release of irritating gases and vapors.

NFPA

Health	Flammability	Instability	Physical hazards
3	0	2	OX

6. Accidental release measures

Personal Precautions Use personal protective equipment as required. Ensure adequate ventilation. Evacuate personnel to safe areas. Keep people away from and upwind of spill/leak.

Environmental Precautions Should not be released into the environment. See Section 12 for additional Ecological Information. Avoid release to the environment. Collect spillage.

Methods for Containment and Clean Up Soak up with inert absorbent material. Keep in suitable, closed containers for disposal.

7. Handling and storage

Handling Wear personal protective equipment/face protection. Do not get in eyes, on skin, or on clothing. Do not breathe mist/vapors/spray. Do not ingest. If swallowed then seek

immediate medical assistance. Ensure adequate ventilation.

Storage. Keep away from combustible material. Keep cool and protect from sunlight. Keep container tightly closed in a dry and well-ventilated place. Do not store in metal containers. Keep only in the original container. Incompatible Materials. Finely powdered metals. copper. Reducing Agent. Strong bases. Combustible material. Organic materials.

8. Exposure controls / personal protection

Exposure Guidelines

Component	ACGIH TLV	OSHA PEL	NIOSH	Mexico OEL (TWA)
Hydrogen peroxide	TWA: 1 ppm	(Vacated) TWA: 1 ppm (Vacated) TWA: 1.4 mg/m³ TWA: 1 ppm TWA: 1.4 mg/m³	IDLH: 75 ppm TWA: 1 ppm TWA: 1.4 mg/m³	TWA: 1 ppm

Legend

ACGIH - American Conference of Governmental Industrial Hygienists
OSHA - Occupational Safety and Health Administration
NIOSH: NIOSH - National Institute for Occupational Safety and Health

Engineering Measures Ensure that eyewash stations and safety showers are close to the workstation location. Ensure adequate ventilation, especially in confined areas.

Personal Protective Equipment

Eye/face Protection Wear appropriate protective eyeglasses or chemical safety goggles as described by OSHA's eye and face protection regulations in 29 CFR 1910.133 or European Standard EN166.

Skin and body protection Wear appropriate protective gloves and clothing to prevent skin exposure.

Respiratory Protection Follow the OSHA respirator regulations found in 29 CFR 1910.134 or European Standard EN 149. Use a NIOSH/MSHA or European Standard EN 149 approved respirator if exposure limits are exceeded or if irritation or other symptoms are experienced.

Recommended Filter type: Particulates filter conforming to EN 143. Inorganic gases and vapours filter. Type B. Grey. conforming to EN14387.

Hygiene Measures Handle in accordance with good industrial hygiene and safety practice.

9. Physical and chemical properties

Physical State	Liquid
Appearance	Clear
Odor	pungent
Odor Threshold	No information available
pH	3.3 (30 %)
Melting Point/Range	-33 °C / -27.4 °F
Boiling Point/Range	108 °C / 226.4 °F @ 760 mmHg
Flash Point	Not applicable
Evaporation Rate	>1.0 (Butyl Acetate = 1.0)
Flammability (solid,gas)	Not applicable
Flammability or explosive limits	
Upper	No data available
Lower	No data available
Vapor Pressure	23 mmHg @ 30 °C
Vapor Density	1.10
Specific Gravity	1.11

Solubility	Miscible with water
Partition coefficient; n-octanol/water	No data available
Autoignition Temperature	No information available
Decomposition Temperature	No information available
Viscosity	No information available
Molecular Formula	H2O2
Molecular Weight	34.01

10. Stability and reactivity

Reactive Hazard Yes

Stability Oxidizer: Contact with combustible/organic material may cause fire. Light sensitive.

Conditions to Avoid Incompatible products. Excess heat. Exposure to light. Combustible material.

Incompatible Materials Finely powdered metals, copper, Reducing Agent, Strong bases, Combustible material, Organic materials

Hazardous Decomposition Products Hydrogen, Oxygen

Hazardous Polymerization Hazardous polymerization does not occur.

Hazardous Reactions None under normal processing.

11. Toxicological information

Acute Toxicity

Product Information

Oral LD50 Category 4. ATE = 300 - 2000 mg/kg.

Dermal LD50 Based on ATE data, the classification criteria are not met. ATE > 2000 mg/kg.

Mist LC50 Category 4. ATE = 1 - 5 mg/l.

Component Information

Component	LD50 Oral	LD50 Dermal	LC50 Inhalation
Water	-	-	-
Hydrogen peroxide	376 mg/kg (Rat) (90%) 910 mg/kg (Rat) (20-60%) 1518 mg/kg (Rat) (8-20% sol)	>2000 mg/kg (Rabbit)	LC50 = 2000 mg/m³ (Rat) 4 h

Toxicologically Synergistic Products No information available

Delayed and immediate effects as well as chronic effects from short and long-term exposure

Irritation Causes burns by all exposure routes

Sensitization No information available

Carcinogenicity The table below indicates whether each agency has listed any ingredient as a carcinogen.

Component	CAS No	IARC	NTP	ACGIH	OSHA	Mexico
Water	7732-18-5	Not listed	Not listed	Not listed	Not listed	Not listed
Hydrogen peroxide	7722-84-1	Not listed	Not listed	A3	Not listed	A3

IARC (International Agency for Research on Cancer)

ACGIH: (American Conference of Governmental Industrial Hygienists)

Mexico - Occupational Exposure Limits - Carcinogens

IARC (International Agency for Research on Cancer)
Group 1 - Carcinogenic to Humans
Group 2A - Probably Carcinogenic to Humans
Group 2B - Possibly Carcinogenic to Humans

A1 - Known Human Carcinogen
A2 - Suspected Human Carcinogen
A3 - Animal Carcinogen

ACGIH: (American Conference of Governmental Industrial Hygienists)

Mexico - Occupational Exposure Limits - Carcinogens
A1 - Confirmed Human Carcinogen

A2 - Suspected Human Carcinogen
A3 - Confirmed Animal Carcinogen
A4 - Not Classifiable as a Human Carcinogen
A5 - Not Suspected as a Human Carcinogen

Mutagenic Effects No information available

Reproductive Effects No information available.

Developmental Effects No information available.

Teratogenicity No information available.

STOT - single exposure None known
STOT - repeated exposure None known

Aspiration hazard No information available

Symptoms / effects,both acute and delayed Ingestion causes severe swelling, severe damage to the delicate tissue and danger of perforation

Endocrine Disruptor Information No information available

Other Adverse Effects The toxicological properties have not been fully investigated.

12. Ecological information

Ecotoxicity

Contains a substance which is:. Harmful to aquatic organisms, may cause long-term adverse effects in the aquatic environment. Do not empty into drains. Do not flush into surface water or sanitary sewer system. Do not allow material to contaminate ground water system.

Component	Freshwater Algae	Freshwater Fish	Microtox	Water Flea
Hydrogen peroxide	EC50 2.5 mg/L/72h	LC50: 16.4 mg/L/96h (P.promelas)	Not listed	EC50 7.7 mg/L/24h

Persistence and Degradability Persistence is unlikely based on information available. Miscible with water

Bioaccumulation/ Accumulation No information available.

Mobility Will likely be mobile in the environment due to its water solubility.

Component	log Pow
Hydrogen peroxide	-1.1

13. Disposal considerations

Waste Disposal Methods Chemical waste generators must determine whether a discarded chemical is classified as a hazardous waste. Chemical waste generators must also consult local, regional, and national hazardous waste regulations to ensure complete and accurate classification.

14. Transport information

DOT

UN-No UN2014
Proper Shipping Name HYDROGEN PEROXIDE, AQUEOUS SOLUTIONS
Hazard Class 5.1
Subsidiary Hazard Class 8
Packing Group II

TDG

UN-No UN2014
Proper Shipping Name HYDROGEN PEROXIDE, AQUEOUS SOLUTION
Hazard Class 5.1
Subsidiary Hazard Class 8

Packing Group II

IATA

UN-No UN2014
Proper Shipping Name HYDROGEN PEROXIDE, AQUEOUS SOLUTION
Hazard Class 5.1
Subsidiary Hazard Class 8
Packing Group II

IMDG/IMO

UN-No UN2014
Proper Shipping Name HYDROGEN PEROXIDE, AQUEOUS SOLUTION
Hazard Class 5.1
Subsidiary Hazard Class 8
Packing Group II

15. Regulatory information

United States of America Inventory

Component	CAS No	TSCA	TSCA Inventory notification - Active-Inactive	TSCA - EPA Regulatory Flags
Water	7732-18-5	X	ACTIVE	-
Hydrogen peroxide	7722-84-1	X	ACTIVE	-

Legend:
TSCA US EPA (TSCA) - Toxic Substances Control Act, (40 CFR Part 710)
X - Listed
'-' - Not Listed

TSCA - Per 40 CFR 751, Regulation of Certain Chemical Substances & Mixtures, Under TSCA Section 6(h) (PBT) Not applicable

TSCA 12(b) - Notices of Export Not applicable

International Inventories
Canada (DSL/NDSL), Europe (EINECS/ELINCS/NLP), Philippines (PICCS), Japan (ENCS), Japan (ISHL), Australia (AICS), China (IECSC), Korea (KECL).

Component	CAS No	DSL	NDSL	EINECS	PICCS	ENCS	ISHL	AICS	IECSC	KECL
Water	7732-18-5	X	-	231-791-2	X	X		X	X	KE-35400
Hydrogen peroxide	7722-84-1	X	-	-	X	X	X	X	X	KE-20204

KECL - NIER number or KE number (http://ncis.nier.go.kr/en/main.do)

U.S. Federal Regulations

SARA 313 Not applicable

SARA 311/312 Hazard Categories See section 2 for more information

CWA (Clean Water Act) Not applicable

Clean Air Act Not applicable

OSHA - Occupational Safety and Health Administration

Component	Specifically Regulated Chemicals	Highly Hazardous Chemicals
Hydrogen peroxide	-	TQ: 7500 lb

CERCLA This material, as supplied, contains one or more substances regulated as a hazardous substance under the Comprehensive Environmental Response Compensation and Liability

Act (CERCLA) (40 CFR 302)

Component	Hazardous Substances RQs	CERCLA EHS RQs
Hydrogen peroxide	-	1000 lb

California Proposition 65 This product does not contain any Proposition 65 chemicals.

U.S. State Right-to-Know Regulations

Component	Massachusetts	New Jersey	Pennsylvania	Illinois	Rhode Island
Water	-	-	X	-	-
Hydrogen peroxide	X	X	X	-	X

U.S. Department of Transportation
Reportable Quantity (RQ): N
DOT Marine Pollutant N
DOT Severe Marine Pollutant N

U.S. Department of Homeland Security This product contains the following DHS chemicals:
Legend - STQs = Screening Threshold Quantities, APA = A placarded amount

Component	DHS Chemical Facility Anti-Terrorism Standard
Hydrogen peroxide	Theft STQs - 400lb (concentration >=35%)

Other International Regulations

Mexico - Grade No information available

Authorisation/Restrictions according to EU REACH

Component	CAS No	REACH (1907/2006) - Annex XIV - Substances Subject to Authorization	REACH (1907/2006) - Annex XVII - Restrictions on Certain Dangerous Substances	REACH Regulation (EC 1907/2006) article 59 - Candidate List of Substances of Very High Concern (SVHC)
Water	7732-18-5	-	-	-
Hydrogen peroxide	7722-84-1	-	Use restricted. See item 75. (see link for restriction details)	-

https://echa.europa.eu/substances-restricted-under-reach

Safety, health and environmental regulations/legislation specific for the substance or mixture

Component	CAS No	OECD HPV	Persistent Organic Pollutant	Ozone Depletion Potential	Restriction of Hazardous Substances (RoHS)
Water	7732-18-5	Listed	Not applicable	Not applicable	Not applicable
Hydrogen peroxide	7722-84-1	Listed	Not applicable	Not applicable	Not applicable

Component	CAS No	Seveso III Directive (2012/18/EC) - Qualifying Quantities for Major Accident Notification	Seveso III Directive (2012/18/EC) - Qualifying Quantities for Safety Report Requirements	Rotterdam Convention (PIC)	Basel Convention (Hazardous Waste)
Water	7732-18-5	Not applicable	Not applicable	Not applicable	Not applicable
Hydrogen peroxide	7722-84-1	Not applicable	Not applicable	Not applicable	Not applicable

16. Other information

Prepared By
Regulatory Affairs
Thermo Fisher Scientific
Email: EMSDS.RA@thermofisher.com

Creation Date	22-Sep-2009
Revision Date	24-Dec-2021
Print Date	24-Dec-2021
Revision Summary	SDS sections updated. 7.

Disclaimer

The information provided in this Safety Data Sheet is correct to the best of our knowledge, information and belief at the date of its publication. The information given is designed only as a guidance for safe handling, use, processing, storage, transportation, disposal and release and is not to be considered a warranty or quality specification. The information relates only to the specific material designated and may not be valid for such material used in combination with any other materials or in any process, unless specified in the text

End of SDS

D

Ethanol Safety Data Sheet

Safety Data Sheet
according to 29CFR1910/1200 and GHS Rev. 3

Effective date : 11.19.2014

Ethanol, Lab Grade, 500mL

SECTION 1 : Identification of the substance/mixture and of the supplier

Product name : **Ethanol, Lab Grade, 500mL**

Manufacturer/Supplier Trade name:

Manufacturer/Supplier Article number: **S25309**

Recommended uses of the product and uses restrictions on use:

Manufacturer Details:

AquaPhoenix Scientific
9 Barnhart Drive, Hanover, PA 17331

Supplier Details:

Fisher Science Education
15 Jet View Drive, Rochester, NY 14624

Emergency telephone number:

Fisher Science Education Emergency Telephone No.: 800-535-5053

SECTION 2 : Hazards identification

Classification of the substance or mixture:

Flammable
Flammable liquids, category 2

Toxic
Acute toxicity (oral, dermal, inhalation), category 3

Health hazard
Reproductive toxicity, category 2
Specific target organ toxicity following repeated exposure, category 2

Irritant
Specific target organ toxicity following single exposure, category 3

Narcotic effects
Flammable Liquid 2
Acute Toxicity 3 (oral)
Specific Target Organ Toxicity, Single Exposure 3
Specific Target Organ Toxicity, Repeat Exposure 1
Reproductive toxicity 2

Signal word :Danger

Hazard statements:
Highly flammable liquid and vapour
Toxic if swallowed
May cause drowsiness or dizziness
May damage fertility or the unborn child
May cause damage to organs through prolonged or repeated exposure

Precautionary statements:
If medical advice is needed, have product container or label at hand
Keep out of reach of children
Read label before use
Do not eat, drink or smoke when using this product
Avoid breathing dust/fume/gas/mist/vapours/spray
Use only outdoors or in a well-ventilated area
Use personal protective equipment as required
Keep away from heat/sparks/open flames/hot surfaces – No smoking
Keep container tightly closed
Ground/bond container and receiving equipment
Use explosion-proof electrical/ventilating/light/…/equipment
Use only non-sparking tools
Take precautionary measures against static discharge
Wear protective gloves/protective clothing/eye protection/face protection
Wash … thoroughly after handling
IF ON SKIN (or hair): Remove/Take off immediately all contaminated clothing. Rinse skin with water/shower
In case of fire: Use … for extinction
Rinse mouth
IF SWALLOWED: Call a POISON CENTER or doctor/physician if you feel unwell
IF INHALED: Remove victim to fresh air and keep at rest in a position comfortable for breathing
Get Medical advice/attention if you feel unwell
Collect spillage
IF exposed or concerned: Get medical advice/attention
Store in a well ventilated place. Keep cool
Store locked up
Store in a well ventilated place. Keep container tightly closed
Dispose of contents/container to …

Other Non-GHS Classification:

WHMIS

B2 

D2B 

D1B 

NFPA/HMIS

NFPA SCALE (0-4)

HMIS RATINGS (0-4)

SECTION 3 : Composition/information on ingredients

Ingredients:		
CAS 64-17-5	Ethanol, denatured	95 %
CAS 67-56-1	Methanol	3-52.25 %
CAS 108-10-1	MIBK	0.95-3.8 %
CAS 67-63-0	Isopropyl Alcohol	3.8-5.7 %
CAS 7732-18-5	Deionized Water	5 %
		Percentages are by weight

SECTION 4 : First aid measures

Description of first aid measures

After inhalation: Move exposed individual to fresh air. Loosen clothing as necessary and position individual in a comfortable position.Seek medical advice if discomfort or irritation persists.

After skin contact: Wash affected area with soap and water. Rinse thoroughly. Seek medical attention if irritation, discomfort or vomiting persists.

After eye contact: Protect unexposed eye. Rinse/flush exposed eye(s) gently using water for 15-20 minutes. Remove contact lens(es) if able to do so during rinsing. Seek medical attention if irritation persists or if concerned.

After swallowing: Rinse mouth thoroughly. Do not induce vomiting. Have exposed individual drink sips of water. Seek medical attention if irritation, discomfort or vomiting persists.

Most important symptoms and effects, both acute and delayed:

Irritation, Nausea,Headache, Shortness of breath.Dizziness. Vomiting;Impact to organs (liver, eyes, other-various). Impact to fetus (if pregnant)

Indication of any immediate medical attention and special treatment needed:

If seeking medical attention, provide SDS document to physician.

SECTION 5 : Firefighting measures

Extinguishing media

Suitable extinguishing agents: If in laboratory setting, follow laboratory fire suppression procedures. Use appropriate fire suppression agents for adjacent combustible materials or sources of ignition. Water. Dry chemical. Foam. Carbon dioxide

For safety reasons unsuitable extinguishing agents:

Special hazards arising from the substance or mixture:

Combustion products may include carbon oxides or other toxic vapors.Dangerous fire hazard when exposed to heat, sparks and open flames.

Advice for firefighters:

Protective equipment: Wear protective equipment. Use NIOSH-approved respiratory protection/breathing apparatus.Use spark-proof tools and explosion-proof equipment.

Additional information (precautions): Move product containers away from fire or keep cool with water spray as a protective measure, where feasible.

SECTION 6 : Accidental release measures

Personal precautions, protective equipment and emergency procedures:

Wear protective equipment. Use respiratory protective device against the effects of fumes/dust/aerosol. Keep unprotected persons away. Ensure adequate ventilation.Keep away from ignition sources. Protect from heat.Stop the spill, if possible. Contain spilled material by diking or using inert absorbent. Transfer to a disposal or recovery container.

Environmental precautions:

Prevent from reaching drains, sewer or waterway. Collect contaminated soil for characterization per Section 13. Collect spilled liquid for recovery, treatment or disposal.

Methods and material for containment and cleaning up:

If in a laboratory setting, follow Chemical Hygiene Plan procedures.Collect liquids using vacuum or by use of absorbents. Place into properly labeled containers for recovery or disposal. If necessary, use trained response staff/contractor.

Reference to other sections:

SECTION 7 : Handling and storage

Precautions for safe handling:

Prevent formation of aerosols. Follow good hygiene procedures when handling chemical materials. Do not eat, drink, smoke, or use personal products when handling chemical substances. If in a laboratory setting, follow Chemical Hygiene Plan.Use only in well ventilated areas.Avoid splashes or spray in enclosed areas.Wash hands before breaks and at the end of work.

Conditions for safe storage, including any incompatibilities:

Store in a cool location. Provide ventilation for containers. Avoid storage near extreme heat, ignition sources or open flame. Store away from foodstuffs. Store away from oxidizing agents.Store in cool, dry conditions in well sealed containers. Keep container tightly sealed.Store in secure flammable storage area away from sources of ignition.Protect from freezing and physical damage.

SECTION 8 : Exposure controls/personal protection

Control Parameters:	108-10-1, MIBK, ACGIH TLV STEL: 75 ppm) 67-63-0, 2-Propanol, OSHA PEL TWA: 400 ppm (980 mg/m3) 67-63-0, 2-Propanol, NIOSH REL: TWA 400 ppm (980 mg/m3) 67-63-0, 2-Propanol, NIOSH REL ST: 500 ppm (1225 mg/m3) 67-63-0, 2-Propanol, ACGIH TLV TWA: 200 ppm 67-63-0, 2-Propanol, ACGIH TLV STEL: 400 ppm 64-17-5, Ethanol, ACGIH TLV TWA: 1000 ppm (1881mg/m3) 64-17-5, Ethanol, OSHA PEL: TWA 1000 ppm (1900 mg/m3) 64-17-5, Ethanol, NIOSH IDLH: 3300 ppm [10%LEL] 64-17-5, Ethanol, NIOSH REL TWA: 1000 ppm (1900 mg/m3) 67-56-1, Methanol, OSHA PEL TWA: 260 mg/m3 (200 ppm) 67-56-1, Methanol, OSHA PEL STEL: 325 mg/m3 (250 ppm) 67-56-1, Methanol, ACGIH TLV TWA: 262 mg/m3 67-56-1, Methanol, ACGIH TLV STEL: 328 mg/m3 (250 ppm) 108-10-1, MIBK, OSHA PEL TWA: 205 mg/m3 (50 ppm) 108-10-1, MIBK, OSHA PEL STEL: 300 mg/m3 (75 ppm) 108-10-1, MIBK, ACGIH TLV TWA 20 mg/m3
Appropriate Engineering controls:	Emergency eye wash fountains and safety showers should be available in the immediate vicinity of use/handling.Provide exhaust ventilation or other engineering controls to keep the airborne concentrations of vapor or mists below the applicable workplace exposure limits (Occupational Exposure Limits-OELs) indicated above.
Respiratory protection:	Not required under normal conditions of use. Use suitable respiratory protective device when high concentrations are present. Use suitable respiratory protective device when aerosol or mist is formed. For spills, respiratory protection may be advisable.
Protection of skin:	The glove material has to be impermeable and resistant to the product/ the substance/ the preparation being used/handled.Selection of the glove material on consideration of the penetration times, rates of diffusion and the degradation.
Eye protection:	Safety glasses with side shields or goggles.
General hygienic measures:	The usual precautionary measures are to be adhered to when handling chemicals. Keep away from food, beverages and feed sources. Immediately remove all soiled and contaminated clothing. Wash hands before breaks and at the end of work. Do not inhale gases/fumes/dust/mist/vapor/aerosols. Avoid contact with the eyes and skin.

SECTION 9 : Physical and chemical properties

Appearance (physical state,color):	Clear, colorless liquid	**Explosion limit lower**: **Explosion limit upper**:	3.3 18
Odor:	Alcohol	**Vapor pressure**:	48 mm Hg
Odor threshold:	10 ppm	**Vapor density**:	1.5
pH-value:	Not determined	**Relative density**:	Approx. 0.8
Melting/Freezing point:	-90 C	**Solubilities**:	infinite solubility
Boiling point/Boiling range:	77 C	**Partition coefficient (n-octanol/water)**:	Not determined
Flash point (closed cup):	15.5 C	**Auto/Self-ignition temperature**:	362.8 C

Evaporation rate:	3.6	**Decomposition temperature**:	Not determined
Flammability (solid,gaseous):	Flammable	**Viscosity**:	a. Kinematic:Not determined b. Dynamic: Not determined
Density: Not determined			

SECTION 10 : Stability and reactivity

Reactivity:
Chemical stability: No decomposition if used and stored according to specifications.
Possible hazardous reactions:
Conditions to avoid: Store away from oxidizing agents, strong acids or bases.Ignition source. Excess heat. Incompatible materials. Open flame
Incompatible materials: Strong acids.Heat. Open flame. Sparks. Strong bases.Potassium dioxide. Acetyl bromide. Acetyl chloride. Bromine pentafluoride. Sodium. Platinum. Strong oxidizers
Hazardous decomposition products: Carbon oxides (CO, CO2).Acrid smoke and fumes. Irritating fumes

SECTION 11 : Toxicological information

Acute Toxicity:		
Inhalation:	64000 mg/kg 4 hr	LD50(rat) (Methanol 64-17-5)
Oral:	7060 mg/kg	LD50 oral-rat: (Ethanol 64-17-5)
Oral:	6200 mg/kg	LD50(rat) (Ethanol 64-17-5)
Oral:	4600 mg/kg	LD50(rat) (MIBK 108-10-1)
Oral:	5628 mg/kg	LD50(rat) (Methanol 67-56-1)
Inhalation:	20000 mg/kg 10 hr	LD50(rat) (Ethanol 64-17-5)
Inhalation:	8.2 mg/kg 4 hr	LD50(rat) (MIBK 108-10-1)
Chronic Toxicity:		
Oral:	May cause damage to the following organs: blood, kidneys, the reproductive system, liver, gastrointestinal tract, upper respiratory tract, skin, central nervous system (CNS), eye, lens or cornea.	Human
Corrosion Irritation:		
Ocular:		May cause eye irritation.
Sensitization:		No additional information.
Single Target Organ (STOT):		Classified as STOT in Section 2 (multiple organs - see above, Section 11)
Numerical Measures:		No additional information.

Carcinogenicity:	IARC: IARC classification (1) for Ethanol, CAS# 64-17-5, is intended for use in alcoholic beverage use only. This product is NOT intended for this use.
Mutagenicity:	No additional information.
Reproductive Toxicity:	No additional information.

SECTION 12 : Ecological information

Ecotoxicity Persistence and degradability: Readily degradable in the environment.
Bioaccumulative potential:
Mobility in soil: Aqueous solution has high mobility in soil.
Other adverse effects:

SECTION 13 : Disposal considerations

Waste disposal recommendations:

Product/containers must not be disposed together with household garbage. Do not allow product to reach sewage system or open water.It is the responsibility of the waste generator to properly characterize all waste materials according to applicable regulatory entities (US 40CFR262.11). Consult federal state/ provincial and local regulations regarding the proper disposal of waste material that may incorporate some amount of this product.

SECTION 14 : Transport information

UN-Number

1170

UN proper shipping name

Ethanol (Mixture)

Transport hazard class(es)

Class:
3 Flammable liquids

Packing group:II
Environmental hazard:
Transport in bulk:
Special precautions for user:

SECTION 15 : Regulatory information

United States (USA)

SARA Section 311/312 (Specific toxic chemical listings):

Reactive, Acute, Chronic, Fire

SARA Section 313 (Specific toxic chemical listings):

67-56-1 Methanol
67-63-0 2-Propanol
108-10-1 MIBK

RCRA (hazardous waste code):

None of the ingredients is listed

TSCA (Toxic Substances Control Act):

All ingredients are listed.

CERCLA (Comprehensive Environmental Response, Compensation, and Liability Act):

None of the ingredients is listed

Proposition 65 (California):

Chemicals known to cause cancer:

None of the ingredients is listed

Chemicals known to cause reproductive toxicity for females:

None of the ingredients is listed

Chemicals known to cause reproductive toxicity for males:

None of the ingredients is listed

Chemicals known to cause developmental toxicity:

108-10-1 Methanol

Canada

Canadian Domestic Substances List (DSL):

All ingredients are listed.

Canadian NPRI Ingredient Disclosure list (limit 0.1%):

64-17-5 Ethanol

Canadian NPRI Ingredient Disclosure list (limit 1%):

67-56-1 Methanol
67-63-0 2-Propanol
108-10-1 MIBK

SECTION 16 : Other information

This product has been classified in accordance with hazard criteria of the Controlled Products Regulations and the SDS contains all the information required by the Controlled Products Regulations.Note:. The responsibility to provide a safe workplace remains with the user.The user should consider the health hazards and safety information contained herein as a guide and should take those precautions required in an individual operation to instruct employees and develop work practice procedures for a safe work environment.The information contained herein is, to the best of our knowledge and belief, accurate.However, since the conditions of handling and use are beyond our control, we make no guarantee of results, and assume no liability for damages incurred by the use of this material.It is the responsibility of the user to comply with all applicable laws and regulations applicable to this material.

GHS Full Text Phrases:

Abbreviations and acronyms:

IMDG: International Maritime Code for Dangerous Goods
PNEC: Predicted No-Effect Concentration (REACH)
CFR: Code of Federal Regulations (USA)
SARA: Superfund Amendments and Reauthorization Act (USA)
RCRA: Resource Conservation and Recovery Act (USA)
TSCA: Toxic Substances Control Act (USA)
NPRI: National Pollutant Release Inventory (Canada)
DOT: US Department of Transportation

IATA: International Air Transport Association
GHS: Globally Harmonized System of Classification and Labelling of Chemicals
ACGIH: American Conference of Governmental Industrial Hygienists
CAS: Chemical Abstracts Service (division of the American Chemical Society)
NFPA: National Fire Protection Association (USA)
HMIS: Hazardous Materials Identification System (USA)
WHMIS: Workplace Hazardous Materials Information System (Canada)
DNEL: Derived No-Effect Level (REACH)

Effective date : 11.19.2014
Last updated : 03.19.2015

E

Digital Thermometer Data Sheet

FEATURES

- Data memory and read function
- Display HOLD function
- Input protection 20 V maximum
- Auto power off
- C / ºF selectable display

RS PRO Digital Thermometer

RS Stock No.: 123-2215

RS Professionally Approved Products bring to you professional quality parts across all product categories. Our product range has been tested by engineers and provides a comparable quality to the leading brands without paying a premium price.

Digital Thermometer

Product Description

RS PRO 1319A is a great value, high accuracy digital thermometer for use with any K-type thermocouple as a temperature sensor. It features a dual LCD display which shows temperature reading (main display) and MAX /MIN / AVERAGE or offset reference value - in RELATIVE mode (secondary display). A digital thermometer can measure temperature to a decimal point rather than a whole number meaning its results are more accurate. The RS PRO 1319A digital thermometer is ideal for areas where accurate temperature readings are required.

General Specifications

Series	RS PRO K-Type
Model Number	1319A
Thermometer Type	Handheld
Probe Type	K
Number of Temperature Inputs	1
Absolute Maximum Temperature Measurement	+1300°C / +1999°F
Temperature Scale	Centigrade/Fahrenheit
Display type	LCD
Resolution	0.1°C / 0.1°F
Best Accuracy	0.3% ± 1°C / 0.3% ± 2°F
Temperature Coefficient	0.1×(spec. Acc'y)/℃ <18℃, >28℃
Data Storage Memory	150 Sets / Yes
Minimum/Maximum Recordings	Yes
Automatic Shut-Off	Yes
Calibrated Certificate	Yes
Operating Temperature	0℃ to 50℃
Storage Temperature	-20℃ to 60℃
Operating Humidity	Below 80% RH
Applications	Food Industry / HVAC / Industrial / Medical

Electrical Specifications

Battery Type	AAA
Battery Life	110 hours

Mechanical Specifications

Dimensions	72 x 35 x 150mm
Length	72mm
Width	35mm
Height	150mm
Weight	235g

Digital Thermometer

Classification

eCl@ss Version	
UNSPSC Version	

Approvals

Compliance/Certifications	EN 61340
Declarations	RoHS Certificate of Compliance

Similar Products

Stock No.	Brand	Product Name	Thermometer Type	Absolute Maximum Temperature Measurement	Probe Type
XXX-XXXX					
XXX-XXXX					

F

COMSOL Simulation Settings

1 Component 1

1.1 DEFINITIONS

1.1.1 Coordinate Systems

Boundary System 1

Coordinate system type	Boundary system
Tag	sys1

COORDINATE NAMES

First	Second	Third
t1	t2	n

1.2 GEOMETRY 1

UNITS

Length unit	mm
Angular unit	deg

1.2.1 Cylinder 1 (cyl1)

POSITION

Description	Value
Position	{0, 0, 0}

AXIS

Description	Value
Axis type	z - axis

SIZE AND SHAPE

Description	Value
Radius	13
Height	50

INFORMATION

Description	Value
Last build time	< 1 second
Built with	COMSOL 6.2.0.339 (win64), Jun 4, 2024, 12:27:30 PM

1.2.2 Helix 1 (hel1)

POSITION

Description	Value
Position	{0, -12, 30}

AXIS

Description	Value
Axis type	y - axis

SIZE AND SHAPE

Description	Value
Number of turns	24
Major radius	2.15
Minor radius	0.127
Axial pitch	1
Radial pitch	0
Chirality	Right - handed

INFORMATION

Description	Value
Last build time	1 seconds
Built with	COMSOL 6.2.0.339 (win64), Jun 4, 2024, 3:38:37 PM

1.2.3 Helix 2 (hel2)

POSITION

Description	Value
Position	{7, -9, 30}

AXIS

Description	Value
Axis type	y - axis

SIZE AND SHAPE

Description	Value
Number of turns	18
Major radius	2.15

Description	Value
Minor radius	0.127
Axial pitch	1
Radial pitch	0
Chirality	Right - handed

INFORMATION

Description	Value
Last build time	< 1 second
Built with	COMSOL 6.2.0.339 (win64), Jun 4, 2024, 3:42:22 PM

1.2.4 Helix 3 (hel3)

POSITION

Description	Value
Position	{-7, -9, 30}

AXIS

Description	Value
Axis type	y - axis

SIZE AND SHAPE

Description	Value
Number of turns	18
Major radius	2.15
Minor radius	0.127
Axial pitch	1
Radial pitch	0
Chirality	Right - handed

INFORMATION

Description	Value
Last build time	< 1 second
Built with	COMSOL 6.2.0.339 (win64), Jun 4, 2024, 3:42:52 PM

1.3 MATERIALS

1.3.1 Nichrome [solid,steady-state]

SELECTION

Geometric entity level	Domain
Selection	Geometry geom1: Dimension 3: Domains 2–4

BASIC

Description	Value	Unit
Density	rho(T)	kg/m³
Thermal conductivity	11.3	W/(m·K)
Heat capacity at constant pressure	480	J/(kg·K)

1.3.2 H2O2 [liquid]

SELECTION

Geometric entity level	Domain
Selection	Geometry geom1: Dimension 3: Domain 1

BASIC

Description	Value	Unit
Density	rho(T)	kg/m³
Heat capacity at constant pressure	2619	J/(kg·K)
Thermal conductivity	0.58576	W/(m·K)
Dynamic viscosity	0.0011459	Pa·s

1.4 SURFACE-TO-SURFACE RADIATION

EQUATIONS

$$J = \varepsilon e_b(T) + \rho_d G$$
$$G = G_m + G_{amb} + G_{ext}$$
$$G_{amb} = F_{amb}\varepsilon_{amb}e_b(T_{amb})$$
$$e_b(T) = n^2\sigma T^4$$

FEATURES

Name	Level
Diffuse Surface 1	Boundary
Initial Values 1	Boundary

1.4.1 Diffuse Surface 1

SETTINGS

Description	Value
Temperature	Temperature (htrad1)

Radiation Direction

SETTINGS

Description	Value
Description	Emitted radiation direction:
Emitted radiation direction	Opacity controlled
Description	This symbol indicates the boundaries that do not radiate for any spectral bands

Ambient

SETTINGS

Description	Value	Unit
Define ambient temperature on each side	Off	
Ambient temperature	User defined	
Ambient temperature	293.15	K
Define ambient emissivity on each side	Off	
Ambient emissivity	Blackbody	
Include diffuse irradiance	On	
Diffuse irradiance	User defined	
Diffuse irradiance	0	W/m²

Surface Emissivity

SETTINGS

Description	Value
Define properties on each side	Off
Emissivity	User defined
Emissivity	0.8

1.4.2 Initial Values 1

Initial Values

SETTINGS

Description	Value
Initial value	Blackbody/Graybody

1.5 LAMINAR FLOW

EQUATIONS

$$\rho\frac{\partial \mathbf{u}}{\partial t}+\rho(\mathbf{u}\cdot\nabla)\mathbf{u}=\nabla\cdot[-p\mathbf{I}+\mathbf{K}]+\mathbf{F}$$

$$\frac{\partial \rho}{\partial t}+\nabla\cdot(\rho\mathbf{u})=0$$

FEATURES

Name	Level
Fluid Properties 1	Domain
Initial Values 1	Domain
Wall 1	Boundary
Inlet 1	Boundary
Outlet 1	Boundary

1.5.1 Fluid Properties 1

SETTINGS

Description	Value
Temperature	Temperature (nitf1)

Fluid Properties

SETTINGS

Description	Value
Constitutive relation	Specify dynamic viscosity
Dynamic viscosity	From material

Model Input

SETTINGS

Description	Value	Unit
Volume reference temperature	User defined	
Volume reference temperature	293.15	K

PROPERTIES FROM MATERIAL

Property	Material	Property group
Dynamic viscosity	H2O2 [liquid]	Basic

1.5.2 Initial Values 1

Initial Values

SETTINGS

Description	Value	Unit
Velocity field, x-component	0	m/s
Velocity field, y-component	0	m/s
Velocity field, z-component	0	m/s
Pressure	0	Pa

Coordinate System Selection

SETTINGS

Description	Value
Coordinate system	Global coordinate system

1.5.3 Wall 1

Boundary Condition

SETTINGS

Description	Value
Wall condition	No slip

Wall Movement

SETTINGS

Description	Value
Translational velocity	Automatic from frame
Sliding wall	Off

1.5.4 Inlet 1

Boundary Condition

SETTINGS

Description	Value
Boundary condition	Fully developed flow
Apply condition on each disjoint selection separately	On

Fully Developed Flow

SETTINGS

Description	Value	Unit
Fully developed flow option	Flow rate	
Flow rate	5E-8	m^3/s

1.5.5 Outlet 1

Boundary Condition

SETTINGS

Description	Value
Boundary condition	Pressure

Pressure Conditions

SETTINGS

Description	Value	Unit
Pressure	0	Pa
Normal flow	Off	
Suppress backflow	On	

1.6 HEAT TRANSFER IN SOLIDS AND FLUIDS

EQUATIONS

$$\rho C_p \frac{\partial T}{\partial t} + \rho C_p \mathbf{u} \cdot \nabla T + \nabla \cdot \mathbf{q} = Q + Q_{ted}$$
$$\mathbf{q} = -k\nabla T$$

FEATURES

Name	Level
Solid 1	Domain
Fluid 1	Domain
Initial Values 1	Domain
Thermal Insulation 1	Boundary
Inflow 1	Boundary
Outflow 1	Boundary
Heat Source 1	Domain
Heat Flux 1	Boundary
Initial Values 2	Domain
Heat Flux 2	Boundary

1.6.1 Solid 1

Heat Conduction, Solid

SETTINGS

Description	Value
Thermal conductivity	From material

Thermodynamics, Solid

SETTINGS

Description	Value
Density	From material
Heat capacity at constant pressure	From material

Coordinate System Selection

SETTINGS

Description	Value
Coordinate system	Global coordinate system

Model Input

SETTINGS

Description	Value
Volume reference temperature	Common model input

PROPERTIES FROM MATERIAL

Property	Material	Property group
Thermal conductivity	Nichrome [solid,steady-state]	Basic
Density	Nichrome [solid,steady-state]	Basic
Heat capacity at constant pressure	Nichrome [solid,steady-state]	Basic

1.6.2 Fluid 1

SETTINGS

Description	Value
Velocity field	Velocity field (nitf1)
Absolute pressure	Absolute pressure (nitf1)

Heat Conduction, Fluid

SETTINGS

Description	Value
Thermal conductivity	From material

Thermodynamics, Fluid

SETTINGS

Description	Value
Fluid type	From material

Coordinate System Selection

SETTINGS

Description	Value
Coordinate system	Global coordinate system

Model Input

SETTINGS

Description	Value	Unit
Volume reference temperature	User defined	
Volume reference temperature	293.15	K

PROPERTIES FROM MATERIAL

Property	Material	Property group
Heat capacity at constant pressure	H2O2 [liquid]	Basic
Thermal conductivity	H2O2 [liquid]	Basic
Density	H2O2 [liquid]	Basic

1.6.3 Initial Values 1

Initial Values

SETTINGS

Description	Value	Unit
Temperature	User defined	
Temperature	473.15	K

1.6.4 Inflow 1

Upstream Properties

SETTINGS

Description	Value	Unit
Upstream temperature	User defined	
Upstream temperature	293.15	K
Specify upstream absolute pressure	Off	

1.6.5 Heat Source 1

Heat Source

SETTINGS

Description	Value	Unit
Heat source	Heat rate	
Heat rate	15	W

1.6.6 Heat Flux 1

Heat Flux

SETTINGS

Description	Value	Unit
Flux type	Convective heat flux	
Heat transfer coefficient	User defined	
Heat transfer coefficient	30	$W/(m^2 \cdot K)$
External temperature	User defined	
External temperature	293.15	K

1.6.7 Initial Values 2

Initial Values

SETTINGS

Description	Value	Unit
Temperature	User defined	
Temperature	873.15	K

1.6.8 Heat Flux 2

Heat Flux

SETTINGS

Description	Value	Unit
Flux type	Convective heat flux	
Heat transfer	User defined	

Description	Value	Unit
coefficient		
Heat transfer coefficient	500	W/(m²·K)
External temperature	User defined	
External temperature	293.15	K

1.7 MULTIPHYSICS

1.7.1 Nonisothermal Flow 1

EQUATIONS

$$Q_{vd} = \tau : \nabla \mathbf{u}$$

Material Properties

SETTINGS

Description	Value
Specify density	From heat transfer interface
Specify reference temperature	From heat transfer interface

Energy Balance

SETTINGS

Description	Value
Include viscous dissipation	On
Include kinetic energy	Off

Coupled Interfaces

SETTINGS

Description	Value
Fluid flow	Laminar Flow (spf)
Heat transfer	Heat Transfer in Solids and Fluids (ht)

1.7.2 Heat Transfer with Surface-to-Surface Radiation 1

EQUATIONS

$$-\mathbf{n} \cdot \mathbf{q} = q_{r,net}$$

Coupled Interfaces

SETTINGS

Description	Value
Heat transfer	Heat Transfer in Solids and Fluids (ht)
Surface-to-surface radiation	Surface-to - Surface Radiation (rad)

1.8 MESH 3

1.8.1 Size (size)

SETTINGS

Description	Value
Maximum element size	5
Minimum element size	0.9
Curvature factor	0.6
Resolution of narrow regions	0.5
Maximum element growth rate	1.5

1.8.2 Size 1 (size1)

SELECTION

Geometric entity level	Domain
Selection	Geometry geom1: Dimension 3: Domain 1

SETTINGS

Description	Value
Calibrate for	Fluid dynamics
Maximum element size	2.6
Minimum element size	0.78
Curvature factor	0.7
Resolution of narrow regions	0.6
Maximum element growth rate	1.2
Predefined size	Coarse

1.8.3 Size 2 (size2)

SELECTION

Geometric entity level	Boundary
Selection	Geometry geom1: Dimension 2: Boundaries 1–2, 5–24

SETTINGS

Description	Value
Calibrate for	Fluid dynamics
Maximum element size	1.38
Minimum element size	0.26
Curvature factor	0.5
Resolution of narrow regions	0.8
Maximum element growth rate	1.13
Predefined size	Fine

1.8.4 Corner Refinement 1 (cr1)

SELECTION

Geometric entity level	Domain
Selection	Geometry geom1: Dimension 3: Domain 1

1.8.5 Free Tetrahedral 1 (ftet1)

SELECTION

Geometric entity level	Domain
Selection	Remaining

SETTINGS

Description	Value
Avoid inverted curved elements	On

INFORMATION

Description	Value
Last build time	34 seconds
Built with	COMSOL 6.2.0.339 (win64), Jun 11, 2024, 8:51:59 PM

1.8.6 Boundary Layers 1 (bl1)

SELECTION

Geometric entity level	Domain
Selection	Geometry geom1: Dimension 3: Domain 1

INFORMATION

Description	Value
Handling of sharp edges	Trimming
Last build time	28 seconds
Built with	COMSOL 6.2.0.339 (win64), Jun 11, 2024, 8:52:27 PM

Boundary Layer Properties 1 (blp1)

SELECTION

Geometric entity level	Boundary
Selection	Geometry geom1: Dimension 2: Boundaries 1–2, 5–24

SETTINGS

Description	Value
Number of layers	2
Thickness adjustment factor	5

G

High Lumen Light Source Data Sheet

Technical Data

CRI:	96
TLCI:	98
Warranty:	Limited 2-Year Warranty (Extend to 3 Years Total With Online Registration)
Color Temperature (Kelvin):	5600K
Lumen Output 5600K:	17672
Beam Angle Flood:	120 Degrees
Dimming:	0-100%
DMX Control:	No
Compatible Wifi Adapter:	NANLINK WS-TB-1 Transmitter box
Wireless Control Type:	2.4GHz Bluetooth
Frequency:	2.4GHz
Mount:	Standard 5/8" Receiver with Rotating Yoke
Light Modifier Bayonet Mount:	Bowens Style

Cooling System:	Active Silent Fan
Power Source:	AC100-240V 50/60Hz
Max Power Consumption:	225W
Includes Rechargeable Battery:	No
Battery Included:	No
Battery Required:	No
Compatible Remote:	Nanlite RC-1 Remote Control, NANLITE WS-RC-C2 Remote Control
Depth Rating:	IP 20